

2017

The Effect of Aging on the Blood Brain Barrier Permeability and Response to Fluoxetine Enantiomers

Ethar Arkan
Wright State University

Follow this and additional works at: https://corescholar.libraries.wright.edu/etd_all



Part of the [Neuroscience and Neurobiology Commons](#), and the [Physiology Commons](#)

Repository Citation

Arkan, Ethar, "The Effect of Aging on the Blood Brain Barrier Permeability and Response to Fluoxetine Enantiomers" (2017). *Browse all Theses and Dissertations*. 1844.
https://corescholar.libraries.wright.edu/etd_all/1844

This Thesis is brought to you for free and open access by the Theses and Dissertations at CORE Scholar. It has been accepted for inclusion in Browse all Theses and Dissertations by an authorized administrator of CORE Scholar. For more information, please contact library-corescholar@wright.edu.

THE EFFECT OF AGING ON THE BLOOD BRAIN
BARRIER PERMEABILITY AND RESPONSE TO
FLUOXETINE ENANTIOMERS

A thesis submitted in partial fulfillment of the
requirements for the degree of
Master of Science

By

ETHAR ARKAN
B.S., Wright State University, 2012

2017

Wright State University

WRIGHT STATE UNIVERSITY
GRADUATE SCHOOL

July 31, 2017

I HEREBY RECOMMEND THAT THE THESIS PREPARED UNDER MY SUPERVISION BY Ethar Arkan ENTITLED The Effect of Aging On The Blood Brain Barrier Permeability And Response To Fluoxetine To Fluoxetine Enantiomers BE ACCEPTED IN PARTIAL FULFILMENT OF THE REQUIREMENTS FOR THE DEGREE OF Master of Science.

Adrian Corbett, Ph.D.
Thesis Director

Eric Bennett, Ph.D.
Department Chair Department of Neuroscience, Cell
Biology, and Physiology

Committee
on Final
Examination

Adrian Corbett, Ph.D.

Debra Mayes, Ph.D.

Kathrin Engisch, Ph.D.

Robert E.W. Fyffe, Ph.D.
Vice President for Research
and Dean of the Graduate
School

ABSTRACT

Arkan, Ethar. M.S., Physiology and Neuroscience, Wright State University, 2017. The effect of aging on the blood brain barrier permeability and response to fluoxetine enantiomers.

We tested the effect of the fluoxetine enantiomers (S-fluoxetine and R-fluoxetine) versus Prozac (50:50 ratio of R- and S- fluoxetine enantiomers) and/or control on blood brain barrier (BBB) permeability in different brain regions in both male and female rats. The rats consumed orally the drug (5 mg/kg) or vehicle for a total of three days, then were injected with sterile Evans blue dye ip, at least 12 hours before euthanasia.. We see significant regional brain differences in BBB permeability (hippocampus has tighter BBB), significant differences based on the age of the animals (young rats show enhanced permeability in lower brain region), and significant differences based on the sex of animals interacting with specific regional differences in BBB permeability (female rats have enhanced permeability in cerebellum). We also see some effect of the fluoxetine enantiomers, with S-fluoxetine enhancing permeability, and R fluoxetine reducing permeability.

TABLE OF CONTENTS

BACKGROUND	1
I.INTRODUCTION	3
1.1 The Blood Brain Barrier	3
1.2 Neurovascular Unit	5
1.2.1 Microglia	6
1.2.2 The Basement Membrane.....	7
1.2.3 Endothelial Cells (ECs).....	7
1.2.4 Astrocytes.....	8
1.3 Tight Junction	9
1.4 Transport across the BBB	14
1.5 BBB Disruption	15
1.6 Fluoxetine	21
1.6.1 Fluoxetine Metabolism.....	21
1.6.2 Fluoxetine Effect on Microglial cells.....	23
1.7 HYPOTHESIS	23
1.7.1 Specific Aims.....	24
II. MATERIALS AND METHODS	26

2.1 Voluntary Drug Administration	26
2.2 Euthanization.....	27
2.3 Cardioperfusion.....	27
2.4 Pellet Homogenization	31
2.5 Bradford Protein Assay	32
2.6 Animal Model	33
2.7 Statistical Analysis.....	34
III. Results.....	35
3.1 Young Male Rats	36
3.2 Old Male Rats	43
3.3 Old Female Rats.....	48
3.4 Young Male Rats versus Old Male Rats.....	54
3.5 Comparison among the Young Males Groups.....	63
3.6 Comparisons among the Old Males Groups	82
3.7 Old Male Rats versus Old Female Rats	89
3.8 Comparison of All treatment groups across a Brain Regions.....	99
3.8.1 Cortex.....	99
3.8.2 Hippocampus.....	102
3.8.3 Brain.....	106
3.8.4 Cerebellum	110

IV. Discussion.....	116
4.1 The results of the total ng EB/mg protein of young versus old male rats (Age difference).....	116
4.2 The results of the total ng EB/mg protein in male versus female (Gender difference).....	117
4.3 Comparison of All treatment groups across a Brain Regions.....	118
4.4 The Treatment Effect among the Different Animal Groups.....	122
4.5 The Activity of the Fluoxetine Metabolites	123
4.6 Previous Research Studies	125
V. Future Directions.....	127
VI. Conclusion.....	128
VII. References	130

LIST OF FIGURES

Figure 1	4
Figure 2	5
Figure 3	10
Figure 4	11
Figure 5	12
Figure 6	14
Figure 7	14
Figure 8	16
Figure 9	21
Figure 10	22
Figure 11	27
Figure 12	29
Figure 13	36
Figure 14	37
Figure 15	38
Figure 16	39
Figure 17	40
Figure 18	41
Figure 19	42
Figure 20	44

Figure 21	45
Figure 22	46
Figure 23	47
Figure 24	49
Figure 25	50
Figure 26	51
Figure 27	52
Figure 28	53
Figure 29	55
Figure 30	56
Figure 31	57
Figure 32	59
Figure 33	60
Figure 34	62
Figure 35	64
Figure 36	65
Figure 37	67
Figure 38	68
Figure 39	70
Figure 40	71
Figure 41	73
Figure 42	74
Figure 43	76
Figure 44	77

Figure 45	79
Figure 46	80
Figure 47	82
Figure 48	83
Figure 49	85
Figure 50	87
Figure 51	88
Figure 52	90
Figure 53	91
Figure 54	93
Figure 55	94
Figure 56	96
Figure 57	97
Figure 58	100
Figure 59	101
Figure 60	103
Figure 61	105
Figure 62	107
Figure 63	109
Figure 64	111
Figure 65	112
Figure 66	126

LIST OF TABLES

Table 1	18-20
Table 2	20
Table 3	35
Table 4	116
Table 5	118
Table 6	119
Table 7	121
Table 8	122
Table 9	123

ACKNOWLEDGEMENTS

I would like to thank Dr. Corbett for letting me do my master's degree in her lab. Being a foreign student with no previous experience in research, I found everything about research foreign as well. Therefore, I had to ask a lot of questions, and always needed additional reassurance to make sure that I am on the right track. I was lucky to have an understanding advisor, Dr. Corbett who took the time to answer all of my questions and she was patient with me till I mastered the lab techniques. She never belittled any of my questions instead Dr. Corbett believed in me and gave me the confidence to complete the master's degree.

This research experience is a very unique experience for me because it is my very first time to get introduced to the field of research. Also, my little sister and I were in Dr. Corbett's lab by accident; we did not plan to be in the same lab.

I would like to thank Dr. Corbett's lab members, my sister who is my main source of encouragement and my Indian friend, Priya who never forget to answer any question or concern that I had.

A very special thanks to my parents who dedicated their lives for me, and without my parents, I will not be where I am today in life.

I dedicate this thesis to my family: my dear father, Dr. Arkan Kadum who supported me in every single step through my education, and my mother, Huda MohammadHassan who always believed in me and gave me the strength that I needed to go through the challenging times, my brother, Ali, and my sister, Nooralhuda.

BACKGROUND

Among elderly people worldwide, neurodegenerative diseases are the major cause of disability and premature death. The most common neurodegenerative diseases include Alzheimer's disease, vascular dementia, frontotemporal dementia, Parkinson disease and Huntington's disease (1).

Neurodegeneration is defined as a progressive loss of neuronal structure and function, which eventually leads to neuronal cell death. It is an important component of age-related pathology. Neurodegenerative diseases begin in mid-life. They are characterized by motor and/or cognitive symptoms that worsen with age, and its symptoms reduce the life expectancy (2). In addition, genetic and environmental factors play a critical role in neurodegenerative diseases development (3, 4), such as Amyotrophic lateral sclerosis (ALS) (5). There are many possible causes for the neurodegenerative diseases. In this study, we are focusing mainly on the changes in the blood brain barrier permeability due to aging.

A tight blood brain barrier is important to keep out peripheral immune cells that may attack and kill cells in the brain. It is critical to regulate the blood brain barrier permeability to ensure a stable environment and an optimal ionic composition that are significant for neural function and synaptic signaling functions. For example, the concentration of potassium is maintained at 4.5 mM in mammalian plasma but it is maintained around 2.5-2.9 mM in cerebrospinal fluid (CSF) and brain interstitial fluid (ISF) in spite of changes that occur after having a meal or exercise (6, 7). Also, the blood brain barrier helps to regulate the amount of neurotransmitters in the blood and it keeps the neurotransmitters in the central and peripheral nervous system separate. For example, blood plasma contains a

high level of neuroexcitatory amino acid glutamate, which if increased in the brain could result in a considerable neurotoxic damage in the neural tissue (8, 9). The blood brain barrier regulates the entry of many macromolecules because high level of certain plasma proteins could lead to nervous tissue damage. For example, high levels of plasma proteins such as albumin, pro-thrombin, and plasminogen cause cellular activation that results in apoptosis and nervous tissue damage (10, 11). For example, thrombin entry into the brain will cause the potentiation of NMDA receptor that will result in glutamate-mediated cell death (12).

The blood brain barrier (BBB) has low permeability to essential water soluble nutrients and metabolites that are important for the nervous tissue' however it has transport systems in the BBB to ensure the supply of nutrients to the central nervous system (8, 13, 14).

Understanding how the BBB changes in permeability with age and in the presence of enantiomers of fluoxetine may provide new approaches to treat the chronic neurodegenerative diseases in the elderly human population that are currently without effective treatment (2). Fluoxetine is used to treat neurodegenerative diseases because of its ability to convert harmful microglia to beneficial microglia, a new role discovered in the Corbett lab.

I.INTRODUCTION

1.1 The Blood Brain Barrier

Paul Ehrlich was the first one to identify the blood brain barrier. He injected basic dyes into the circulatory system and found out that it did not stain the brain but it stained most other organs. Therefore, a conclusion was made that the blood brain barrier separates the central and the peripheral nervous system in order to maintain ion hemostasis state in the CNS by regulating the entry of toxic and pathogenic substances in and out of the CNS except for lipid soluble molecules (15). That separation is important to insure the integrity of neural network connectivity and to insure the longevity of neurons. Also, maintaining ion hemostasis is critical for neuron signaling (16).

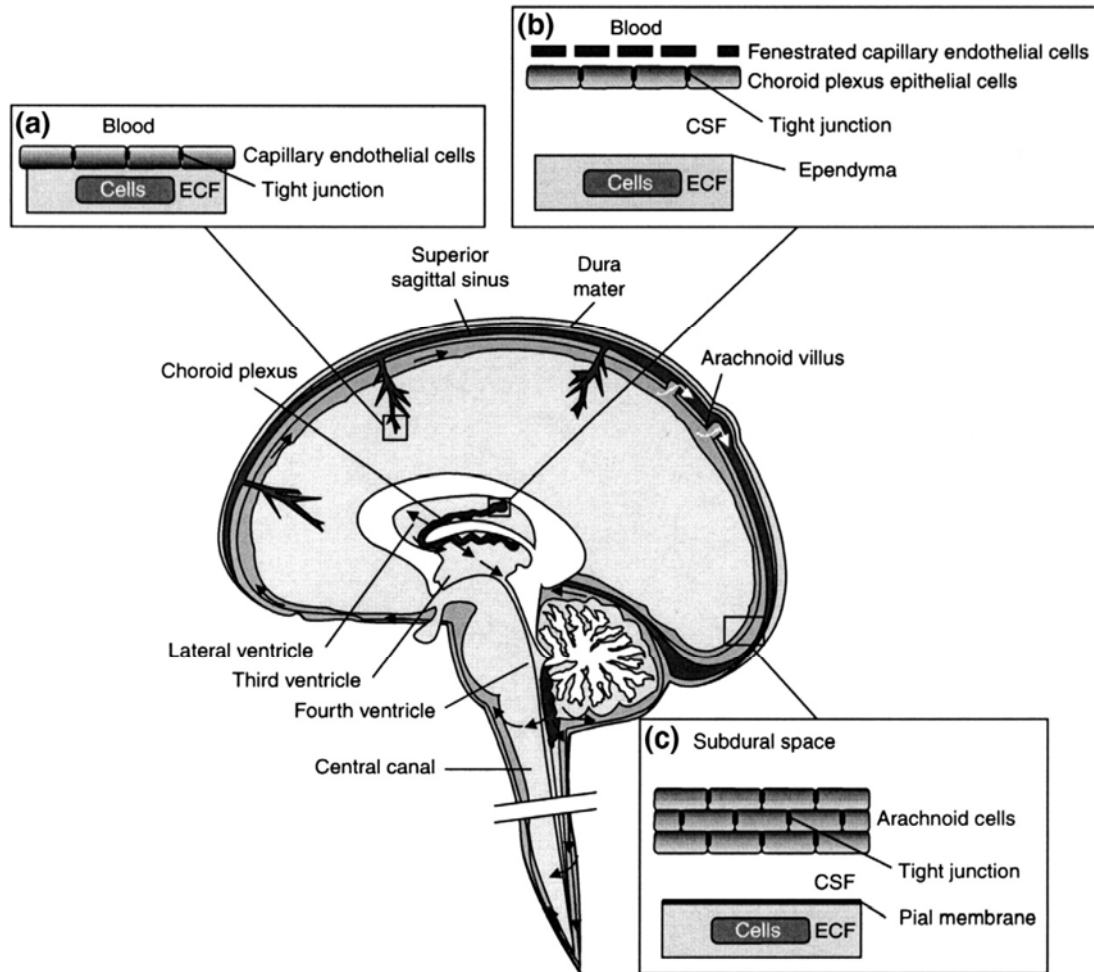


Figure1: The brain interfaces include the following: the blood brain barrier, the blood-CSF barrier, and the arachnoid barrier (17).

The choroid plexus is a structure that is located within the brain ventricles. It is composed of monolayer of epithelial cells. These epithelial cells are derived from the ependymal cells of the brain ventricles (18). Mitochondria are found in the choroid plexus epithelial cells to provide energy that is needed for the active transport and secretion (19). These epithelial cells are connected by the tight junctions in order to limit the paracellular diffusion (20). From the capillaries total surface area in the brain, the epithelial surface area of the microvilli in the choroid plexus is composed of about 25 to 50% of the total surface

area (21) . At the choroid plexuses, the blood flow rate is about five times more than the blood flow rate at other brain regions (20).

The arachnoid barrier limits the exchange between the blood and the CNS because of its avascular epithelium surface and its small surface area (17). The barrier is composed of tight junctions. It functions as a physical barrier by separating the dural layer from the cerebrospinal fluid that is found in the subarachnoid space. It is considered as the most complex barrier among the different barriers of the brain (22-24). The arachnoid barrier is found at the meninges of the brain under the dura layer of the brain (8).

1.2 Neurovascular Unit

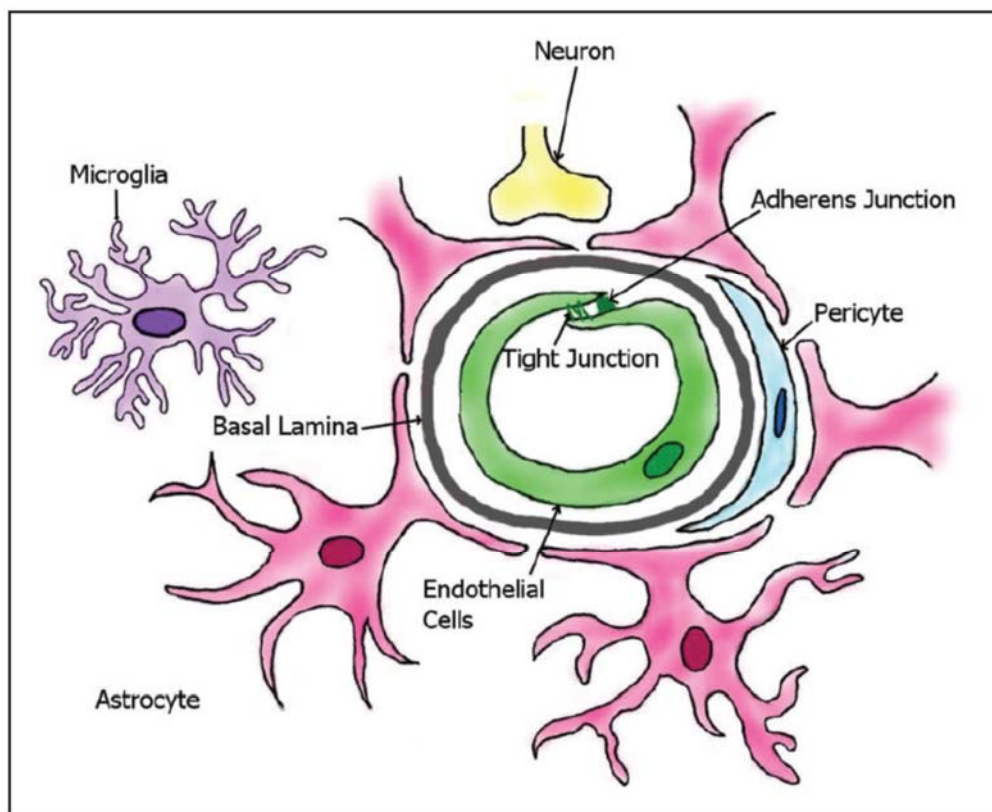


Figure 2: Cellular elements of the BBB (2).

“Modular” Neurovascular unit (NVU) is made of a capillary segment with basal lamina, pericytes, perivascular astrocytes, and microglial cells (16). Also, different neurons types (e.g. noradrenergic, serotonergic, cholinergic, GABAergic) have been observed to be part of the neurovascular unit (25).

1.2.1 Microglia

The first one to describe microglia was the Spanish neuroanatomist Del Rio-Hortega. The microglial cells represent about 20% of the total glial cell population within the CNS (26). The microglial cells are characterized by a small cell body (5-10 μm) and they possess many radial cell processes extending from the cell body. Branched microglia are involved in extracellular fluid cleansing and neurotransmitter deactivation which contributes to the maintenance of homeostasis. Microglial cells lack endocytic and phagocytic activity under normal physiological conditions (27). Diseases or trauma could lead to microglial activation, and this activation is directly correlated to the type and severity of brain injury (28). Activated microglia have a relatively large cell body and short cytoplasmic processes. Activated microglia secrete high levels of neurotoxic mediators such as nitric oxide, peroxide, inflammatory cytokines, proteases and complement components (28, 29). Excessive production of these substances further lead to cell injury in the CNS which in turn leads to astrocyte activation which leads to further microglial activation. That will eventually lead to neuronal cell death (25). Dysfunction of the BBB is characterized by changes in tight junction protein expression and enhanced paracellular permeability which is directly associated with the activation of microglia (30). The microglial functional state determines the expression of ion channels in the microglia (31-34). There are several ion channels in the microglia including multiple potassium, calcium, sodium and chloride

channels (35). In addition, microglia express glutamate receptors (36) and transporters such as GLUT-1 (37). Furthermore, these cells express membrane proteins, which are involved in drug transport. The microglial cells are involved in a variety of physiological functions including proliferation, ramification and maintenance of membrane potential. They are also involved in intracellular pH regulation and cell volume regulation (31-34) .

1.2.2 The Basement Membrane

The basement membrane (BM) is an important component of the neurovascular unit. It surrounds all the cerebral capillaries (38). Collagen type IV, I, fibronectin, thrombospondin (39), laminin, nidogen, heparin sulfate proteoglycans, and agrin (40) are the main components of the basement membrane. There are two types of the basement membrane. The vascular basement membrane and the parenchymal basement membrane. The vascular basement membrane is an extracellular matrix secreted by the endothelial cells and pericytes and it contains laminins $\alpha 4$ and $\alpha 5$. In contrast, the parenchymal basement membrane is secreted by astrocytic processes and it contains laminins $\alpha 1$ and $\alpha 2$ (41, 42). The basement membrane plays an important role as an anchor for signaling processes at the vasculature and it provides an additional barrier for molecules and cells to cross before accessing the neural tissue. BBB dysfunction and leukocyte infiltration during the neurodegenerative diseases can result from the disruption of the basement membrane by matrix metalloproteinases (43).

1.2.3 Endothelial Cells (ECs)

Endothelial cells are simple squamous epithelial cells that line the interior of all blood vessels. They are derived from the mesoderm layer (44, 45). The phenotypic characteristics

of the ECs depend primarily on the location of the ECs. The CNS endothelial cells are very thin cells: they are 39% less thick (46) than the vascular endothelial cells that are found in the skeletal muscle (43). They make the inner walls of the blood vessels by folding onto itself to form the lumen of the vessel. Endothelial cells are considered as the major cell that is responsible for the blood brain barrier integrity. They regulate the CNS homeostasis by providing a combination of a physical barrier, and a molecular barrier. The endothelial cells that forms the BBB are characterized by having a high numbers of mitochondria that are essential to generate ATP in order to transfer the ions across the the cells using transporters. Also, they are characterized by lacking fenestrations in their cell membrane and having a reduced pinocytotic activity. The endothelial cells limit the paracellular movement of solutes at the BBB by forming intercellular tight junctions (22, 47, 48). In addition, they limit the transcellular movement of solutes by limiting the vesicle-mediated transcellular movement of solutes. Furthermore, they express very low level of leukocyte adhesion molecules in order to limit the amount of immune cells that enter the CNS (43, 49, 50). There two main categories of transporters are found in the CNS endothelial cells. At the luminal surface of the endothelia are found the efflux transporters which transport the lipophilic molecules (51-53). Highly specific nutrient transporters are the second type of transporters which transport nutrients across the BBB into the CNS and remove the waste products from the CNS into the blood (54).

1.2.4 Astrocytes

Astrocytes are the most abundant glial cell type in the brain. The astrocytic end feet contain an array of proteins including connexins, dystroclycan, dystrophin, and aquaporin 4 that surround the cerebral capillaries of the brain (43). The close proximity of the

astrocytic end feet to the capillary network and its close relation to the neuron makes the astrocytes participate in a significant role to ensure development and maintenance of the BBB. The astrocytes maintain the metabolic and the nutritive support of the neuron (15). The endfeet of the astrocyte is linked to the basement membrane by the dystroglycan-dystrophin complex by binding agrin (43). This linkage is critical to place aquaporin 4 in a position to regulate water homeostasis in the CNS. Also, astrocytes disperse vascular nutrients away from the blood vessel in support of neuron in that region. Astrocytes induce tight junction formation by secreting soluble factors (15) . Some of the examples of the glial derived factors that are secreted by the astrocytes and result in the induction of the BBB phenotype in endothelial cells include: transforming growth factor (55), anipoetin 1, basic fibroblast growth factor, and glial derived neurotrophic factor (56).

Astrocytes act as a cellular link between the capillaries and the neurons. That link is significant to regulate the contraction/dilation of vascular muscle cells that surround the capillaries by responding to changes in neuronal activity (43). Moreover, astrocytes participate in the regulation of cerebral microvascular permeability via Ca signaling (57, 58). In addition, astrocytes have a high-affinity transporter for glutamate that contributes to maintaining low excitatory neurotransmitter concentrations in the brain. Furthermore, astrocytes act as a secondary barrier for CNS drug permeation by preventing the drug to reach their action site either by sequestering the drug within the astrocyte cytoplasm or by keeping the drugs at the brain extracellular fluids (25).

1.3 Tight Junction

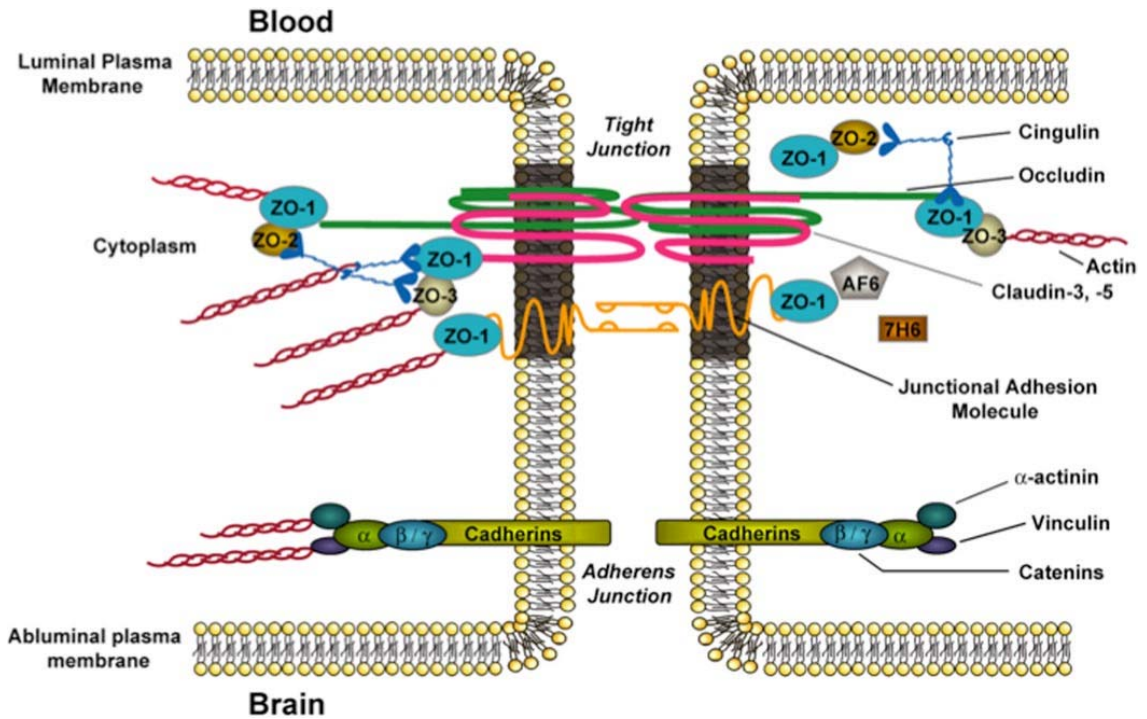


Figure 3: Tight junction proteins (25). ZO-1 stands for zona occludin protein-1. 7H6 stands for cytoplasmic tight junction-associated protein (59). AF-6 stands for afadin (60).

The tight junction is an almost impermeable continuous barrier that interconnects the BBB endothelial cells to prevent the entry of foreign substances with the exception of small lipid-soluble molecules (61). Tight junctions are formed by transmembrane proteins which include occludin, claudins, junction adhesion molecules (JAMs) that are connected to the cytoskeleton through accessory proteins (e.g., zonula occlude 1, 2, and 3) (62).

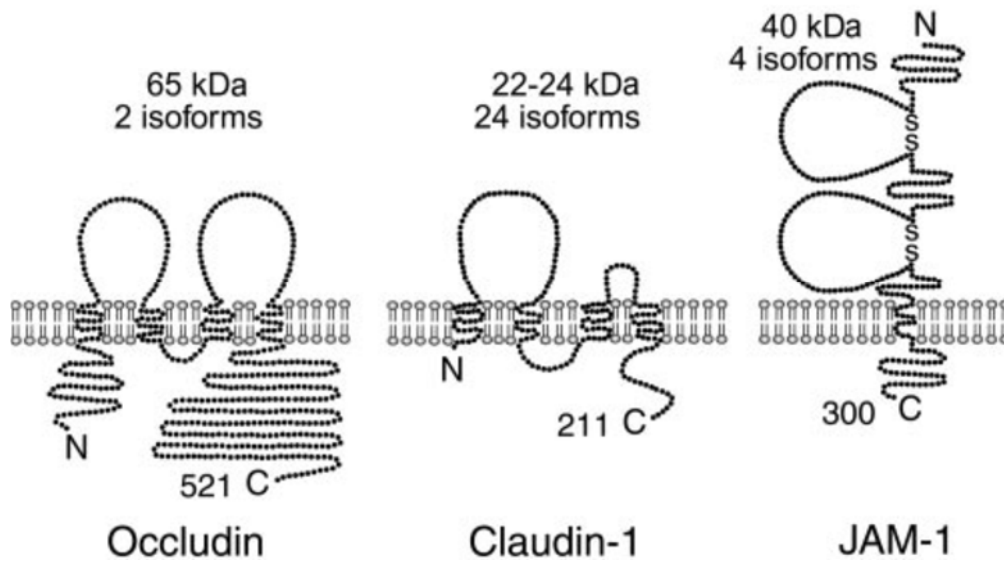


Figure 4: Basic Structure of selected tight junction proteins (63).

Occludin is considered as the first identified membrane protein within the tight junction. It consists of four transmembrane domains, two extracellular domains, and three cytoplasmic domains. It has a molecular weight of 60-65 kDa (64). It has two extracellular loops that span the intercellular cleft and are separated by a short cytoplasmic loop. The amino (N-terminus) and carboxy (C-terminus) are both cytoplasmic terminal domains (65).

Claudins are 20-24 KDa proteins (62). They have a similar basic structure to occludin, with much smaller cytoplasmic chains (65). It forms that primary “seal” of the tight junction (25). Junctional adhesion molecules (JAM) has several isoforms at the BBB including junction adhesion molecules-1 (JAM-1), junction adhesion molecules-2 (JAM-2) and junction adhesion molecules-3 (JAM-3) (62, 66). Junctional adhesion molecules-1 (JAM-1) is 40-KDa, and it play a role in the early developmental stages of the BBB. Junctional adhesion molecules-1 (JAM-1) mediates the early attachment of endothelial cells during the development of the BBB (67). Moreover, it regulates the transendothelial migration of leukocytes during inflammation (66). Loss of junctional adhesion molecules

(JAM) protein expression is correlated with BBB breakdown (68, 69) but it is not a sufficient marker for the BBB breakdown (70).

Accessory proteins including Membrane-associated guanylate kinase-like (MAGUK) family, cingulin, AF-6, 7H6 and EMP-1 (62, 71) are involved in coordination and clustering of tight junction protein complexes to the cell membrane (72). Three proteins of the membrane-associated guanylate kinase-like (MAGUK) family have been identified at the tight junction: ZO-1, -2, and -3. The protein that was directly involved with tight junction complexes is ZO-1 (73). It connects the transmembrane proteins of the tight junction to the actin cytoskeleton (74). In addition, ZO-1 acts as a signaling molecule that communicates the state of the tight junction to the cellular interior (75). ZO-2 is a protein that binds structural tight junction constituents, signaling molecules and transcription factors (76). ZO-3 function is still not known yet (25).

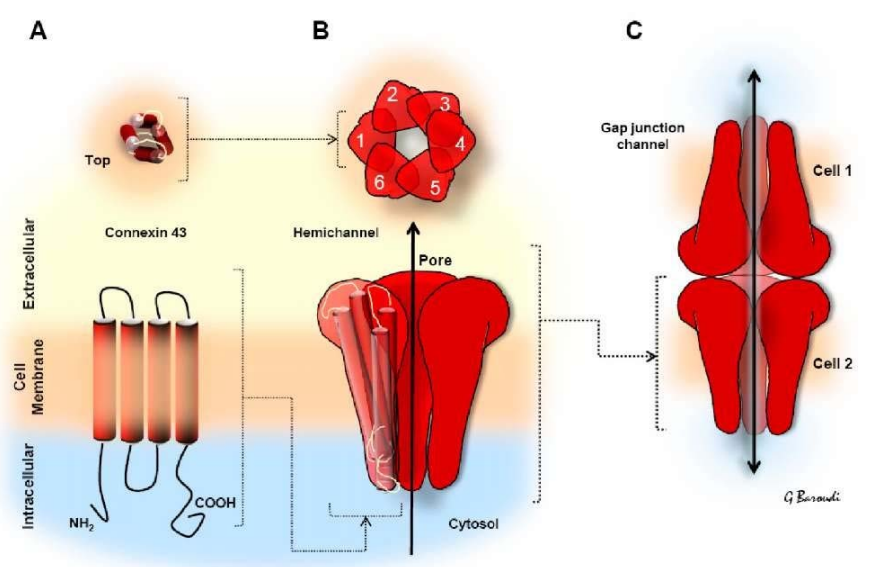


Figure 5: the structure of connexin 43 (77).

Connexins have many different types (at least twenty-one) that are named according to their molecular weights. The above figure represents the structure of connexin 43. About 150 amino acids form the structure of the connexin's C-terminus (78, 79). Arginine, aspartic acid, asparagine, serine and proline are the most common amino acids that are found in the connexin 43. Protein interactions and kinases target the proline and serines composition of the connexin 43 (80). It is made of four transmembrane segments with two extracellular loops and one intracellular loop. Also, two terminals that are found in the cytosol: an amino terminal and a carboxy terminal that has multiple phosphorylation sites as figure shows it. Hemichannel is formed by six connexin that surrounds the aqueous pore. Two hemichannels form the gap junctions (77). Cell to cell communication occurs through gap junction (81) that allows cytoplasmic contents to pass through the opening of the hemichannels to the extracellular fluid. Gap junctions are considered as a dynamic structure because of cell ability to modify the number of the gap junctions through connexins biosynthesis, degradation and endocytosis (81). Some of the integral membrane proteins show half-lives of more than 75hrs (82, 83). In contrast, some other integral membrane proteins has a half-life of less than 5hrs (82-84). Regarding connexin degradation, it has a half-life of 1.5-5 hours. It shows that half-life in both vivo and in cultured cells (85-87).

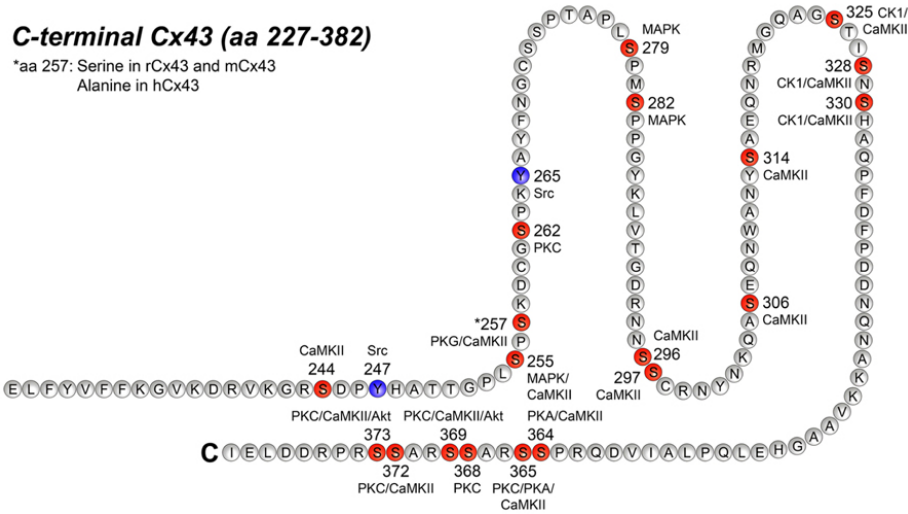


Figure 6: phosphorylation sites at the connexin carboxy terminus (88).

1.4 Transport across the BBB

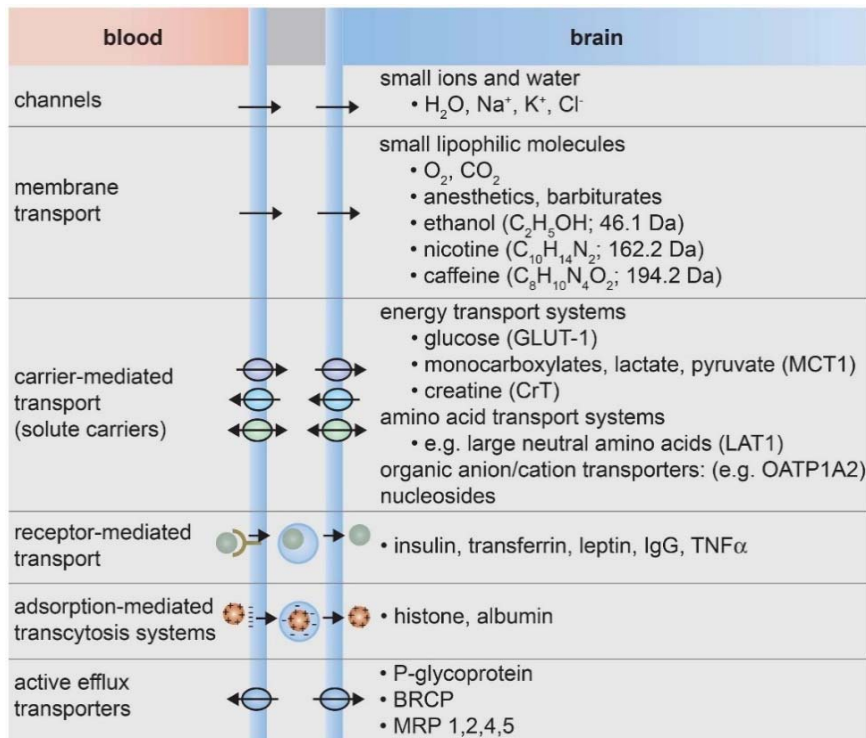


Figure 7: Transport across the BBB (89).

There are several ways to transport across the blood brain barrier. Passive diffusion (membrane transport in Figure 5) is for small lipophilic molecules with a molecular weight less than 500 Da (90, 91). An example of small molecules that passively diffuse through the cell membrane are barbiturates, ethanol, and caffeine. Also, gaseous lipophilic molecules can diffuse through the cell membrane such as O₂ and CO₂ (92, 93). Carrier-mediated transport is for small polar molecules, such as glucose, amino acids, organic anions and cations, and nucleosides (94). Large molecules and 98% of all small molecules do not cross the BBB (92, 93). Previous studies have shown that catecholamines do not cross the blood brain barrier (95).

1.5 BBB Disruption

Any disturbance to the function of these proteins will result in destabilizing the junctions, and it will enhance the paracellular diffusion. In the basal region of the lateral plasma membranes, there are adherens junctions below the tight junctions. Catenins connect cadherins to the cytoskeleton, and cadherins stabilize adhesion between basal endothelial cells in the adherens junctions.

Any disruption to the blood brain barrier permeability could lead to many central nervous system diseases such as Alzheimer's disease, amyotrophic lateral sclerosis, cerebrovascular disease (e.g. stroke), epilepsy, seizures, brain infection, meningitis, inflammatory disease, brain tumors, neurotrauma (89). Changes in ion balance, disrupting transport systems, and alternating the enzymatic barrier from being effective could be the results from BBB dysfunction. The blood brain barrier has tight junctions which limits the entry of certain molecules such as polar molecules and large molecules. Also, it limits

the entry of solute carrier protein along with ectoenzyme and endoenzyme that is found inside the endothelial cells. Therefore, it functions as an enzymatic (metabolic barrier) (16).

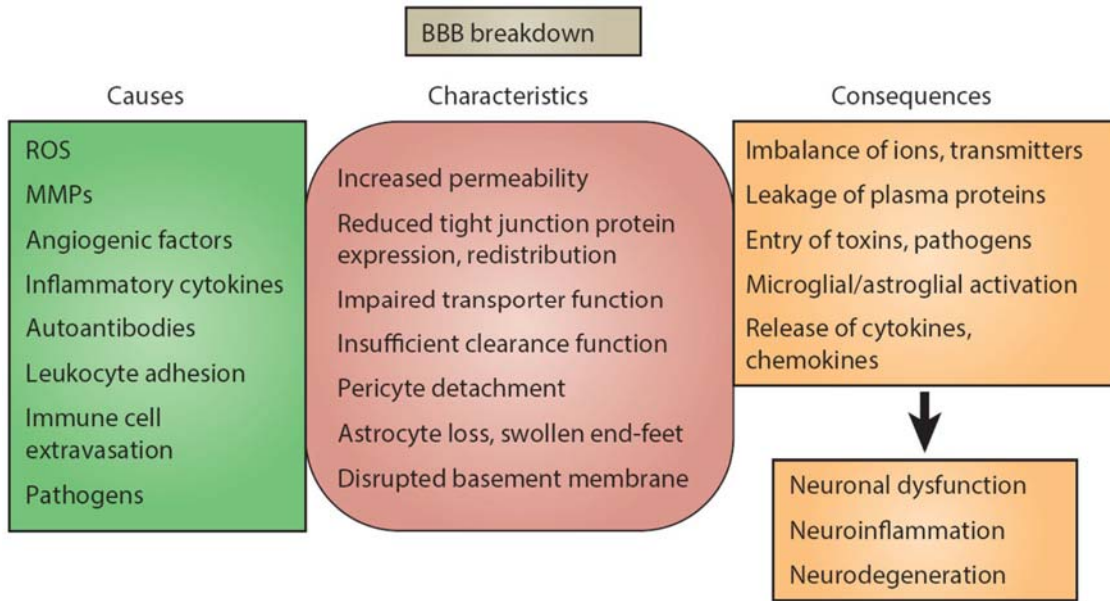


Figure 8: causes, characteristics, and consequences of BBB breakdown (5).

As the above figure shows that there are several factors that could lead to the blood brain barrier breakdown. Examples for the different causes that could cause the blood brain barrier permeability include the following: reactive oxygen species, matrix metalloproteinases (MMPs), angiogenic factors, inflammatory cytokines, autoantibodies, leukocyte adhesion, immune cell extravasation and pathogens. The characteristics of the blood brain barrier breakdown include the following: increased permeability, reduced tight junction protein expression and redistribution, impaired transporter function, insufficient clearance function, pericyte detachment, astrocyte loss and a disrupted basement membrane. The blood brain barrier breakdown leads to the following: imbalance of ions, leakage of plasma protein, entry of toxins, microglial activation and release of cytokines

and chemokines. That will eventually lead to neuronal dysfunction, inflammation and degeneration.

Previous studies have indicated that it is not certain yet that the blood brain barrier disruption is always caused by or a consequence of the oxidative stress (5). Nevertheless, some neurological diseases have blood brain barrier disruption associated with oxidative stress such as stroke, multiple sclerosis (MS) and amyotrophic lateral sclerosis (ALS) (96-98). Oxidative stress refers to having many reactive oxygen species (ROS) that are more than necessary or required, possibly because of a damaged intrinsic antioxidant defense system. There are several mechanisms by which elevated reactive oxygen species could lead to the BBB dysfunction. One of the mechanisms is that the reactive oxygen species could cause destruction and damage to the cellular molecules such as proteins, lipids and DNA. Other mechanisms include the following: increasing the response to the inflammatory mediators, damaging the tight junction proteins, causing cytoskeletal reorganization and causing the activation of the matrix metalloproteinases (MMPs) (99).

Blood brain barrier disruption could lead to an abnormal neuronal activity that is caused by the imbalance of certain molecules in the interstitial fluid (e.g. ions, transmitters and metabolic products). An example of this situation occurs in seizures. Several neurological diseases have seizures such as epilepsy, central nervous system infections, stroke and neurodegenerative diseases (100). It is not known yet if epilepsy is a cause or a consequence of damaged blood brain barrier (101). Inflammation could lead to neurological diseases by causing a blood brain barrier disruption. An example of this situation is the neurological disease neuromyelitis optica (NMO). It is an inflammatory

disease that attack the central nervous system. It mainly affects the spinal cord and the optic nerve (102).

The table below lists the blood brain barrier disruption as either a primary or a secondary result of certain diseases.

Diseases linked to BBB dysfunction

Disease	Level of BBB effect	Comment
Stroke	Primary	Microvascular injury induced by oxidative stress during ischemia/reperfusion
Epilepsy	Primary	Systemic inflammation can disturb brain homeostasis by allowing entry of ions and epileptogenic substances across the BBB
	Secondary	Seizures reduce BBB integrity, which enables entry of plasma proteins into the brain that sustain the epileptogenic state
AD	Primary	BBB dysfunction, including defective amyloid-beta clearance from brain and congophilic angiopathy
Familial ALS	Primary	Loss of BBB integrity at an ultrastructural level, associated with expression of mutant SOD1 in brain capillary endothelial cells
PD	Secondary	Increased BBB permeability and decreased transport activity across the BBB, including inefficient efflux of toxic molecules via P-glycoprotein
MS	Secondary	Extravasation of autoreactive T cells and monocytes across a compromised BBB
Natalizumab- ab-PML with IRIS	Secondary	Infiltration of T cells in perivascular space and parenchyma after discontinuation of Natalizumab in context of PML

Disease	Level of BBB effect	Comment
NMO	Primary	BBB breakdown including loss of AQP4 and of astrocytes caused by AQP4-IgG
Primary CNS vasculitis	Primary	Inflammation of cerebral vessels without systemic disorder
Secondary CNS vasculitis	Primary	Inflammation of cerebral vessels associated with systemic inflammatory illness
VZV vasculopathy	Primary	Viral infection (primary or upon reactivation) of cerebral arteries
Cerebral malaria	Primary	Sequestration of parasitized red blood cells in lumen of cerebral microvasculature
Primary CNS lymphoma	Secondary	Leaky angiogenic vessels in malignant tissue
Glioblastoma	Secondary	Leaky neo-angiogenic vessels and loss of BBB integrity in pre-existing vessels (by subcellular mislocalization of astroglial AQP4) in malignant tissue
PRES	Primary	Vascular injury by systemic influence, such as disorders of clotting or bleeding, and chemotherapy agents (particularly those which inhibit VEGFR kinase)
TBI	Secondary	Mechanical disruption of BBB followed by post-traumatic BBB dysfunction
Migraine	Secondary	Cortical spreading depression with subsequent vascular reaction
Diabetes	Secondary	Increased BBB permeability, possibly leading to cognitive impairment

*Primary level of BBB effect indicates that the cerebrovasculature is probably compromised upstream from CNS pathogenesis whereas secondary level of BBB effect is interpreted as happening downstream from the initial insult and aggravating disease.

AD, Alzheimer’s disease; ALS, Amyotrophic lateral sclerosis; PD, Parkinson’s disease; MS, Multiple sclerosis; PML, Progressive multifocal leukoencephalopathy; IRIS, Immune reconstitution inflammatory syndrome; NMO, Neuromyelitis optica; VZV, Varizella zoster virus; PRES, Posterior reversible encephalopathy syndrome; TBI, Traumatic brain injury

Table 1: Diseases and blood brain barrier disruption (5).

Table 2. Changes in the BBB constituents with aging (2).

BBB elements	Properties
ECs	<i>Capillary wall thickness:</i> increased in humans decreased in rats decreased in monkeys <i>Number of ECs:</i> decreased in humans <i>Number of mitochondria:</i> decreased
Tight junctions	<i>Expression of tight junction proteins:</i> decreased
Basal lamina	<i>Thickness of basement membrane:</i> Increased <i>Concentration of collagen IV and agrin:</i> Increased <i>Concentration of laminin:</i> decreased
Astrocytes	<i>Astrocyte proliferation:</i> Increased number and size <i>GFAP expression:</i> Increased
Microglia	<i>Changes to amoeboid morphology</i> <i>Production of neurotoxic proinflammatory mediators</i>
Pericytes	<i>Number of pericytes:</i> Degeneration and loss of pericytes <i>Ultrastructural changes:</i> vesicular and lipofuscin-like inclusions, increased size of mitochondria, foamy transformation
Neurons	<i>Deterioration of synaptic plasticity</i> <i>Deficit in long-term potentiation</i> <i>Impaired neurogenesis.</i> <i>Increased apoptosis,</i> <i>Neuronal damage due cytokine release</i>

The above table lists the changes that occur in the blood brain barrier permeability with aging (2). We see that the tight junction proteins are decreased with age. Also, we noticed more neuronal damage with age caused due to cytokine release. Most of the animal models used in the above table were mice.

1.6 Fluoxetine

Fluoxetine is (R, S)-N-methyl-3-phenyl-3-(4-(trifluoromethyl) phenoxy) propan-1-amine. It is the first selective serotonin uptake inhibitor approved by the United States Food and Drug Administration (FDA)(103). It is used to treat diseases that are related to the Central Nervous System. For examples, it is used to treat major depressive disorder, obsessive-compulsive disorder, acute depressive episodes in Bipolar I disorder, panic disorder bulimia nervosa, and premenstrual dysphoric disorder (104),

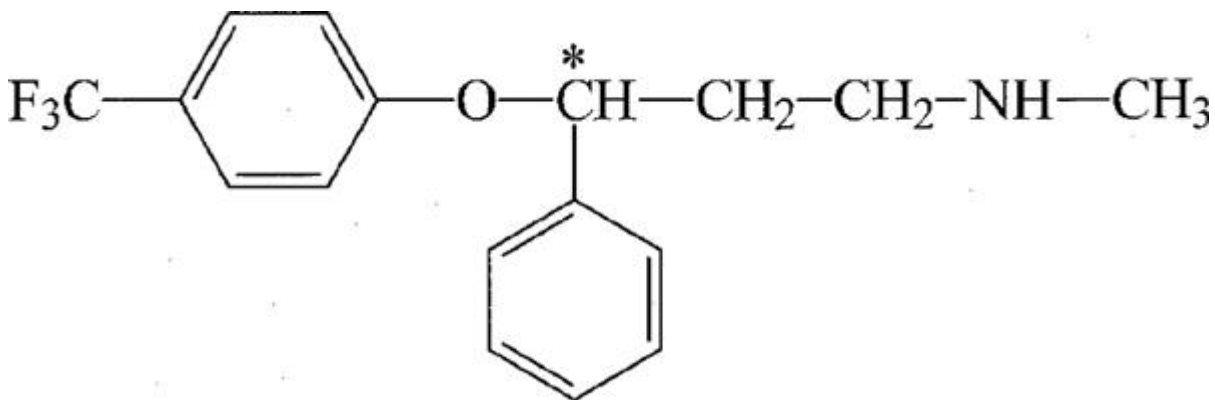


Figure 9: Chemical Structure of Fluoxetine (105).

1.6.1 Fluoxetine Metabolism

Fluoxetine has the largest volume of distribution among SSRI drugs. Fluoxetine has a long half-life and low plasma protein binding. It takes between 1 and 22 months to achieve steady state due to its long half-life according to depression studies. Also, it is

almost completely absorbed following oral administration. High performance liquid chromatography (HPLC) was used to detect the presence of fluoxetine and its active metabolites in the serum and the brain of the Sprague Dawley rats after drug ingestion (106, 107).

Fluoxetine is metabolized in the liver by cytochrome P450 that results in forming different metabolites.

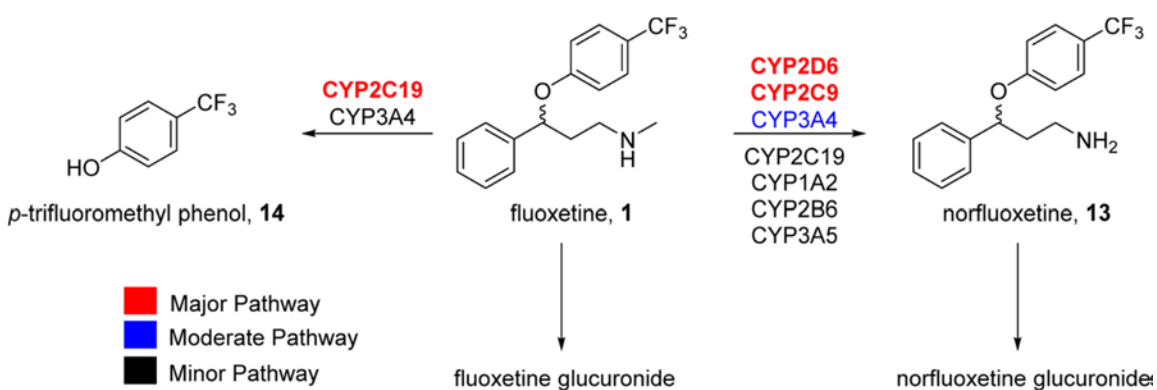


Figure 10: Structures of the oxidative and conjugative metabolites of fluoxetine. The major metabolite is norfluoxetine, equipotent to fluoxetine for the S-enantiomer but with a significantly longer half-life than fluoxetine 1. The phenolic metabolite is inactive. The single enantiomers (S)-1 and (R)-1 showed divergent 2D6 metabolism (108) .

Fluoxetine is excreted as either norfluoxetine or as fluoxetine glucuronide or norfluoxetine glucuronide. The norfluoxetine metabolite is formed mainly by CYP2D6 while the inactive phenolic metabolite 14 is formed by CYPs 2C19. Norfluoxetine is pharmacologically similar to fluoxetine for the S-enantiomer, but not the R-enantiomer, yet it has a longer half-life (4-16 days). Fluoxetine is both a substrate and an inhibitor of CYP2D6 while norfluoxetine is both substrate and an inhibitor of CYP3A4. Both

Fluoxetine and norfluoxetine have R and S enantiomers. (S)-fluoxetine is 1.5 times more potent than (R)-fluoxetine while (S)-norfluoxetine is 5 to 20 times more potent than (R)-norfluoxetine (108).

1.6.2 Fluoxetine Effect on Microglial cells

Neuroinflammation involves microglial activation (109). Pro-inflammatory factors which include reactive oxygen species, chemokines and cytokines are secreted during microglial activation. Neuronal damages occur due to the accumulation of the previous pro-inflammatory factors. Toxic soluble factors get released from the damaged neurons. These toxic soluble factors amplify microglial activation. Hence, preventing the microglial activation that is associated with neuroinflammation represent a therapeutic potential to the neurological disorders that are caused by neuroinflammation. Fluoxetine has an important role in neuroprotection. It inhibits the release of a microglial transcription factor, NF-KB that results in the production of cytotoxic factors and proinflammatory factors. In addition, fluoxetine decreases the morphological changes that are associated with activated microglia. These changes involve a larger cell body, irregular shapes and thicker processes (110). The fluoxetine exert its effect though affecting the immune system. It activates M2 through IL-4 induction and inhibits M1 through LPS + INF induction (111).

1.7 HYPOTHESIS

In this study, we predict that aging will cause more neurodegenerative diseases by increasing the blood brain barrier permeability. Also, we expect that certain drugs such as fluoxetine will change the blood brain barrier permeability by either making it tighter or

by increasing its permeability. Each enantiomer of fluoxetine will have a different effect on the permeability of the blood brain barrier. We expect that our results will match the results of the stroke study. In stroke animals, our lab saw that R-fluoxetine is increased the permeability while S-fluoxetine is decreased the permeability of the blood brain barrier. However, this will be the first test of these enantiomers in a normal, uninjured brain. The research study that was conducted by Dr. Debra's Mayes by using an artificial blood brain barrier found that R-fluoxetine tighten the blood brain barrier while S-fluoxetine loosen the blood brain barrier.

1.7.1 Specific Aims

Specific Aim 1: The main aim of this study is to test the effect of Prozac enantiomers (R-fluoxetine and S-fluoxetine) on the blood brain barrier permeability in different brain regions (cortex, hippocampus, striatum-caudate putamen-hypothalamus (brain), and the cerebellum). We chose the cortex and the hippocampus regions because they are aged related regions that are associated with neurodegenerative diseases such as Alzheimer. Previous stroke studies have chosen cerebellum region to study.

Specific Aim 2: We will determine if there are age and gender difference in the blood brain barrier permeability across the different tested brain regions among the males (at different ages) and females rats (at an older age). Males and females animals showed no difference in blood brain barrier permeability as previous studies have shown (112). During this study, we did not have enough funding to include young females.

Specific Aim 3: We are comparing the results of this study in the discussion with previous studies that have been conducted on stroke injured animals, to examine changes in normal versus injured brains.

II. MATERIALS AND METHODS

2.1 Voluntary Drug Administration

The purified R-enantiomer and S-enantiomer of 5mg/kg fluoxetine have been given to the Sprague Dawley rats. Also, its 50/50 combined racemic mixture (trade name Prozac) has been given to the young male rats at a dosage of 5mg/kg. Prozac was purchased from a pharmacy while the enantiomers of fluoxetine were purchased from Sigma-Aldrich. The drug Prozac is a combination of 50:50 R-fluoxetine/S-fluoxetine. Studies have shown that subcutaneous drug administration could increase the level of stress to the animal by increasing the level of stress hormones such as corticosterone, particular if the drugs need to be administered on a daily basis (113). In order to reduce the amount of stress that the animals might experience during this study, the medicine was delivered to the animal encased in sugar cookie dough that weighted about 4 grams. The control animals were only given the cookie dough without medicine. Each animal received the drugs for a total of 3 days and were euthanized on the fourth day.

The animals were injected ip with sterile 2% Evans blue in PBS (1 ml for young animals; 2.5 mls for old animals) late on the third day of drug administration. During this study, we had to give the animals the medicine first then injecting them with Evan's blue because the animals did not eat their medications if they were given Evans' blue dye first. After 12-16 hours later, the animals were euthanized, and cardioperfused.

In order to avoid bias, randomization and blinding were applied during this study (114). During this study, I did not know any information about the animal except their numbers.

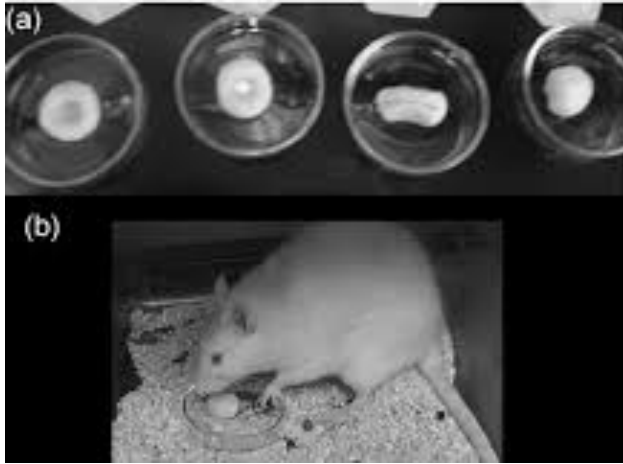


Figure 11: method for voluntary drug administration (113).

2.2 Euthanization

Intraperitoneal injection of Euthasol (100 mg/kg pentobarbital) was performed in order to euthanize the animals. The tail-pinch method was applied to check the consciousness of the rat. When the animal reached the stage of surgical anesthesia by showing no pain reflexes, the animal was ready to go through the cardioperfusion procedure.

2.3 Cardioperfusion

An incision was made at the diaphragm region extended to the upper thorax. We basically removed a flap of the ribs covering the heart, so that the heart was fully exposed. Then, a hemostat was placed at the apex of the heart and loosely held. A scissor was used to cut the apex heart muscle held in the hemostat, and a cannula was pushed through into

the left ventricle. After the perfusion needle (cannula) was inserted into the apex of the heart, the hemostat was clamped. The perfusion needle was supplied with ice cold phosphate buffered saline (PBS). The heart was slightly tilted toward the left to locate the thinner right ventricle. Then, a cut was made at the right atria to let the blood flow out of the body of the rat.

Brain Dissection

Once perfusion is completed, generally after 150 mls of buffer is passed through the heart, we see a change in the color of the liver to a lighter color. The head of the rat was decapitated. Then, the skin that covered the skull was removed starting from the base of the skull near the spinal cord. A smooth curved rongeurs was slid under the skull bone, around the midline of the skull. Then, it was lifted away from the brain to remove the skull, and we made sure not to damage the brain tissue. A curved spatula was placed under the anterior of the brain, near the olfactory bulbs and then the brain was lifted upward. The optic nerves were cut and the brain was removed from the head of the rat. A microtome blade was used to dissect the brain sections.

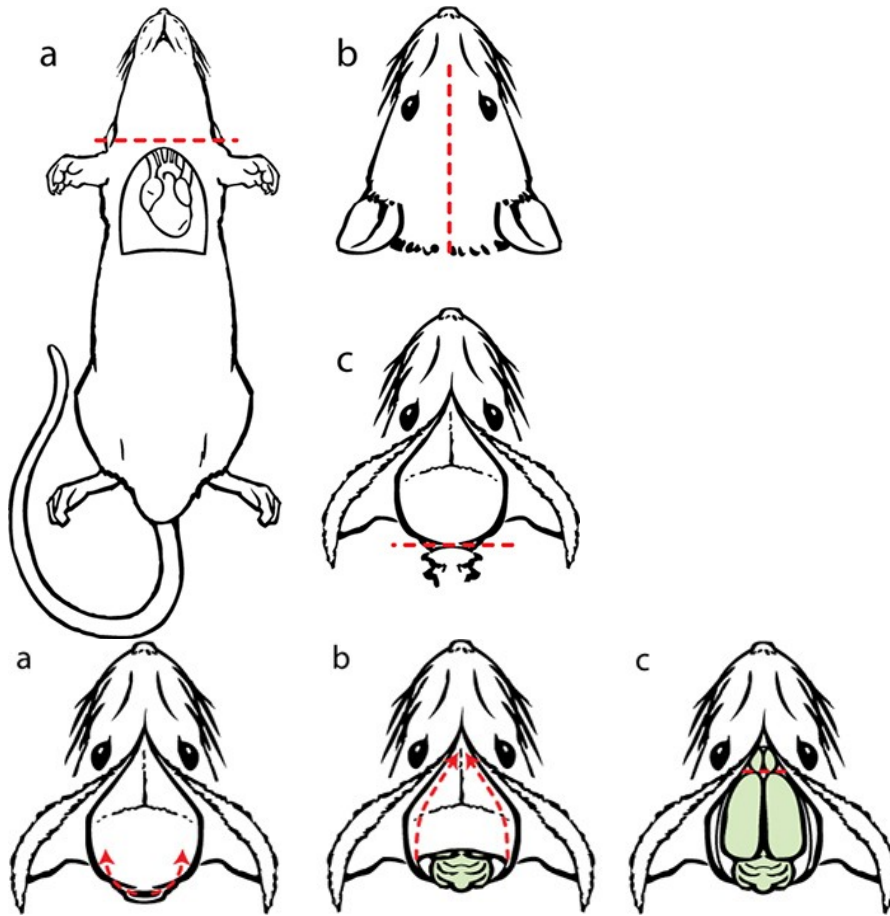


Figure 12: Steps to dissect the rat brain (115).

The dissected brain sections, including the cortex, the peri-ventricular and hippocampus region, the lower brain region (composed of the striatum-caudate putamen-hypothalamus) and the cerebellum, were individually placed in a beaker filled with dry ice and isopentane for about 10 sec to quick freeze the brain sections. The vials with these quick frozen brain sections were weighed while they were empty and weighed again with the brain tissue in order to find the weight (mg) of the dissected brain tissue.

Evans Blue Protocol

A 50% trichloroacetic acid (TCA) stock solution is prepared by mixing 10 ml of cerebrospinal fluid (ACSF) with 5 grams of TCA. Brain tissues were homogenized in 1:3 ACSF: TCA stock which was prepared by adding 375 μ l of TCA stock solution and 125 μ l of ACSF to every single brain section. Then, they were spun at 10,000 relative centrifugal force for 20 minutes. The pellets and the supernatants were separated and have been collected into different vials, and they were kept at the freezer with -80 degree Celsius.

Calibration Curve Solutions Preparations

Two stocks solutions were prepared in order to prepare the calibration standard. The first stock solution is the 1:3 TCA solution which was prepared by mixing 1.25 ml of the ACSF with 3.75 ml of TCA stock, described above. The second stock solution was 1 mg/ml Evans blue (for Evans blue calibration curve) or 1 mg/ml bovine serum albumin (BSA; for protein assay) dissolved in the 1:3 TCA solution (calibration stock).

Four test tubes were labeled with 0 μ g/ml, 2 μ g/ml, 5 μ g/ml, and 10 μ g/ml sequentially. Then, 1ml of 1:3 TCA stock solution was added to the first tube, 2 μ l of 1 mg/ml Evans blue stock with 998 μ l of 1:3 TCA were added to the second tube, 5 μ l of 1 mg/ml Evans blue stock with 995 μ l of stock 1:3 TCA were added to the third tube, and 10 μ l Evans blue with 990 μ l of 1:3 TCA were added to the last tube. Then, the test tubes were mixed well and vortexed. These were the calibration curve stocks for Evans blue assay.

Microtiter plate Preparation

Supernatants and homogenized pellets from each brain sample (four different regions for each animal) were read using a microtiter plate. An empty blank sheets were filled with the numbers and the labeling of the brain tissues in order to help with filling out the real microtiter plate, using 3 replicates for each sample. Then 30 μ l of each the calibration stocks and each sample of the brain (supernatant or homogenized pellet) were added to the microtiter plate (3 replicate wells for each). Later, 90 μ l of 95% ethanol was added to each well on the plate. The plates were taken to a spectrofluorometer microtiter plate reader in order to be read. The fluorescence values for the spectrophotometer were 620nm for the excitation value and 680nm for the emission value. In order to determine the number of nanograms of evans blue detected per milligram of brain tissue is available, the standard calibration curve was analyzed for its slope and y-intercept. These values were used to determine the number of nanograms of evans blue in each 30 ul brain sample, using the formula:

$$Ng\ Evans\ blue = (average\ brain\ sample\ fluorescence - y\ intercept) / slope.$$

2.4 Pellet Homogenization

Two rat brain sample pellets were homogenized at the same time. First, 0.5 ml of phosphate buffered solution (PBS) was added to the pellet. Then, the each pellet was ground by using the PTFE pestle. Next, the pellet was homogenized by using a Tissumizer rotor. After that, the pellet's solution was transferred to a Dounce tissue grinder in order to be thoroughly homogenized, breaking up all clumps of tissue. Later, another 0.5 ml of PBS was added and the homogenized pellet was mixed by using the Tissumizer. After the pellet is completely homogenized in a total of 1ml PBS, it was transferred with to a new vial and labeled.

2.5 Bradford Protein Assay

Bradford Solution Preparation

Bradford solution is prepared in steps: in the first step 100mg of Coomassie blue G is mixed with 850 ml of distilled water overnight. That solution should be dark in color due to the presence of Coomassie blue. In the second step, 50 ml of ethanol is added to the solution and it will cause the solution to turn bright blue. Finally, 100 ml of phosphoric acid (85%) is added to the solution and the solution is expected to turn brown.

Calibration Standard Stocks Preparation

Six test tubes will be labeled with the following numbers: 0 $\mu\text{g/ml}$, 1 $\mu\text{g/ml}$, 2 $\mu\text{g/ml}$, 5 $\mu\text{g/ml}$, 10 $\mu\text{g/ml}$, and 20 $\mu\text{g/ml}$. Then, 1ml of distilled water is added to the 0 $\mu\text{g/ml}$. Then, 20 μl of BSA with 980 μl were added to the 1 $\mu\text{g/ml}$ labeled tube. Next, 40 μl of 1mg/ml BSA with 960 μl distilled water were added to 2 $\mu\text{g/ml}$ labeled tube. Later, 100 μl of 1mg/ml BSA with 900 μl of distilled water were added to the 5 $\mu\text{g/ml}$ labeled tube. After that, 200 μl of 1mg/ml BSA with 800 μl of distilled water were added to the 10 $\mu\text{g/ml}$ labeled tube. Finally, 400 μl of 1mg/ml BSA with 600 μl distilled water were added to the 20 $\mu\text{g/ml}$ labeled tube.

Pellets Dilution Preparation

At least two dilutions of each pellet were prepared for protein determination. The dilution factor was determined based on the amount of the protein that was present in the vial. Most of the time the dilution was 1:2 and 1:4 for the cortex, striatum-caudata putamen and the cerebellum. For the peri-ventricular and hippocampus, the dilution was 1:1 and 1:2.

All brain pellets were homogenized into 1 ml of PBS before they were assayed for protein content.

The 1:2 dilution stock was prepared by adding 75 μ l of the homogenized pellet sample with 75 μ l of PBS while the 1:4 dilution was prepared by adding 50 μ l of the homogenized pellet sample with 150 μ l of the PBS. Then, 50 μ l of pellet dilution stock was added to each of the two test tubes label with 1:1 dilution. After all the tubes are completed, 50 μ l of water was added to all the tubes. Two replicated was prepared for each tube from the calibration stock solution by taking 50 μ l from the calibration stock solution. Then, 50 μ l of PBS was added to each replicate to ensure that the chemical composition of the protein in the standards and the protein in the samples is matched. Later, Bradford solution was added to all of the test tubes. About 30 mins had passed until the spectrophotometer reading were taken. First the blank test tube is placed inside the spectrophotometer. While placing the spectrophotometer on transmission, the spectrophotometer was zeroed by blocking transmission and then full transmission was set to 100. Following this, the spectrophotomer was set to absorbance at 595 nm, and each tube was read.

2.6 Animal Model

Sprague-Dawley rats males and females were used during this research study. Young rats weighed 100gm (1.5 months) while the old male rats weighed about 500 grams (10-12 months) and old female rats weighed about 300 grams. The rats were kept in cages provided with water and ad libitum food. The animals were obtained from the laboratory animal resource department. The research study was conducted in accordance with the federal guidelines for the care and use of laboratory animals for scientific purposes.

2.7 Statistical Analysis

Graph prism 7 software was used to determine the statistical differences between the groups. One-way and two-way ANOVA were the statistical methods that have been used in this research study. ROUT analysis was used to identify outliers.

III. Results

In Table 1, the animal treatment groups used in this study are shown, with the amount of drug they were given by voluntary oral administration for three days, and the abbreviation that is used for that group. On the third day, after drug administration, animals were injected ip with Evans blue and were euthanized and cardioperfused approximately 16-20 hours later. Since we only used Prozac in the young rats, we will only compare it to the enantiomers of fluoxetine and the control in the young rats. Also we do not have a young rat control for the female rats, so we will only compare male old rats with female old rats to analyze for gender differences

Animal Age and Gender	Drug Treatment	Abbr.
1.5 month male rats	Control	CYM
1.5 month male rats	5 mg/kg S-fluoxetine	SYM
1.5 month male rats	5 mg/kg R-fluoxetine	RYM
1.5 month male rats	5 mg/kg Prozac	PYM
10 month male rats	Control	COM
10 month male rats	5 mg/kg S-fluoxetine	SOM
10 month male rats	5 mg/kg R-fluoxetine	ROM
10 month female rats	Control	COF
10 month female rats	5 mg/kg S-fluoxetine	SOF
10 month female rats	5 mg/kg R-fluoxetine	ROF

Table 3: Abbreviations for the animals age, gender and drug treatments that have been used in this study.

3.1 Young Male Rats

One Way ANOVA of Total ng EB/mg Protein

In the next set of figures, we presented the total ng Evans blue per protein (mg) for the different young male groups (the control young male, the young male that have taken R-fluoxetine and the young male that have taken the S-fluoxetine). The data was normalized by dividing the total amount of Evans blue in ng per the amount of protein concentration in mg that was determined by using the Bradford protein assay.

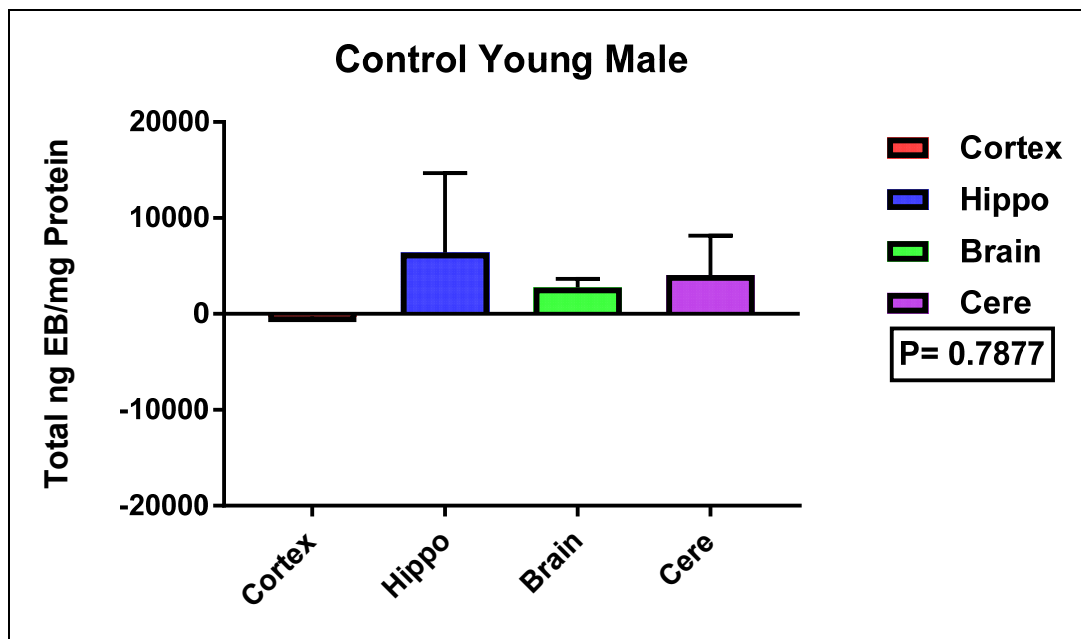


Figure 13: Young male rats that have not taken any drug (Control Young Male). The x-axis represents the different brain regions: the red color represents the cortex, the blue color represents peri-ventricular and hippocampus, the green color represents the striatum-caudate putamen-hypothalamus (brain), and the purple color represents the cerebellum. The y-axis represents the total ng EB/mg protein. One-way ANOVA was

performed. Columns represent the mean for each group and error bars show standard error of mean (SEM). $P = 0.7877$. The animal number, $n = 10$.

Figure 13 shows that there was no significant difference between the different brain regions ($P = 0.7877$). The cortex showed the lowest blood brain barrier permeability among the different brain regions. The mean \pm the standard error of the mean (SEM) for the different brain regions are as follow: cortex: -246.7 ± 379 , peri-ventricular and hippocampus: 6386 ± 8309 , striatum-caudate putamen-hypothalamus (brain): 2755 ± 908.5 and the cerebellum: 4048 ± 4099 . Outliers were determined by ROUT software at medium setting. In the hippocampus region the outlier: 80868.926 was located while 40375.985 was located in the cerebellum.

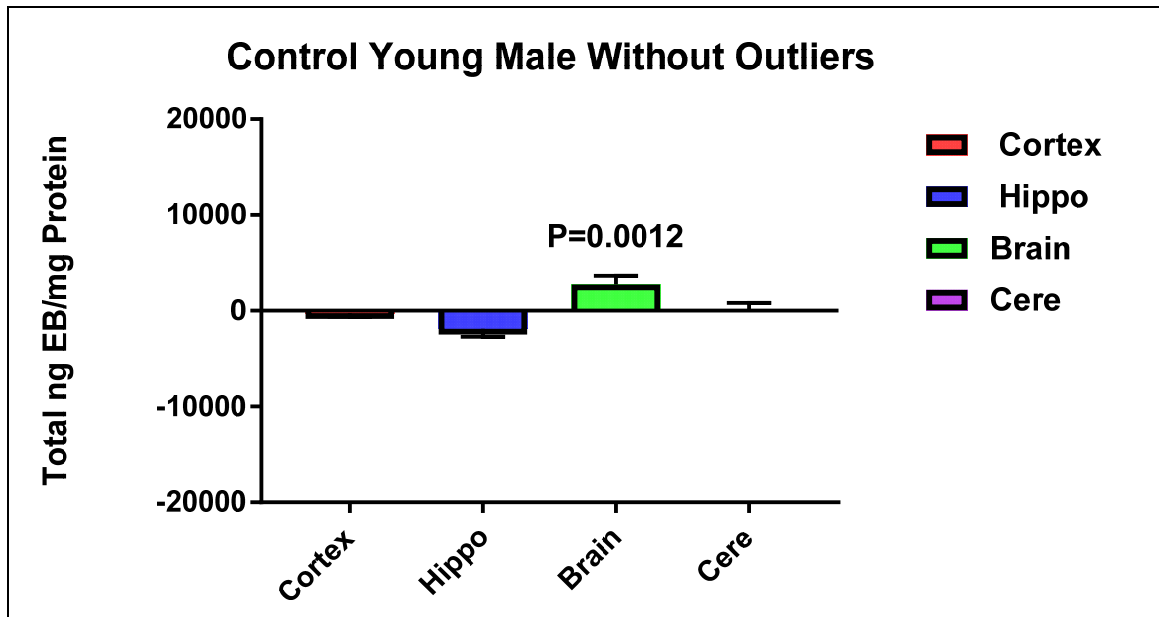


Figure 14: Young male rats that have not taken any drug (Control Young Male) without outliers. The x-axis represents the different brain regions: the red color represents the cortex, the blue color represents peri-ventricular and hippocampus, the green color represents the striatum-caudate putamen-hypothalamus (brain), and the purple color

represents the cerebellum. The y-axis represents the total ng EB/mg protein. One-way ANOVA was performed. Columns represent the mean for each group and error bars show standard error of mean (SEM). $P= 0.0012$. The n for the animal groups are as follow: the n for the cortex =10, the n for the hippo = 9, the n for the lower brain =10 and the n for the cerebellum =9.

Figure 14 shows that there was a significant difference between the different brain regions ($P= 0.0012$). The brain region (striatum-caudate putamen-hypothalamus) showed the highest blood brain barrier permeability among the different brain regions. The mean \pm the standard error of the mean (SEM) for the different brain regions are as follow: cortex: -246.7 ± 379 , peri-ventricular and hippocampus: -1890 ± 825.8 , striatum-caudate putamen-hypothalamus (brain): 2755 ± 908.5 and the cerebellum: 12.1 ± 796.3 .

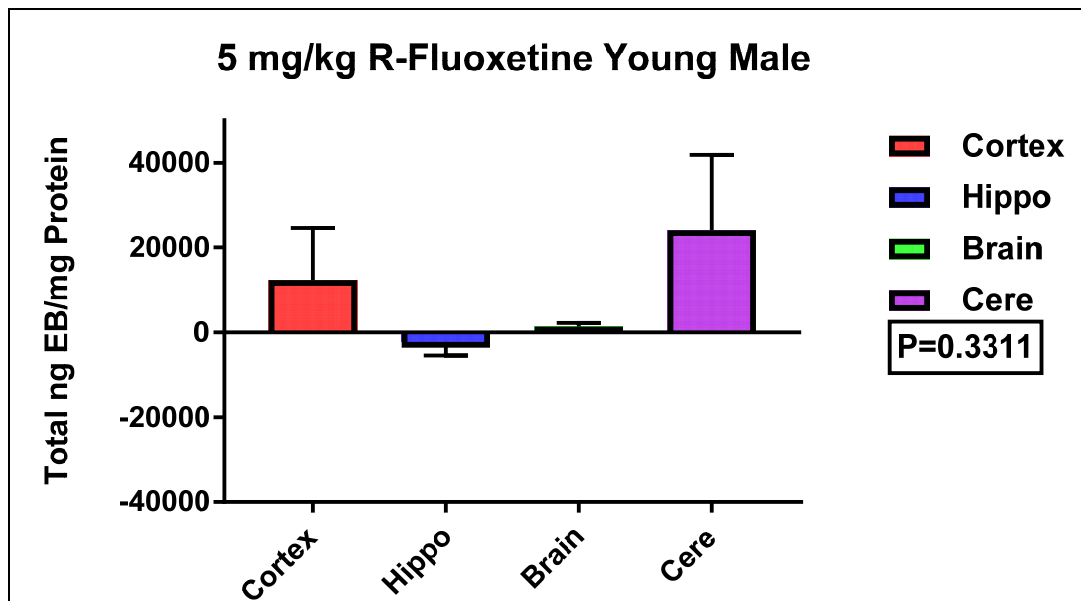


Figure 15: Young male rats that have taken 5 mg/kg R-fluoxetine (RYM) for three days. The x-axis represents the different brain regions: the red color represents the cortex, the blue color represents peri-ventricular and hippocampus, the green color represents the

striatum-caudate putamen-hypothalamus, and the purple color represents the cerebellum. The y-axis represents the total ng EB/mg protein. One-way ANOVA was performed. Columns represent the mean for each group and error bars show standard error of mean (SEM). P=0.3311. The animal number, n= 11.

Figure 15 shows that there was no significant difference between the different brain regions (P=0.3311). The mean \pm the standard error of the mean (SEM) for the different brain regions are as follow: cortex: 12308 \pm 12294, peri-ventricular and hippocampus: -2205 \pm 3224, striatum-caudate putamen-hypothalamus: 1397 \pm 851.6 and the cerebellum: 24093 \pm 17789. Outliers were determined by ROUT software at medium setting. In the cerebellum the following outliers were found: 24064.006, 41496.548, and 197113.230. In the cortex region the following outlier was found: 134723.409.

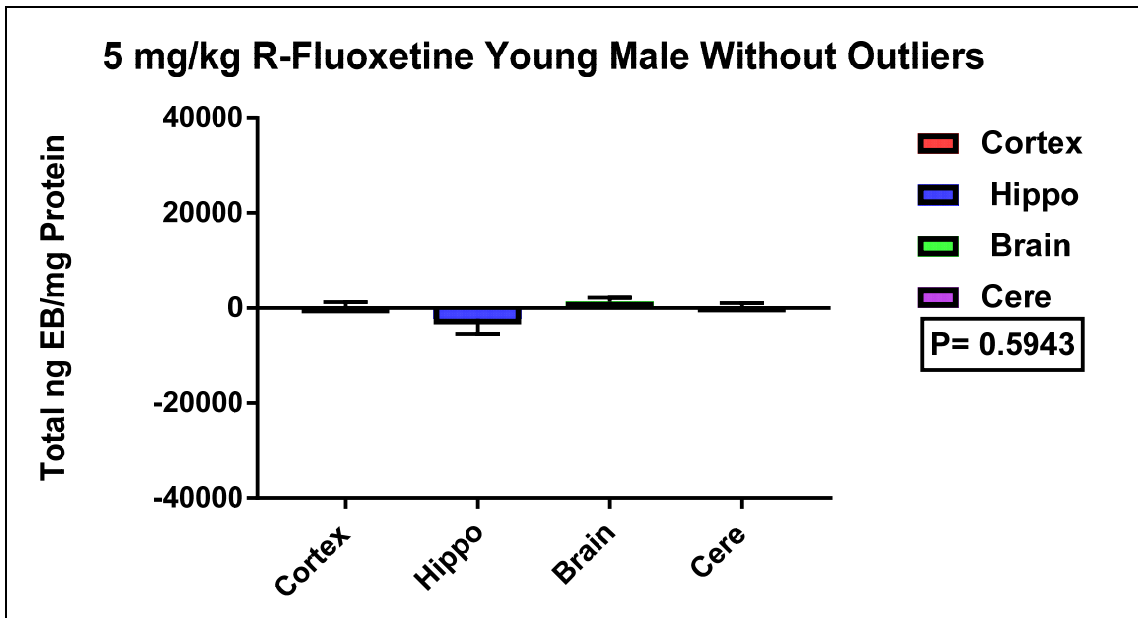


Figure 16: *Young male rats that have taken 5mg/kg R-fluoxetine for three days (RYM) without outliers. The x-axis represents the different brain regions: the red color represents the cortex, the blue color represents peri-ventricular and hippocampus, the green color*

represents the striatum-caudate putamen-hypothalamus, and the purple color represents the cerebellum. The y-axis represents the total ng EB/mg protein. One-way ANOVA was performed. Columns represent the mean for each group and error bars show standard error of mean (SEM). $P=0.5943$. The animal number, n for the cortex = 9, n for the hippo = 11, n for the lower brain = 11, n for the cerebellum = 8.

Figure 16 shows that there was no significant difference between the different brain regions ($P=0.5943$). The mean \pm the standard error of the mean (SEM) for the different brain regions are as follow: cortex: 66.77 ± 1253 , peri-ventricular and hippocampus: -2205 ± 3224 , striatum-caudate putamen-hypothalamus: 1397 ± 851.6 and the cerebellum: 293.1 ± 824.6 .

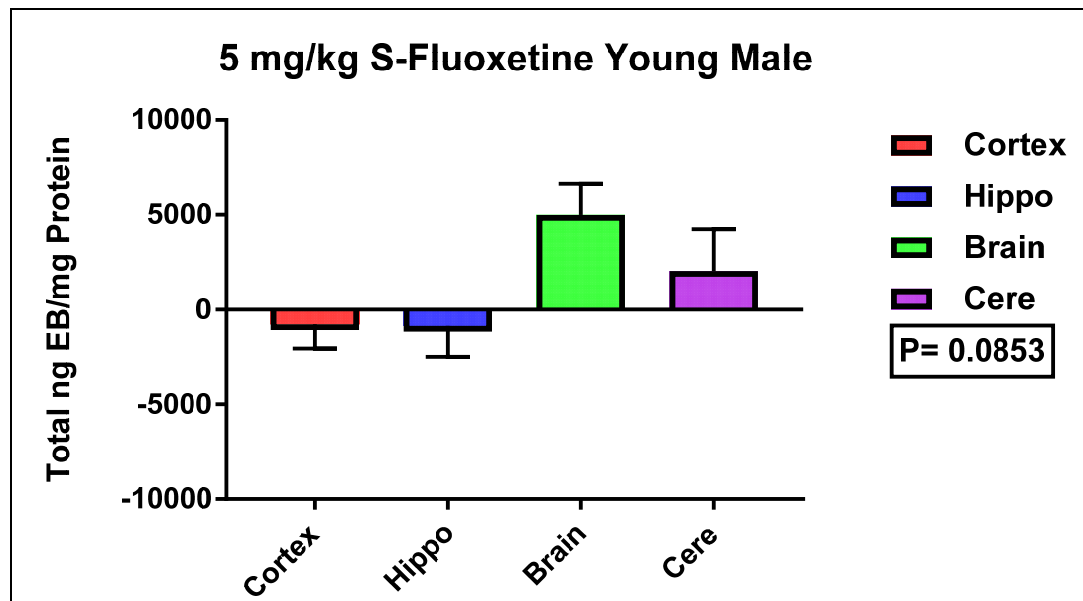


Figure 17: Young male rats that have taken 5 mg/kg S-fluoxetine (SYM) for three days. The x-axis represents the different brain regions: the red color represents the cortex, the blue color represents peri-ventricular and hippocampus, the green color represents the striatum-caudate putamen-hypothalamus, and the purple color represents the cerebellum.

The y-axis represents the total ng EB/mg protein. One-way ANOVA was performed. Columns represent the mean for each group and error bars show standard error of mean (SEM). $P=0.0853$. The animal number, $n = 7$.

Figure 17 shows that there was no significant difference between the different brain regions ($P=0.0853$). There is a strong trend towards a significant difference between the permeability of the lower brain region and the cortex and hippocampus. The mean \pm the standard error of the mean (SEM) for the different brain regions are as follow: cortex: -778.2 ± 1282 , peri-ventricular and hippocampus: -853.8 ± 1635 , striatum-caudate putamen-hypothalamus (brain): 4991 ± 1649 and the cerebellum: 2018 ± 2218 . Outlier was determined by ROUT software at medium setting, and it was located in the cerebellum: 15175.114 .

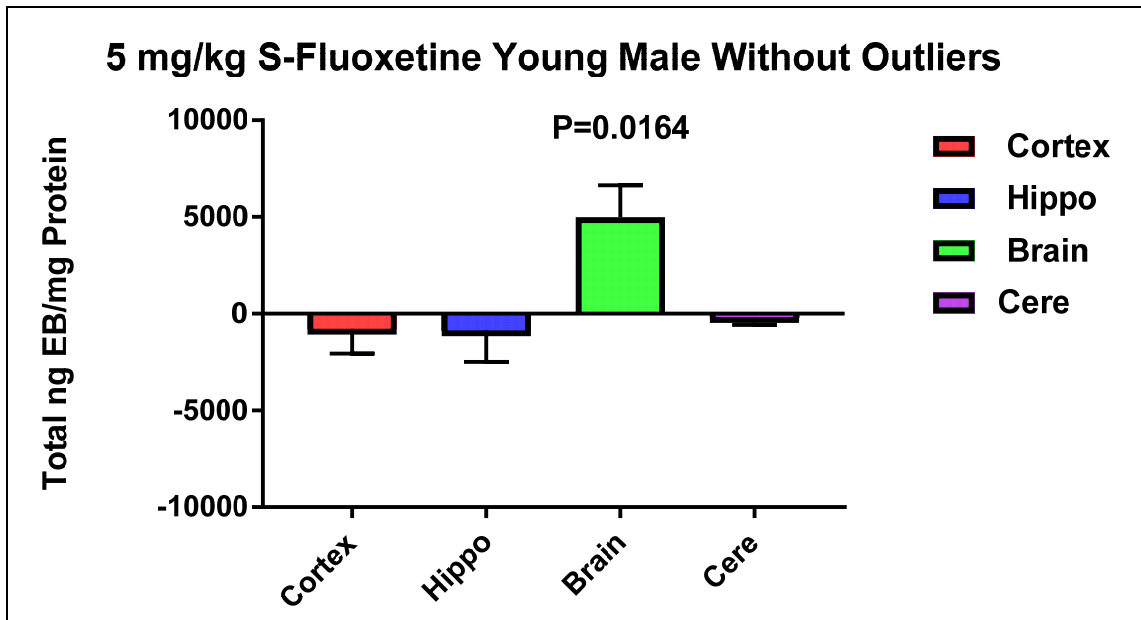


Figure 18: Young male rats that have taken 5mg/kg S-fluoxetine for three days (SYM). The x-axis represents the different brain regions: the red color represents the cortex, the blue color represents peri-ventricular and hippocampus, the green color represents the striatum-caudate putamen-hypothalamus, and the purple color represents the cerebellum.

The y-axis represents the total ng EB/mg protein. One-way ANOVA was performed. Columns represent the mean for each group and error bars show standard error of mean (SEM). $P=0.0164$. The n for the animal groups was as follow: the n for the cortex = 6, the n for the hippo = 7, the n for the lower brain = 7, the n for the cerebellum = 6.

Figure 18 shows that there was a significant difference between the different brain regions ($P=0.0164$). The brain region showed the highest blood brain barrier permeability among the different brain regions. The mean \pm the standard error of the mean (SEM) for the different brain regions are as follow: cortex: -778.2 ± 1282 , peri-ventricular and hippocampus: -853.8 ± 1635 , striatum-caudate putamen-hypothalamus (brain): 4991 ± 1649 and the cerebellum: -174.7 ± 392.8 .

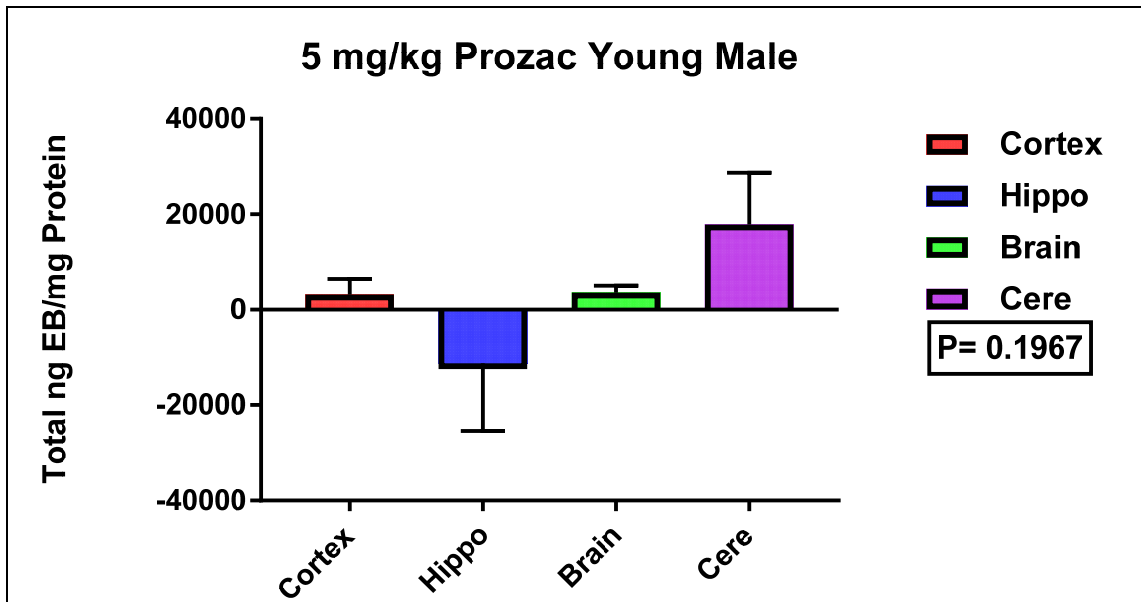


Figure 19: Young male rats that have taken 5mg/kg Prozac (PYM) for three days. The x-axis represents the different brain regions: the red color represents the cortex, the blue color represents peri-ventricular and hippocampus, the green color represents the striatum-caudate putamen-hypothalamus (brain), and the purple color represents the

cerebellum. The y-axis represents the total ng EB/mg protein. One-way ANOVA was performed. Columns represent the mean for each group and error bars show standard error of mean (SEM). P= 0.1967. The animal number, n = 7.

Figure 19 shows that there was no significant difference between the different brain regions (P= 0.1967), and the cerebellum showed the highest blood brain barrier permeability among the different brain regions. The mean \pm the standard error of the mean (SEM) for the different brain regions are as follow: cortex: 3193 \pm 3273, peri-ventricular and hippocampus: -11231 \pm 14227, striatum-caudateputamen-hypothalamus(brain): 3593 \pm 1440 and the cerebellum: 17815 \pm 10890.

Summary: When total ng Evans blue in regions is normalized by the amount of protein measured from the tissue in milligrams, we see that control young males have show a statistical difference in the permeability of Evans blue in the lower brain region compared to the cortex, hippocampus and cerebellum, showing enhanced permeability in that region. S-fluoxetine did produce increased permeability (statistically different) in the lower brain region, while R-fluoxetine tightened the BBB permeability in this region, removing statistical differences in BBB permeability between the regions. Prozac, which is a mixture of R- and S-fluoxetine, did not show any significant differences in permeability between the brain regions tested.

3.2 Old Male Rats

One Way ANOVA total ng EB/mg protein

In the next set of figures, we normalized the amount of Evans blue in a region by dividing the total ng Evans blue in that region by the protein concentration in mg, determined by a Bradford protein assay for the old male rats.

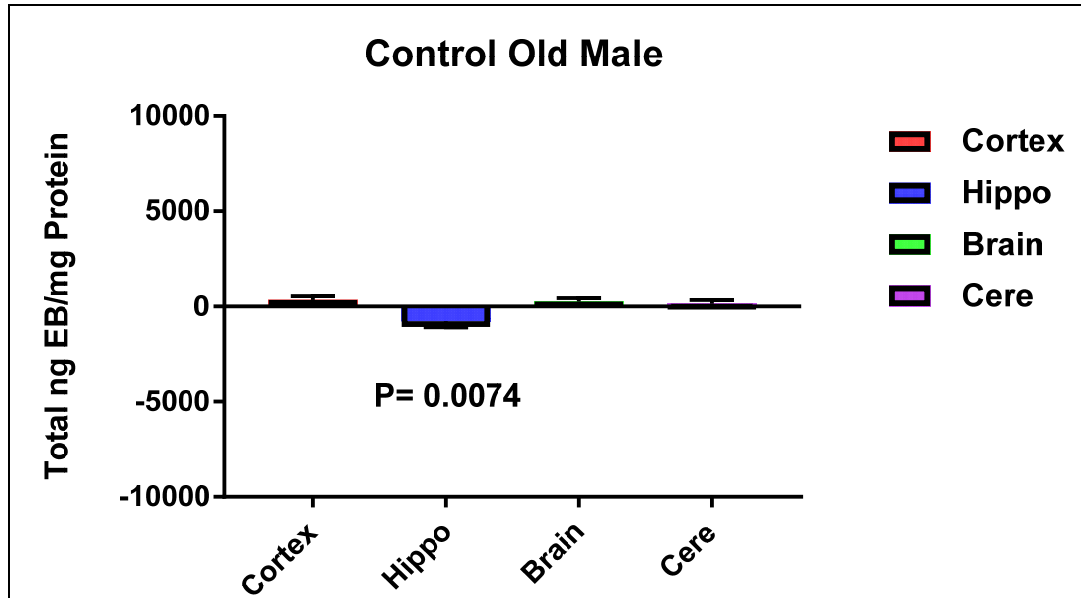


Figure 20: Old male rats that have not taken any drug (COM). The x-axis represents the different brain regions: the red color represents the cortex, the blue color represents peri-ventricular and hippocampus, the green color represents the striatum-caudate putamen-hypothalamus (brain), and the purple color represents the cerebellum. The y-axis represents the total ng EB/mg protein. One-way ANOVA was performed. Columns represent the mean for each group and error bars show standard error of mean (SEM). $P = 0.0074$. The animal number, $n = 7$.

Figure 20 shows that there was a significant difference between the different brain regions ($P = 0.0074$), and the hippocampus region showed the lowest blood brain barrier permeability among the different brain regions. The mean \pm the standard error of the mean for the different brain regions are as follow: cortex: 347.2 ± 188.8 , peri-ventricular and

hippocampus: -771.1 ± 317.7 , striatum-caudate putamen-hypothalamus (brain): 263 ± 179.6 and the cerebellum: 140.8 ± 207 .

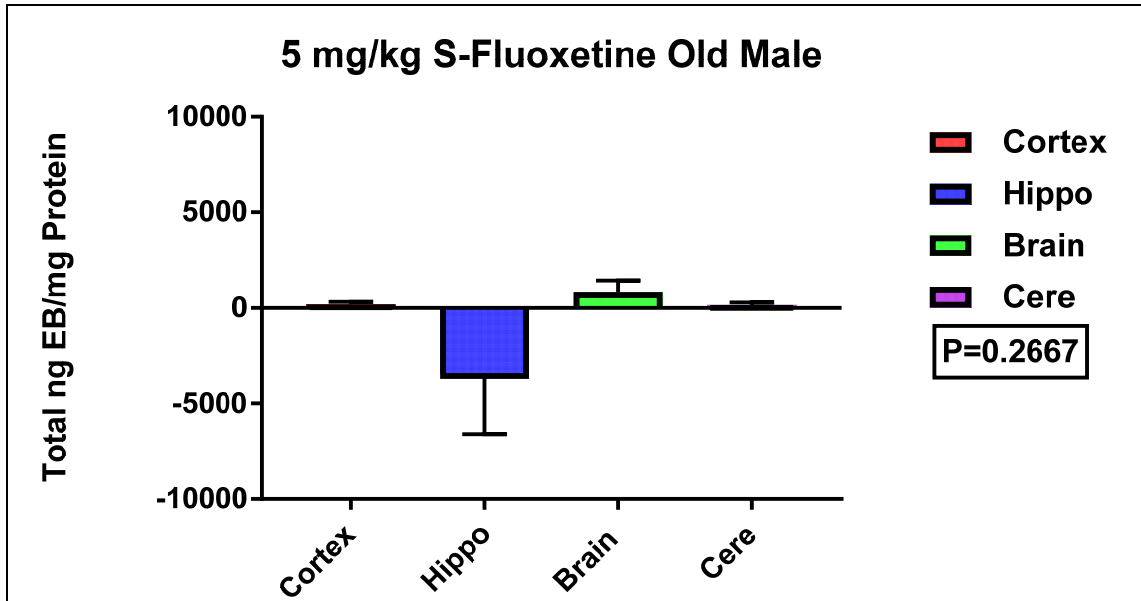


Figure 21: Old male rats that given 5 mg/kg S-fluoxetine (SOM) for three days. The x-axis represents the different brain regions: the red color represents the cortex, the blue color represents peri-ventricular and hippocampus, the green color represents the striatum-caudate putamen-hypothalamus (brain), and the purple color represents the cerebellum. The y-axis represents the total ng EB. One-way ANOVA was performed. Columns represent the mean for each group and error bars show standard error of mean (SEM). $P= 0.2667$. The animal number, $n = 7$.

Figure 21 shows that there was no significant difference between the different brain regions ($P=0.2667$). The hippocampus showed the lowest blood brain barrier permeability. The mean \pm the standard error of the mean for the different brain regions are as follow: cortex: 194.2 ± 135.1 , peri-ventricular and hippocampus: -3411 ± 3191 , striatum-caudate putamen-hypothalamus (brain): 820 ± 603.6 and the cerebellum: 4306.474579 . Outliers

were determined by ROUT software at medium setting. The outlier: 22521.990 was located in the hippocampus region. The outlier: 4306.475 was located in the brain region.

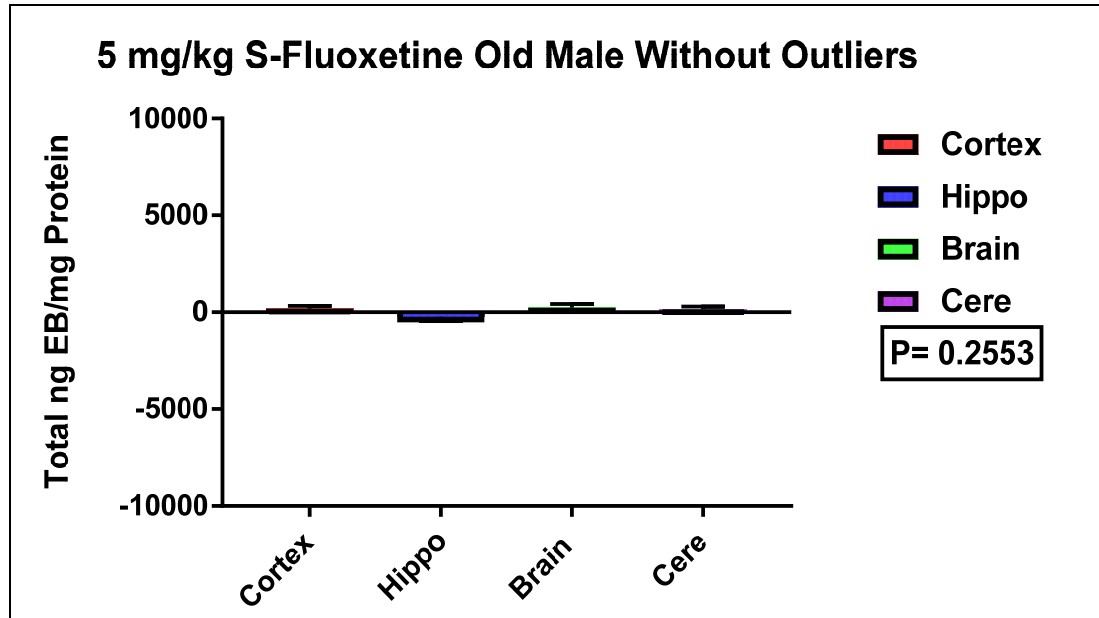


Figure 22: Old male rats that given 5 mg/kg S-fluoxetine (SOM) for three days without outliers. The x-axis represents the different brain regions: the red color represents the cortex, the blue color represents peri-ventricular and hippocampus, the green color represents the striatum-caudate putamen-hypothalamus (brain), and the purple color represents the cerebellum. The y-axis represents the total ng EB. One-way ANOVA was performed. Columns represent the mean for each group and error bars show standard error of mean (SEM). $P = 0.2553$. The n for the animal numbers are as follow: the n for the cortex = 7, the n for the hippo = 6, the n for the lower brain = 6, the n for the cerebellum = 7.

Figure 22 shows that there was no significant difference between the different brain regions ($P=0.2553$). The mean \pm the standard error of the mean for the different brain regions are as follow: cortex: 194.2 \pm 135.1, peri-ventricular and hippocampus: -

226.3±237.1, striatum-caudate putamen-hypothalamus (brain): 238.9±193.4 and the cerebellum: 161.2±127.9.

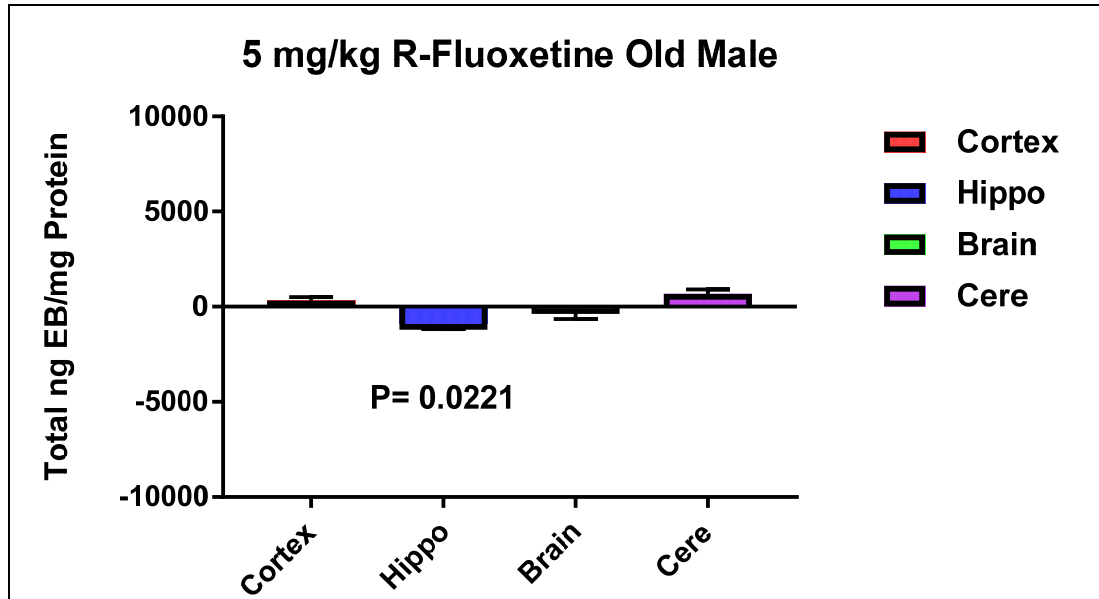


Figure 23: Old male rats that have taken 5 mg/kg R-fluoxetine (ROM) for three days. The x-axis represents the different brain regions: the red color represents the cortex, the blue color represents peri-ventricular and hippocampus, the green color represents the striatum-caudate putamen-hypothalamus (brain), and the purple color represents the cerebellum. The y-axis represents the total ng EB/mg protein. One-way ANOVA was performed. Columns represent the mean for each group and error bars show standard error of mean (SEM). $P = 0.0221$. The animal number, $n = 7$.

Figure 23 shows that there was a significant difference between the different brain regions ($P = 0.0221$), and the hippocampus showed the lowest blood brain barrier permeability among the different brain regions. The mean \pm the standard error of the mean for the different brain regions are as follow: cortex: 326.1±180.3, peri-ventricular and

hippocampus: -902 ± 267 , striatum-caudate putamen-hypothalamus (brain): -72.23 ± 565.1
and the cerebellum: 671.2 ± 231 .

Summary: When total ng Evans blue in regions is normalized by the amount of protein measured from the tissue in milligrams, we see that there is a significant difference in the blood brain barrier regions among the old male rats that have not taken any medicine and the old male rats that have taken 5mg/kg of R-fluoxetine, with the hippocampus showing statistically lower permeability compared to the other brain regions. The old male rats that have taken 5mg/kg of S-fluoxetine did not show any significant difference in the blood brain barrier permeability.

3.3 Old Female Rats

One Way ANOVA total ng EB/mg protein

The following figures represent the one-way ANOVA for the different female rats (control female rats, the female rats that have taken R-fluoxetine, and the female rats that have taken S-fluoxetine). The figures represent the normalized measurements of Evans blue in the different brain regions of the female rats. The Evans blue was normalized by measuring the total amount of Evans blue per the protein concentration (mg). The protein was measured by using the Bradford protein assay.

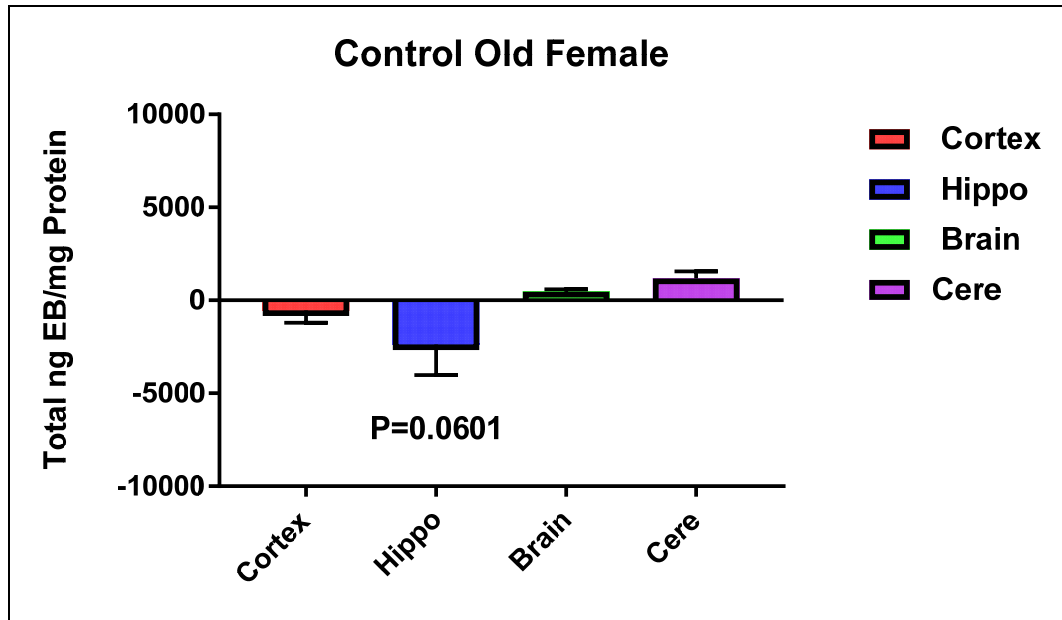


Figure 24: Old female rats that have not taken any drug (COF). The x-axis represents the different brain regions: the red color represents the cortex, the blue color represents peri-ventricular and hippocampus, the green color represents the striatum-caudate putamen-hypothalamus (brain), and the purple color represents the cerebellum. The y-axis represents the total ng EB/mg protein. One-way ANOVA was performed. Columns represent the mean for each group and error bars show standard error of mean (SEM). $P = 0.0601$. The animal number, $n = 7$.

Figure 24 shows that there was a strong trend for a significant difference between the different brain regions ($P = 0.0601$). The hippocampus showed the lowest blood brain barrier permeability among the different brain regions. The mean for the different brain regions are as follow: cortex: -540.4 ± 675.7 , peri-ventricular and hippocampus: -2376 ± 1649 , striatum-caudate putamen-hypothalamus (brain): 455.9 ± 139.6 and the cerebellum: 1172 ± 393.9 . Outliers were determined by ROUT software at medium setting.

The outlier -4503.975 was located in the cortex while the outlier -12021.576 was located in the hippocampus.

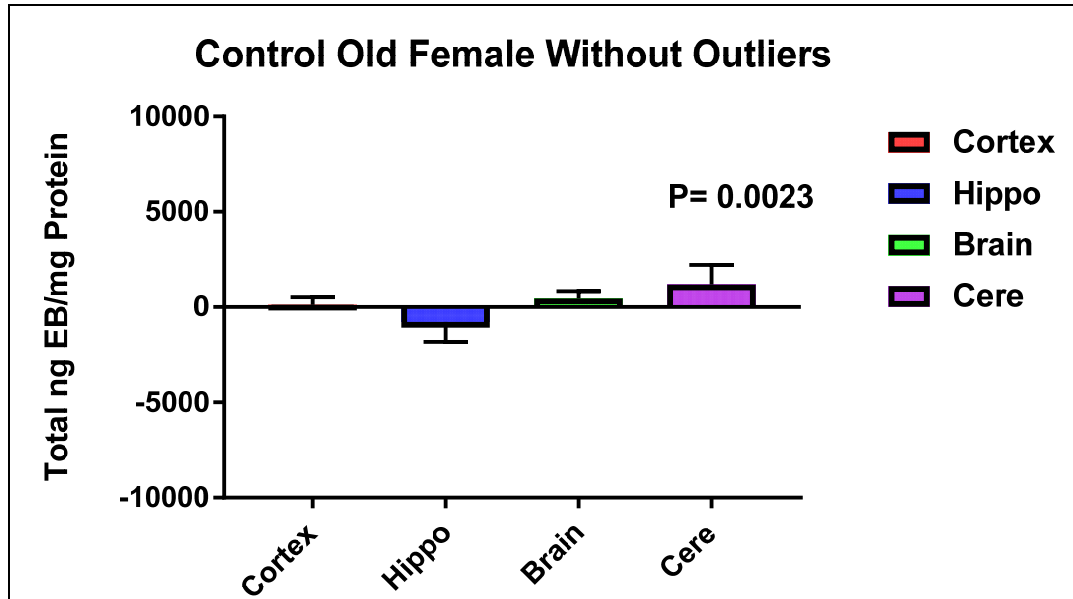


Figure 25: Old female rats that have not taken any drug (COF). The x-axis represents the different brain regions: the red color represents the cortex, the blue color represents periventricular and hippocampus, the green color represents the striatum-caudate putamen-hypothalamus (brain), and the purple color represents the cerebellum. The y-axis represents the total ng EB/mg protein. One-way ANOVA was performed. Columns represent the mean for each group and error bars show standard error of mean (SEM). $P= 0.0023$. The animal numbers, n for the different brain regions are as follow: the n for cortex = 6, the n for the hippo = 6, the n for the lower brain = 7, the n for the cerebellum = 7.

Figure 25 shows that there was a significant difference between the different brain regions ($P= 0.0023$), with the cerebellum showing enhanced permeability compared to the other brain regions. The mean \pm the standard error of the mean for the different brain

regions are as follow: cortex: 120.2 ± 168.3 , peri-ventricular and hippocampus: -768 ± 434.8 , striatum-caudate putamen-hypothalamus (brain): 455.9 ± 139.6 and the cerebellum: 1172 ± 393.9 .

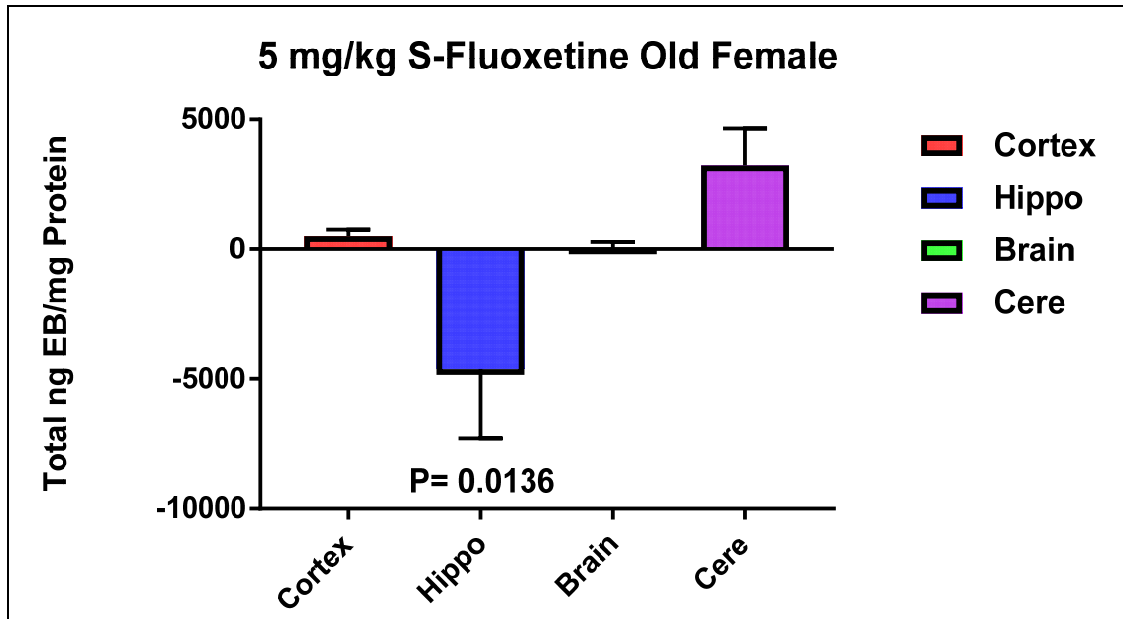


Figure 26: Old female rats that have taken 5 mg/kg S-fluoxetine (SOF) for three days. The x-axis represents the different brain regions: the red color represents the cortex, the blue color represents peri-ventricular and hippocampus, the green color represents the striatum-caudate putamen-hypothalamus, and the purple color represents the cerebellum. The y-axis represents the total ng EB/mg protein. One-way ANOVA was performed. Columns represent the mean for each group and error bars show standard error of mean (SEM). $P = 0.0136$. The animal number, $n = 6$.

Figure 26 shows that there was a significant difference between the different brain regions ($P = 0.0136$). The hippocampus showed the lowest blood brain barrier permeability

among the different brain regions, and the cerebellum showed the highest permeability. The mean \pm the standard error of the mean for the different brain regions are as follow: cortex: 509.7 ± 252.4 , peri-ventricular and hippocampus: -4622 ± 2673 , striatum-caudate putamen-hypothalamus (brain): 29.63 ± 250.6 and the cerebellum: 3232 ± 1428 .

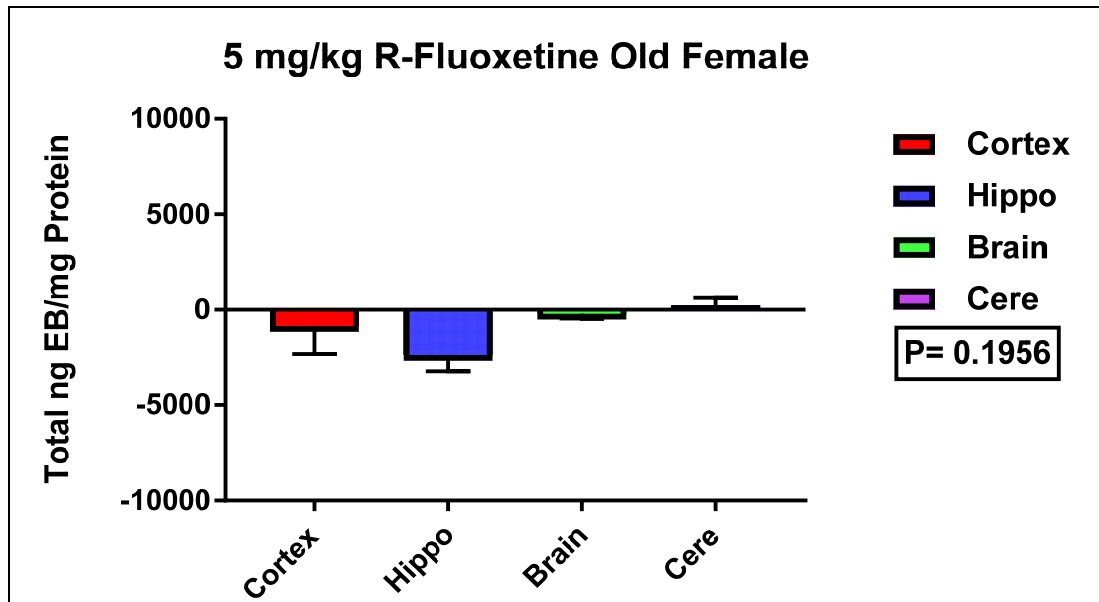


Figure 27: Old female rats that have taken 5 mg/kg R-fluoxetine (ROF) for three days. The x-axis represents the different brain regions: the red color represents the cortex, the blue color represents peri-ventricular and hippocampus, the green color represents the striatum-caudate putamen-hypothalamus (brain), and the purple color represents the cerebellum. The y-axis represents the total ng EB/mg protein. One-way ANOVA was performed. Columns represent the mean for each group and error bars show standard error of mean (SEM). $P = 0.1956$. The animal number, $n = 7$.

Figure 27 shows that there was no significant difference between the different brain regions ($P=0.1956$). The hippocampus showed the lowest blood brain barrier permeability among the different brain region. The mean \pm the standard error of the mean for the

different brain regions are as follow: cortex: -856.5 ± 1463 , peri-ventricular and hippocampus: -2369 ± 847.8 , striatum-caudate putamen-hypothalamus (brain): -207.1 ± 250.5 and the cerebellum: 240.8 ± 390.3 . The outlier was determined by using ROUT analysis at medium setting. It was located at the cortex region. The outlier was -9420.832 .

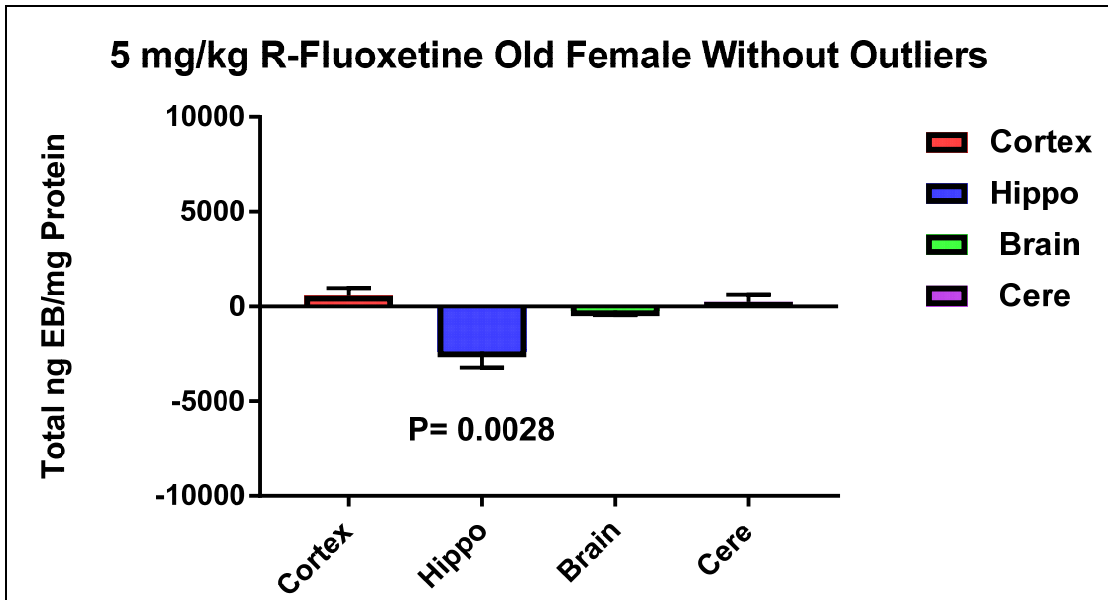


Figure 28: Old female rats that have taken 5 mg/kg R-fluoxetine (ROF) for three days without outliers. The x-axis represents the different brain regions: the red color represents the cortex, the blue color represents peri-ventricular and hippocampus, the green color represents the striatum-caudate putamen-hypothalamus (brain), and the purple color represents the cerebellum. The y-axis represents the total ng EB/mg protein. One-way ANOVA was performed. Columns represent the mean for each group and error bars show

standard error of mean (SEM). P= 0.0028. The animal number, n for the cortex = 6, n for hippo = 7, n for the lower brain = 7, n for the cerebellum = 7.

Figure 28 shows that there was significant difference between the different brain regions (P=0.0028), with the hippocampus showing statistically lower permeability. The mean \pm the standard error of the mean for the different brain regions are as follow: cortex: 570.8 \pm 380.8, peri-ventricular and hippocampus: -2369 \pm 847.8, striatum-caudate putamen-hypothalamus (brain): -207.1 \pm 250.5 and the cerebellum: 240.8 \pm 390.3.

Summary: Total ng Evans blue in regions was normalized by the amount of protein measured from the tissue in milligrams. Our statistical analysis showed that there was a significant difference in the blood brain barrier permeability in the different brain regions with the hippocampus showing the lowest blood brain barrier permeability and the cerebellum showing higher blood brain barrier permeability in both control and S-fluoxetine groups.

3.4. Young Male Rats versus Old Male Rats

Two-Way ANOVA of total ng EB/mg Protein

The following set of figures represents the two-way ANOVA of the comparison between the different groups of the old males and the young males. The measurements of Evans blue were normalized by measuring the total amount of Evans blue in ng and then dividing it by the amount of protein concentration in mg. The Bradford protein assay was used to measure the amount of the protein concentration.

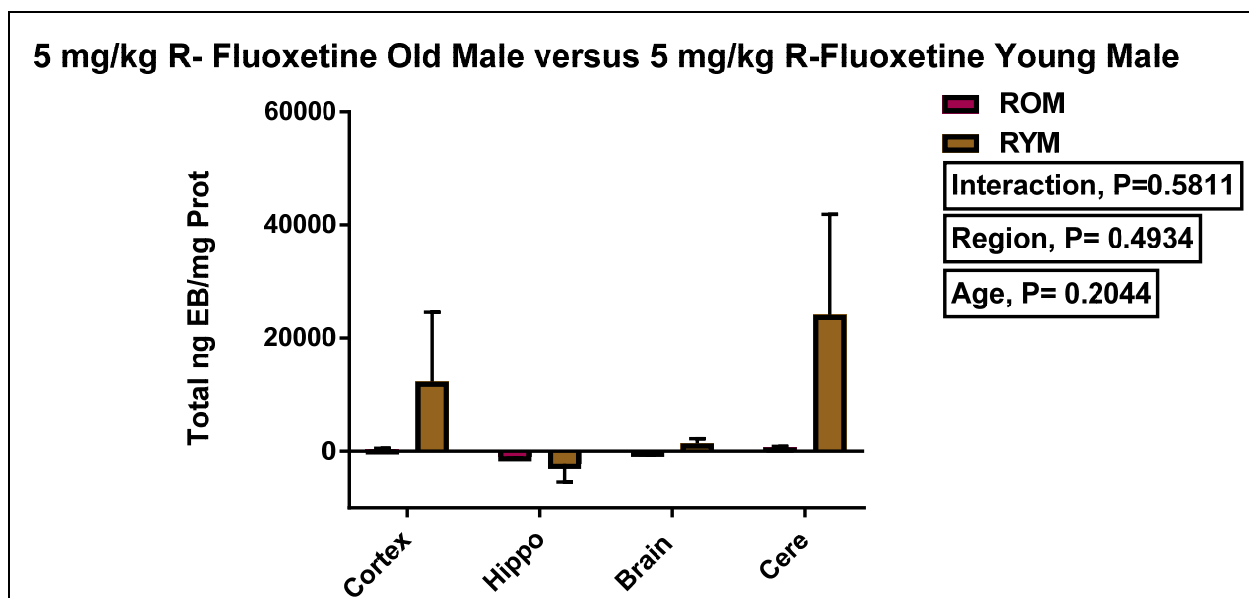


Figure 29: Comparison between young male and old male rats that have given 5 mg/kg R-fluoxetine (RYM vs. ROM) for three days. The x-axis represents the different brain regions: cortex, peri-ventricular and hippocampus, striatum-caudate putamen-hypothalamus (brain), cerebellum. The y-axis represents the total ng EB/mg protein. Two-way ANOVA was performed. Columns represent the mean for each group and error bars show standard error of mean (SEM). Interaction, $P=0.5811$. Region, $P=0.4934$. Age, $P=0.2044$. The number of the animals, n was as follow: the n for the ROM =7, the n for the RYM =11.

Figure 29 shows that there was no significant difference for interaction between the different brain regions and age groups ($P = 0.5811$). Also, there was no significant difference between the different brain regions between the groups ($P = 0.4934$). In addition, there was no significant difference between the young and the old males ($P = 0.2044$). The root mean square error, which is defined as the residual mean square. It is used to estimate the common within-group standard deviation which also known as the standard error of the estimate were as the following. The mean \pm the standard error of the mean for ROM:

5.78±338.6, RYM: 8898±5930. The mean ± the standard error of the mean: ROM: 5.787 ± 4783.159, RYM: 8410.804 ± 4079.092. The mean ± the standard error of the mean for the different brain regions are as follow: cortex: 6317.183 ± 6541.099, hippo: -2528.268 ± 6541.099, brain: 662.374 ± 6541.099, cerebellum: 12381.893 ± 5450.916.

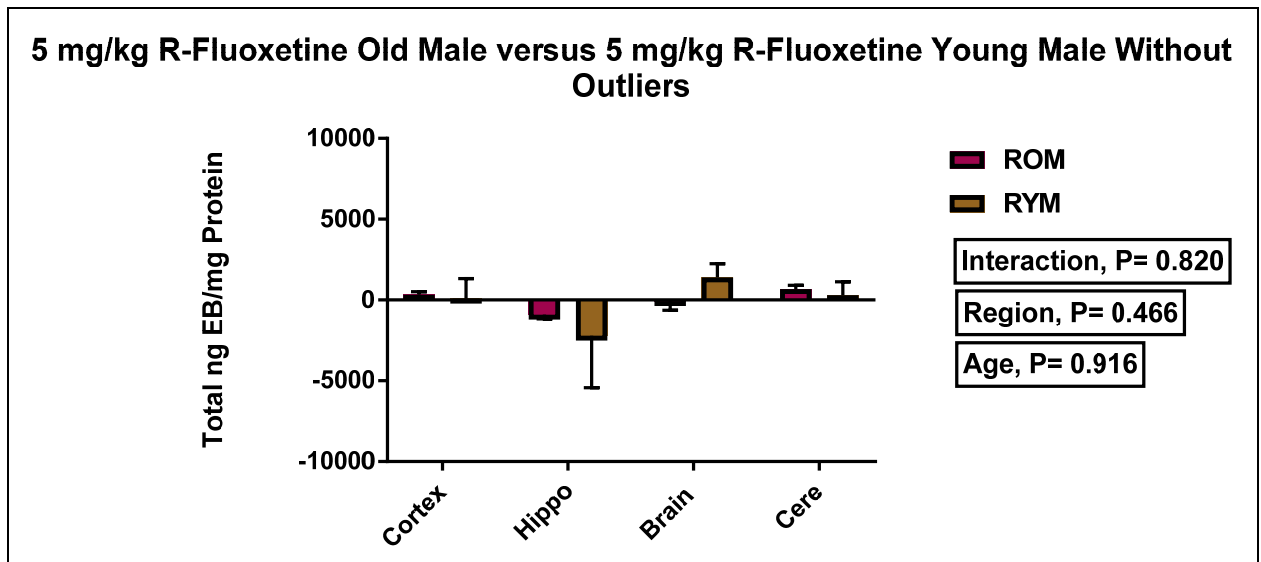


Figure 30: Comparison between old male rats that have given R-fluoxetine for three days, and young male rats that R-fluoxetine (ROM vs. RYM). The x-axis represents the different brain regions: cortex, peri-ventricular and hippocampus, striatum-caudate putamen-hypothalamus (brain), and cerebellum. The y-axis represents the total ng EB. Two-way ANOVA was performed. Columns represent the mean for each group and error bars show standard error of mean (SEM). Interaction, P=0.820. Region, P=0.466. Age, P=0.916. The n for the animal numbers was as follow: the n for the ROM = 7, the n for the animal

groups of the RYM was as follow: the n for the cortex was 9, the n for the hippo was 11, the n for the brain was 11 and the n for the cerebellum was 8.

Figure 30 shows that there was no significant difference for interaction between the different brain regions and age groups (P = 0.820). Also, there was no significant difference between the different brain regions between the groups (P = 0.466). In addition, there was no significant difference between the young and the old males (P =0.916). The root mean square error, which is defined as the residual mean square. It is used to estimates the common within-group standard deviation which also known as the standard error of the estimate were as the following. The mean \pm the standard error of the mean for the different brain regions are as follow: cortex: 196.441 ± 1133.443 , peri-ventricular and hippocampus:- 1553.296 ± 1112.027 , striatum-caudate putamen-hypothalamus (brain): 662.367 ± 998.075 and the cerebellum: 482.149 ± 1190.354 . The mean \pm the standard error of the mean for the treatment groups was as follow: RYM: -111.950 ± 691.300 , ROM: 5.780 ± 869.311 .

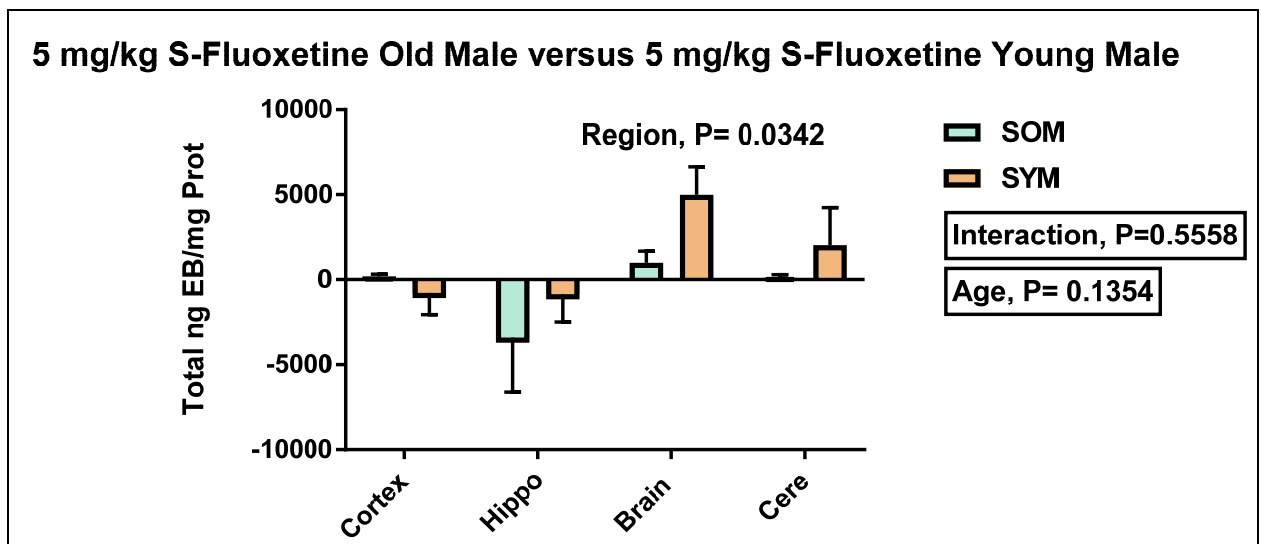


Figure 31: Comparison between young male and old male rats that have given 5 mg/kg S-

fluoxetine (SYM vs. SOM) for three days. The x-axis represents the different brain regions: cortex, peri-ventricular and hippocampus, striatum-caudate putamen-hypothalamus (brain), cerebellum. The y-axis represents the total ng EB/mg protein. Two-way ANOVA was performed. Columns represent the mean for each group and error bars show standard error of mean (SEM). Interaction, $P=0.5558$. Region, $P=0.0342$. Age, $P=0.1354$. The animal numbers, n for the different animal groups were as follow, the n for the SOM =7, the n for the SYM =7.

Figure 31 shows that there was no significant difference for interaction between the different brain regions and age groups ($P = 0.5558$). Also, there was a significant difference between the different brain regions between the groups ($P = 0.0342$). In addition, there was no significant difference between the young and the old males ($P = 0.1354$). The root mean square error, which is defined as the residual mean square. It is used to estimates the common within-group standard deviation which also known as the standard error of the estimate were as the following. The mean \pm the standard error of the mean for SOM: -559.023 \pm 806.390, SYM: 534.440 \pm 823.019. The mean \pm the standard error of the mean for the different brain regions: cortex: -292.006 \pm 1186.974, hippo: -1888.090 \pm 1140.408, brain: 1041.251 \pm 1140.408, cerebellum: 1089.678 \pm 1140.408.

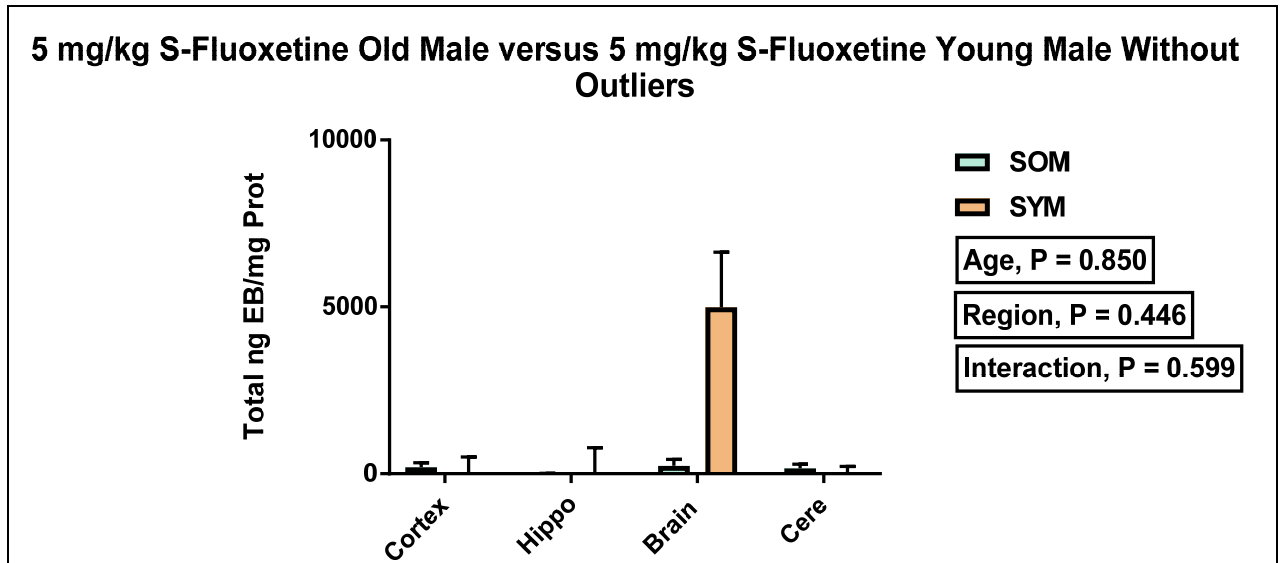


Figure 32: Comparison between old male rats that have given S-fluoxetine, and young male rats that have given S-fluoxetine (SOM vs. SYM) for three days without outliers. The x-axis represents the different brain regions: cortex, peri-ventricular and hippocampus, striatum-caudate putamen-hypothalamus (brain), and cerebellum. The y-axis represents the total ng EB. Two-way ANOVA was performed. Columns represent the mean for each group and error bars show standard error of mean (SEM). Interaction, $P = 0.599$. Region, $P = 0.446$. Age, $P = 0.850$. The animal numbers, n for the SOM of the cortex was 7, the hippocampus was 6, the brain was 6 and the cerebellum was 7. The n for the SYM was as follow: the n for the cortex was 6, the n for the hippo was 7, the n for the brain was 7, and the n for the cerebellum was 6.

Figure 32 shows that there was no significant difference for interaction between the different brain regions and age groups ($P = 0.599$). Also, there was no significant difference between the different brain regions between the groups ($P = 0.446$). In addition, there was no significant difference between the young and the old males ($P = 0.850$). The root mean square error, which is defined as the residual mean square. It is used to estimate the

common within-group standard deviation which also known as the standard error of the estimate were as the following. The mean \pm the standard error of the mean for SOM: 91.98 \pm 107.3, SYM: 796.1 \pm 1407. The mean \pm the standard error of the mean for the different brain regions: cortex: -292.006 \pm 576.364, hippo: -295.543 \pm 576.364, brain: 750.708 \pm 492.705, cerebellum: -6.736 \pm 576.364.

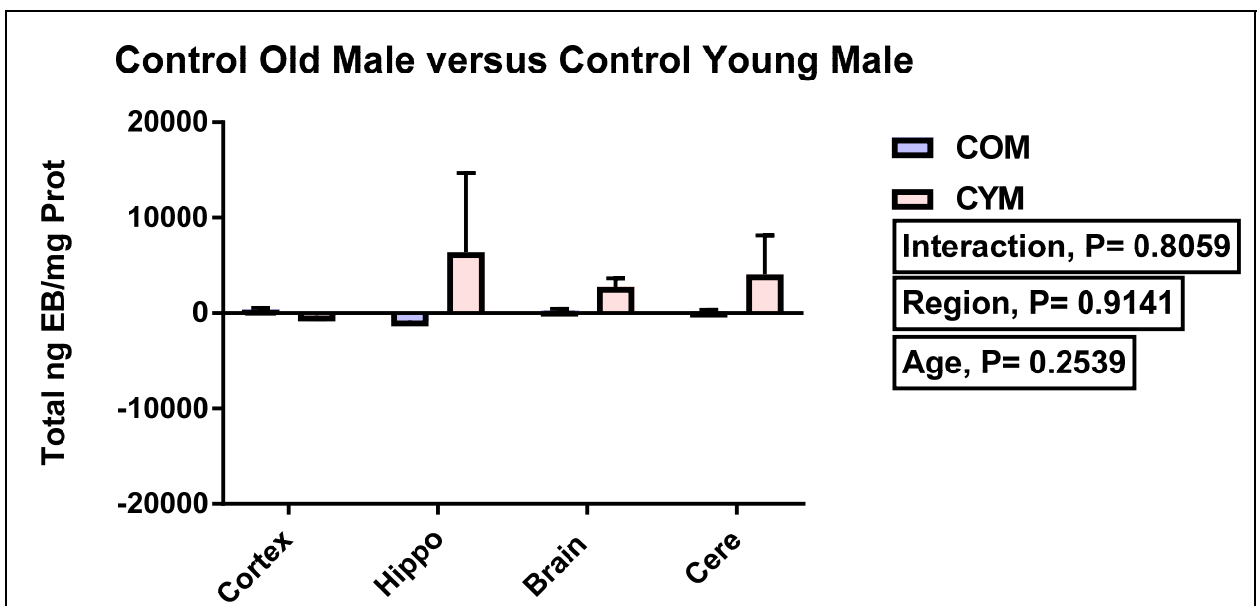


Figure 33: Comparison between young male and old male rats that have not given any drug (CYM vs. COM). The x-axis represents the different brain regions: cortex, periventricular and hippocampus, striatum-caudate putamen-hypothalamus (brain), cerebellum. The y-axis represents the total ng EB/mg protein. Two-way ANOVA was performed. Columns represent the mean for each group and error bars show standard error of mean (SEM). Interaction, $P=0.8059$. Region, $P=0.9141$. Age, $P=0.2539$. The

animal numbers, n for the different animal groups were as follow, the n for the COM =7, the n for the CYM =10.

Figure 33 shows that there was no significant difference for interaction between the different brain regions and age groups ($P = 0.8059$). Also, there was no significant difference between the different brain regions between the groups ($P = 0.9141$). In addition, there was no significant difference between the young and the old males ($P = 0.2539$). The root mean square error, which is defined as the residual mean square. It is used to estimate the common within-group standard deviation which also known as the standard error of the estimate were as the following. The mean \pm the standard error of the mean for COM: -5.023 ± 258.9 , SYM: 3236 ± 1383 . The mean \pm the standard error of the mean was as follow: COM -5.023 ± 2157.676 , CYM: 3235.603 ± 1805.242 . The mean \pm the standard error of the mean for the different brain regions was as follow: cortex: $50.286 \pm$, hippo: 2807.251 , brain: 1508.976 , cerebellum: 2094.647 .

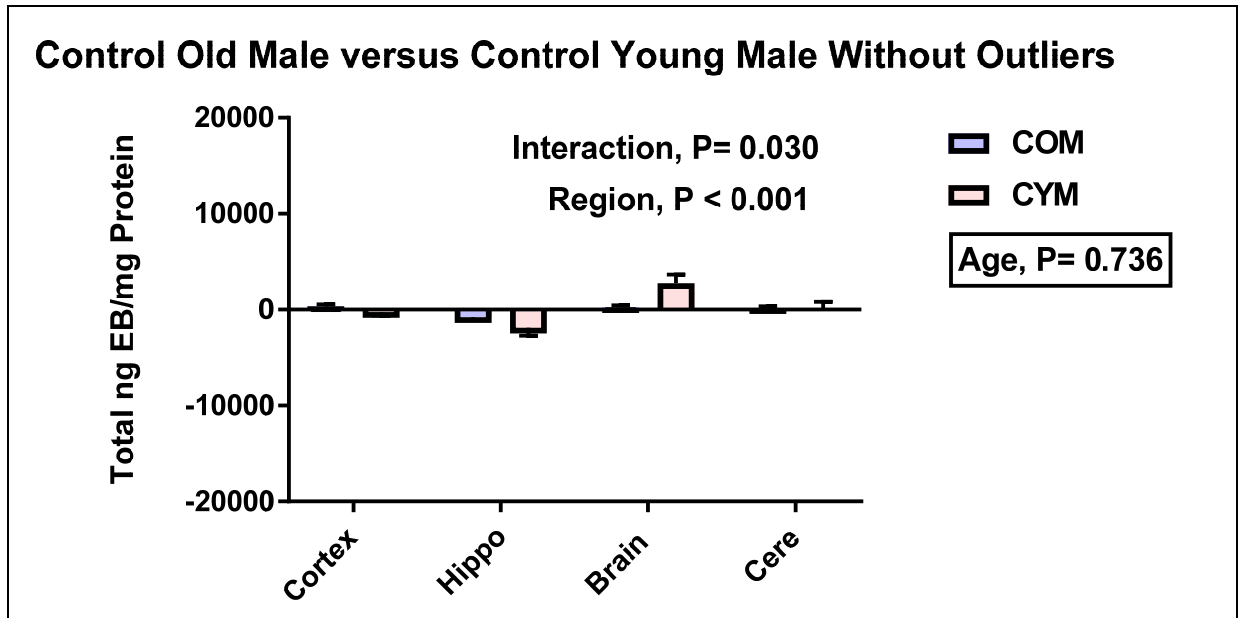


Figure 34: Comparison between old male rats that have not taken a drug (COM), and young male rats that have not taken a drug (CYM). The x-axis represents the different brain regions: cortex, peri-ventricular and hippocampus, striatum-caudate putamen-hypothalamus (brain), and cerebellum. The y-axis represents the total ng EB. Two-way ANOVA was performed. Columns represent the mean for each group and error bars show standard error of mean (SEM). Interaction, $P=0.030$. Region, $P<0.001$. Age, $P=0.736$. The animal numbers, n for the different animal groups were as follow: the n for the COM =7, the n for the CYM for the different brain regions were as follow: the n for the cortex was 10, the n for the hippocampus was 9, the n for the brain is 10 and n for the cerebellum was 9.

Figure 34 shows that there was significant difference for interaction between the different brain regions and age groups ($P = 0.030$). Also, there was significant difference between

the different brain regions between the groups ($P < 0.001$). In addition, there was no significant difference between the young and the old males ($P = 0.736$). The root mean square error, which is defined as the residual mean square. It is used to estimate the common within-group standard deviation which also known as the standard error of the estimate were as the following. The mean \pm the standard error of the mean for the different brain regions are as follow: cortex: 50.288 ± 486.556 , peri-ventricular and hippocampus: 1330.710 ± 497.562 , striatum-caudate putamen-hypothalamus (brain): 1508.976 ± 433.586 and the cerebellum: 76.453 ± 497.562 . The mean \pm the standard error of the mean for the treatment groups was as follow: CYM: 157.526 ± 301.182 , COM: -5.023 ± 373.171 .

Summary: Total ng Evans blue in regions was normalized by the amount of protein measured from the tissue in milligrams. We compared the amount of total ng Evans blue among the different groups (control, S-fluoxetine and R-fluoxetine) between the young and the old males. The R-fluoxetine groups showed no significant difference in interaction, region nor age. The S-fluoxetine showed a significant difference in interaction and region. The young males in the S-fluoxetine showed the highest blood brain barrier permeability in the lower brain regions among the different brain regions in the brain. The S-fluoxetine has increased the blood brain barrier permeability in the brain region. The control group showed a significant interaction in the interaction and the region. In the control group, the brain showed the highest blood brain barrier permeability among the different brain regions.

3.5 Comparison among the Young Males Groups

Two Way ANOVA of total ng EB/mg Protein

In the figures that are listed below, we compared the total ng Evans Blue per mg of protein for the different groups of the young males. We normalized the data by dividing the total ng of Evans blue by the protein concentration (mg) which was measured by Bradford protein assay.

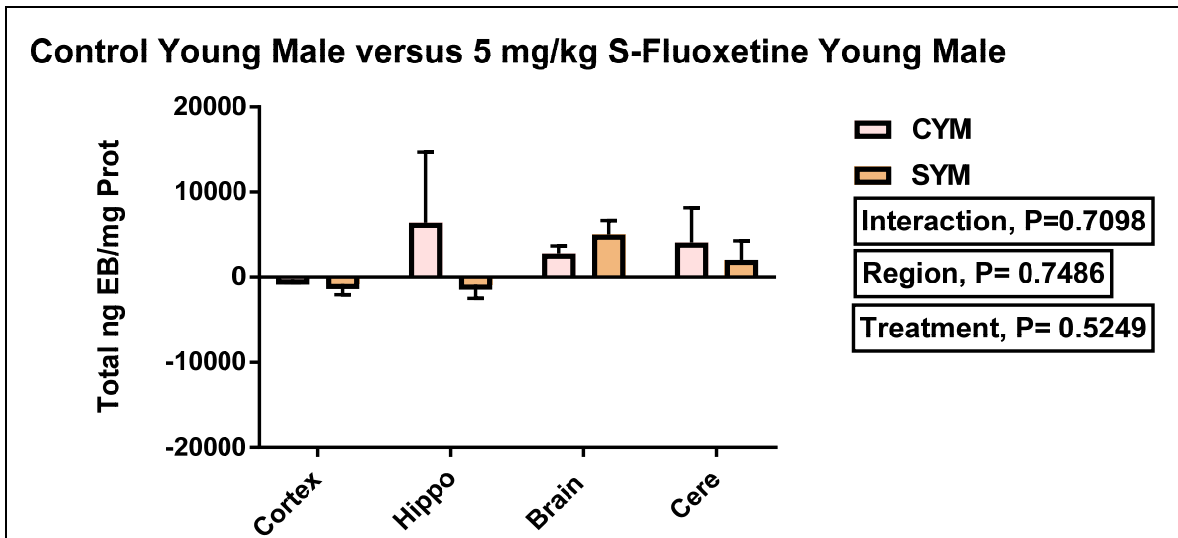


Figure 35: Comparison between young male rats that have given 5 mg/kg S-fluoxetine for three days, and young male rats that have not given any drug (SYM vs. CYM). The x-axis represents the different brain regions: cortex, peri-ventricular and hippocampus, striatum-caudate putamen-hypothalamus (brain), cerebellum. The y-axis represents the total ng Evans Blue/mg protein. Two-way ANOVA was performed. Columns represent the mean for each group and error bars show standard error of mean (SEM). Interaction, $P=0.7098$. Region, $P=0.7486$. Treatment, $P=0.5249$. The n for the different animal groups were as follow: the n for the CYM =10, the n for the SYM =7.

Figure 35 shows that there was no significant difference in ng Evans Blue/mg protein in young male rats for interaction between the different brain regions and the drug treatment groups ($P=0.7098$). Also, there was no significant difference between the different brain

regions between the groups ($P = 0.7486$). In addition, there was no significant difference between the different drug treatment groups ($P = 0.5249$). ROUT analysis at medium setting was used to find out the outliers. The SYM had an outlier (15175.114) at the cerebellum region of the brain. The CYM had two outliers. The first outlier (80868.926) was located at the hippocampus region while the second outlier (40375.985) was located at the cerebellum region. The root mean square error, which is defined as the residual mean square. It is used to estimate the common within-group standard deviation which also known as the standard error of the estimate were as the following. The mean \pm the standard error of the mean: CYM: 3235.604 ± 1874.775 , SYM: 1344.297 ± 2286.992 . The mean \pm the standard error of the mean for the different brain regions was as follow: Cortex: -512.418 ± 3061.495 , hippo: 2765.933 ± 2921.626 , brain: 3872.970 ± 2921.626 , cerebellum: 3033.315 ± 2921.626 .

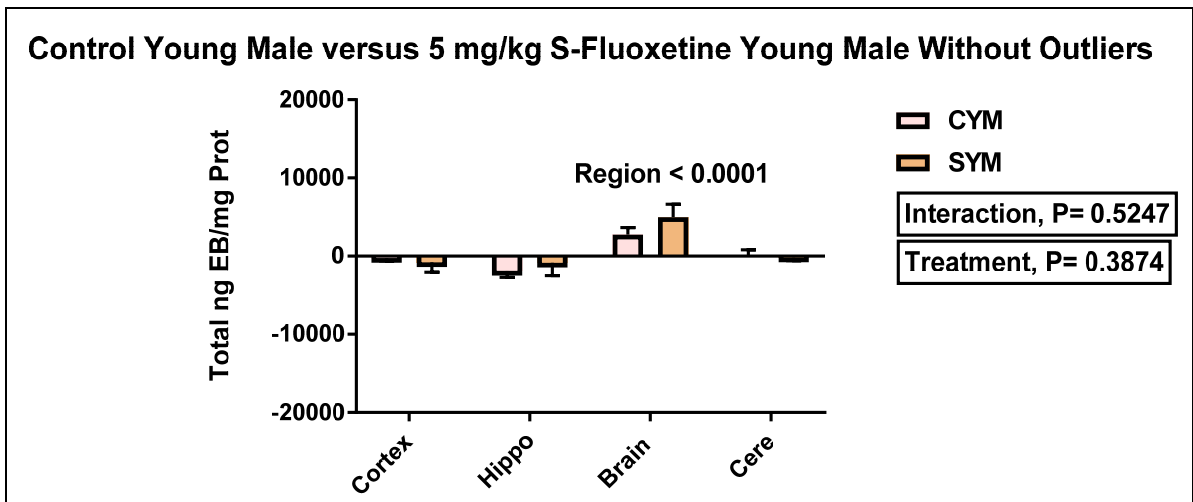


Figure 36: Comparison between young male rats that have given 5 mg/kg S-fluoxetine for three days, and young male rats that have not given any drug (SYM vs. CYM). The x-axis represents the different brain regions: cortex, peri-ventricular and hippocampus, striatum-

caudate putamen-hypothalamus (brain), cerebellum. The y-axis represents the total ng EB/mg protein. Two-way ANOVA was performed. Columns represent the mean for each group and error bars show standard error of mean (SEM). Interaction, $P= 0.5247$. Region, $P < 0.0001$. Treatment, $P= 0.3874$. The n for the animal groups of the CYM was as follow: the n for the cortex was 10, the n for the hippocampus was 9, the n for the brain was 10 and the n for the cerebellum was 9. The n for the SYM was as follow: the n for the cortex was 6, the n for the hippocampus was 7, the n for the brain was 7, and the n for the cerebellum 6.

Figure 36 shows data from Figure 35 that has removed the statistical outliers. This data indicates there was no significant difference in ng Evans Blue/mg protein for the interaction between the different brain regions and the drug treatment groups ($P = 0.5247$). However, there was a significant difference in ng Evans Blue/mg protein between the different brain regions for the young male ($P < 0.0001$), with the lower brain region showing a higher permeability. There was no significant difference between the different drug treatment groups ($P = 0.3874$; control versus S-fluoxetine) in the young male rats. The root mean square error, which is defined as the residual mean square. It is used to estimate the common within-group standard deviation which also known as the standard error of the estimate were as the following. The mean \pm the standard error of the mean for CYM: 157.526 ± 466.809 , SYM: 796.089 ± 565.238 . The mean \pm the standard error of the mean for the different brain regions are as follow: cortex: -512.418 ± 741.965 , hippo: -1372.028 ± 724.084 , brain: 3872.970 ± 708.067 , cerebellum: -81.294 ± 757.265 .

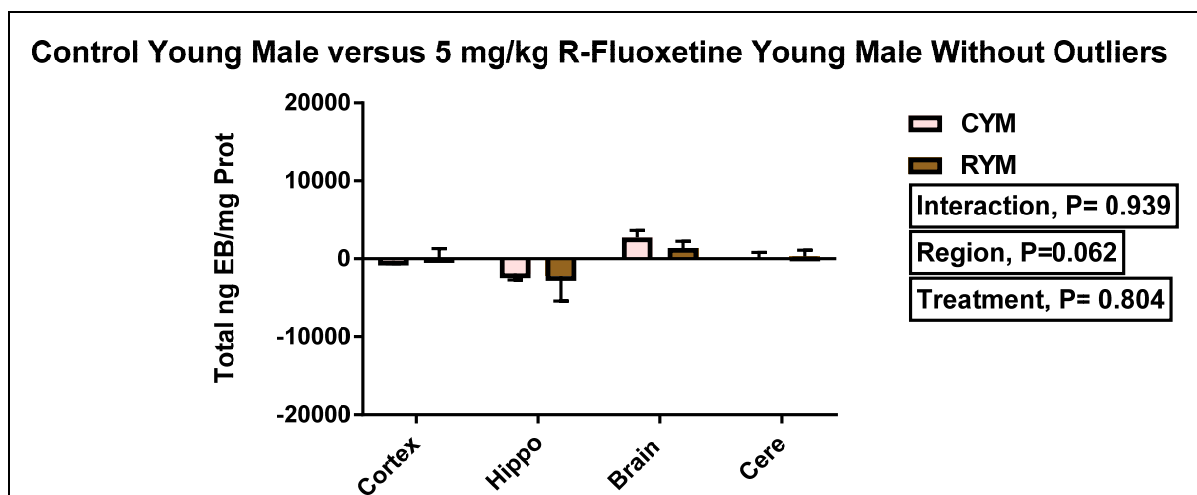


Figure 37: Comparison between young male rats that have given 5 mg/kg R-fluoxetine for three days, and young male rats that have not given any drug (RYM vs. CYM). The x-axis represents the different brain regions: cortex, peri-ventricular and hippocampus, striatum-caudate putamen-hypothalamus (brain), cerebellum. The y-axis represents the total ng EB/mg protein. Two-way ANOVA was performed. Columns represent the mean for each group and error bars show standard error of mean (SEM). Interaction, $P = 0.939$. Region, $P = 0.062$. Treatment, $P = 0.804$. The animal numbers (n) for the different animal groups were as follow: the n for the CYM =10, the n for the RYM =11.

Figure 37 shows there was no significant difference in ng Evans Blue/ mg protein for the interaction between the different brain regions and the drug treatment groups ($P = 0.939$; control versus R-fluoxetine). Also, there was no significant difference between the different brain regions for the young male rats ($P = 0.062$). In addition, there was no significant difference between the drug treatment groups ($P = 0.804$; control versus R-fluoxetine). The statistical outliers were determined by using the ROUT analysis at medium setting. The CYM had two outliers. The first outlier (80868.926) was located at the hippocampus region while the second outlier (40375.985) was located at the cerebellum

region. The RYM group had four outliers. The first outlier (134723.409) was located at the cortex. In contrast, the rest of the outliers (24064.006, 41496.548 and 197113.231) were located at the cerebellum. The root mean square error, which is defined as the residual mean square. It is used to estimate the common within-group standard deviation which also known as the standard error of the estimate were as the following. The mean \pm the standard error of the mean: CYM: 3235.604 ± 4171.233 , RYM: 8898.305 ± 3720.250 . The mean \pm the standard error of the mean for the brain regions was as follow: cortex: 6060.813 ± 5763.387 , hippo: 2090.514 ± 5763.387 , brain: 2075.962 ± 5030.697 , Cere: 14070.529 ± 5763.387 .

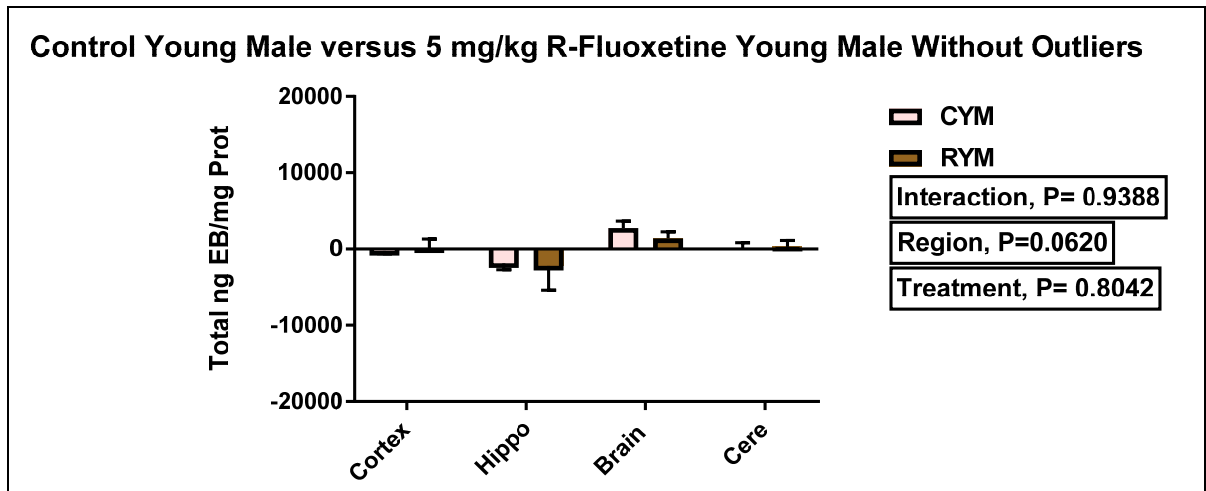


Figure 38: Comparison between young male rats that have given 5 mg/kg R-fluoxetine for three days, and young male rats that have not given any drug (RYM vs. CYM). The x-axis represents the different brain regions: cortex, peri-ventricular and hippocampus, striatum-caudate putamen-hypothalamus (brain), cerebellum. The y-axis represents the total ng EB/mg protein. Two-way ANOVA was performed. Columns represent the mean for each group and error bars show standard error of mean (SEM). Interaction, $P= 0.9388$. Region, $P=0.0620$. Treatment, $P= 0.8042$.

$P = 0.0620$. Treatment, $P = 0.8042$. The n for the animal numbers for the different animal groups were as follow: the n for the CYM for the different brain regions were as follow: the n for the cortex was 10, the n for the hippocampus was 9, the n for the brain was 10 and the n for the cerebellum was 9. The n for the RYM was as follow: the n for the cortex was 9, the n for the hippocampus was 11, the n for the brain was 11 and the n for the cerebellum was 8.

Figure 38 shows the data from Figure 37 with the statistical outlier removed. The data indicates there was no significant difference in the ng Evans Blue/mg protein for interaction between the different brain regions and the drug treatment groups ($P = 0.9388$; control versus R-fluoxetine). Also, there was no significant difference between the different brain regions between the groups ($P = 0.0620$), but the P value does indicate a very strong trend here. In addition, there was no significant difference between the treatment groups ($P = 0.8042$). The root mean square error, which is defined as the residual mean square. It is used to estimates the common within-group standard deviation which also known as the standard error of the estimate were as the following. The mean \pm the standard error of the mean for the different brain regions are as follow: cortex: -89.943 ± 1063.861 , periventricular and hippocampus: -2047.447 ± 1069.221 , striatum-caudate putamen-hypothalamus (brain): 2075.962 ± 1039.401 and the cerebellum: 152.580 ± 1155.921 . The mean \pm the standard error of the mean for the treatment groups was as follow: CYM: 157.526 ± 772.877 , RYM: -111.950 ± 758.648 .

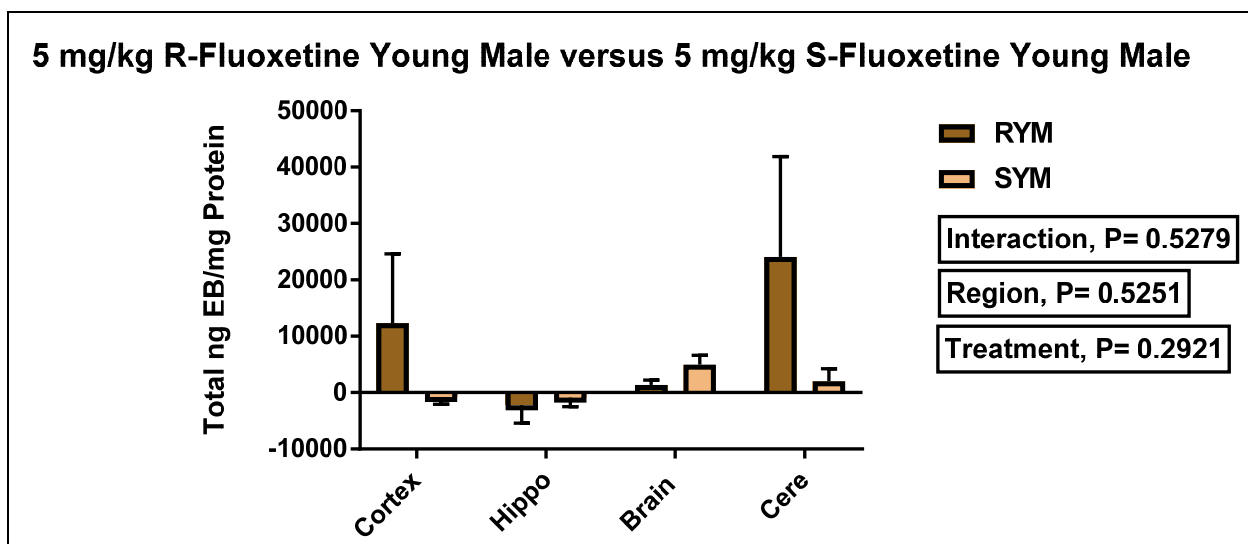


Figure 39: Comparison between young male rats that have given 5 mg/kg R-fluoxetine for three days, and young male rats that have given 5 mg/kg of S-fluoxetine (RYM vs. SYM). The x-axis represents the different brain regions: cortex, peri-ventricular and hippocampus, striatum-caudate putamen-hypothalamus (brain), cerebellum. The y-axis represents the total ng EB/mg protein. Two-way ANOVA was performed. Columns represent the mean for each group and error bars show standard error of mean (SEM). Interaction, $P = 0.5279$. Region, $P = 0.5251$. Treatment, $P = 0.2921$. The n for the animal numbers of the different animal groups were as follow: the n for the RYM =11, the n for the SYM =7.

Figure 39 shows that the data indicates that there was no significant difference in the ng Evans blue/ mg protein for interaction between the different brain regions and drug treatment groups ($p = 0.5279$; R-fluoxetine vs. S-fluoxetine treatment group). Also, there was no significant difference between the different brain regions between the groups ($P = 0.5251$). In addition, there was no significant difference between the treatment groups ($P = 0.2921$). The ROUT analysis at medium setting was used to determine the outliers. The

SYM had an outlier at the cerebellum. The outlier was 15175.114. The RYM had four outliers. The first outlier was 134723.409. It was found at the cortex. The other outliers were found at the cerebellum. These outliers include: 24064.006, 41496.548, and 197113.231. The root mean square error, which is defined as the residual mean square. It is used to estimate the common within-group standard deviation which also known as the standard error of the estimate were as the following. The mean \pm the standard error of the mean, RYM: 8898.305 ± 4378.361 , SYM: 1344.297 ± 5601.744 . The mean \pm the standard error of the mean for the different brain regions: cortex: 5765.054 ± 7369.880 , hippo: -1529.182 ± 7020.997 , brain: 3193.973 ± 7020.997 , cerebellum: 13055.360 ± 7020.997 .

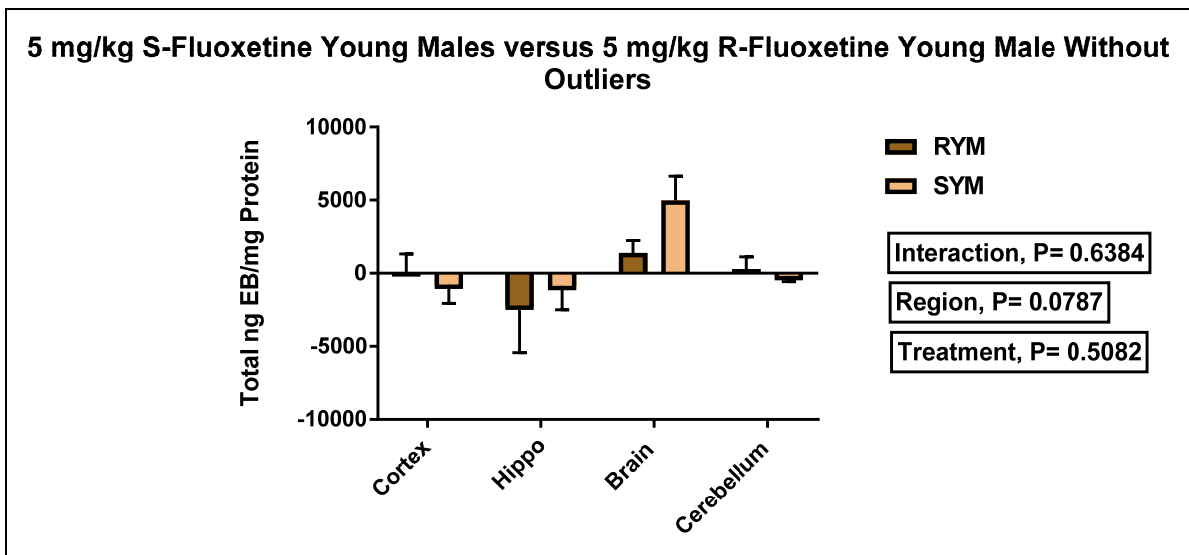


Figure 40: Comparison between young male rats that have given 5 mg/kg R-fluoxetine for three days, and young male rats that have given 5 mg/kg of S-fluoxetine (RYM vs. SYM). The x-axis represents the different brain regions: cortex, peri-ventricular and hippocampus, striatum-caudate putamen-hypothalamus (brain), cerebellum. The y-axis represents the total ng EB/mg protein. Two-way ANOVA was performed. Columns represent the mean for each group and error bars show standard error of mean (SEM).

Interaction, P = 0.6384. Region, P = 0.0787. Treatment, P = 0.5082. The n for the animal numbers of the different animal groups were as follow: the n for the RYM for the different brain regions were as follow: the n for the cortex was 9. The n for the hippocampus was 11, the n for the brain was 11 and the n for the cerebellum was 8, the n for the SYM was as follow: the n for the cortex was 6, the n for the hippocampus was 7, the n for the brain was 7, and the n for the cerebellum was 6.

Figure 40 shows the data from Figure 39, but with the statistical outliers removed. The data shows there was no significant difference in ng Evans Blue/mg protein for the interaction between the different brain regions and the drug treatment groups ($P = 0.6384$; R-fluoxetine versus S-fluoxetine). Also, there was no significant difference between the different brain regions between the groups ($P = 0.0787$), but the P value does show a very strong trend here. In addition, there was no significant difference between the treatment groups ($P = 0.5082$). The root mean square error, which is defined as the residual mean square. It is used to estimate the common within-group standard deviation which also known as the standard error of the estimate were as the following. The mean \pm the standard error of the mean: RYM: -111.950 ± 901.296 , SYM: 1344.297 ± 1090.216 . The mean \pm the standard error of the mean: cortex: -355.702 ± 1459.425 , hippo: -1529.182 ± 1366.432 , brain: 3193.973 ± 1366.432 , cerebellum: 1155.606 ± 1462.679 .

Summary: Total ng Evans blue in regions was normalized by the amount of protein measured from the tissue in milligrams. Our analysis showed that there were no significant difference in the interaction, region and treatment in the comparison between the CYM versus RYM. Also, there were no significant difference in the interaction, region and

treatment in the comparison between RYM versus SYM. There was a significant difference in the region for the SYM group in the comparison of CYM versus SYM.

5 mg/kg Prozac young male versus different treatment groups among young males

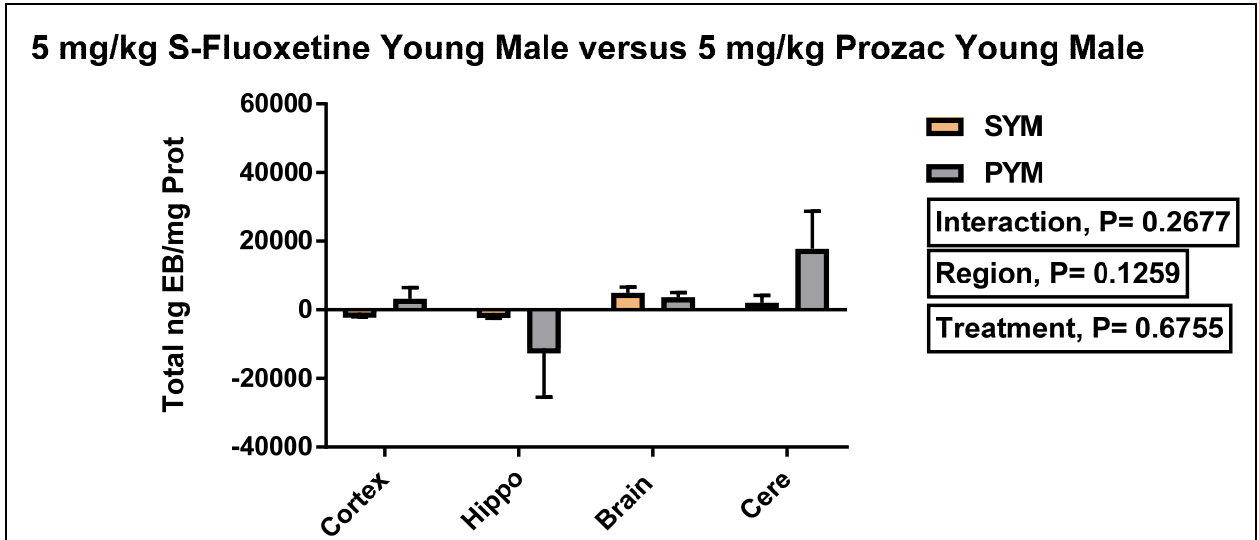


Figure 41: Comparison between young male rats that have given 5 mg/kg S-fluoxetine, and young male rats that have given 5 mg/kg Prozac (SYM vs. PYM) for three days. The x-axis represents the different brain regions: cortex, peri-ventricular and hippocampus, striatum-caudate putamen-hypothalamus (brain), cerebellum. The y-axis represents the total ng EB/mg protein. Two-way ANOVA was performed. Columns represent the mean for each group and error bars show standard error of mean (SEM). Interaction, P=0.2677. Region, P=0.1259. Treatment, P=0.6755. The n for the animal groups was as follow: SYM=7, PYM=7.

Figure 41 shows there was no significant difference in ng Evans Blue/mg protein for interaction between the different brain regions and the drug treatment groups (P = 0.2677; S-fluoxetine versus Prozac). Also, there was no significant difference between the different

brain regions between the groups ($P = 0.1259$). In addition, there was no significant difference the drug treatment groups ($P = 0.6755$). Outlier was determined by using the ROUT analysis at medium settings. The outlier was located at the SYM group at the cerebellum (15175.114). The root mean square error, which is defined as the residual mean square. It is used to estimate the common within-group standard deviation which also known as the standard error of the estimate were as the following. The mean \pm the standard error of the mean for the SYM: 1344.297 ± 2976.671 , PYM: 3342.441 ± 3109.031 . The mean \pm the standard error of the mean for the different brain regions was as follow: the cortex: 1207.318 ± 4576.370 , the hippo: -6042.555 ± 4396.834 , the brain: 4292.009 ± 3807.770 , the cerebellum: 9916.704 ± 4396.834 .

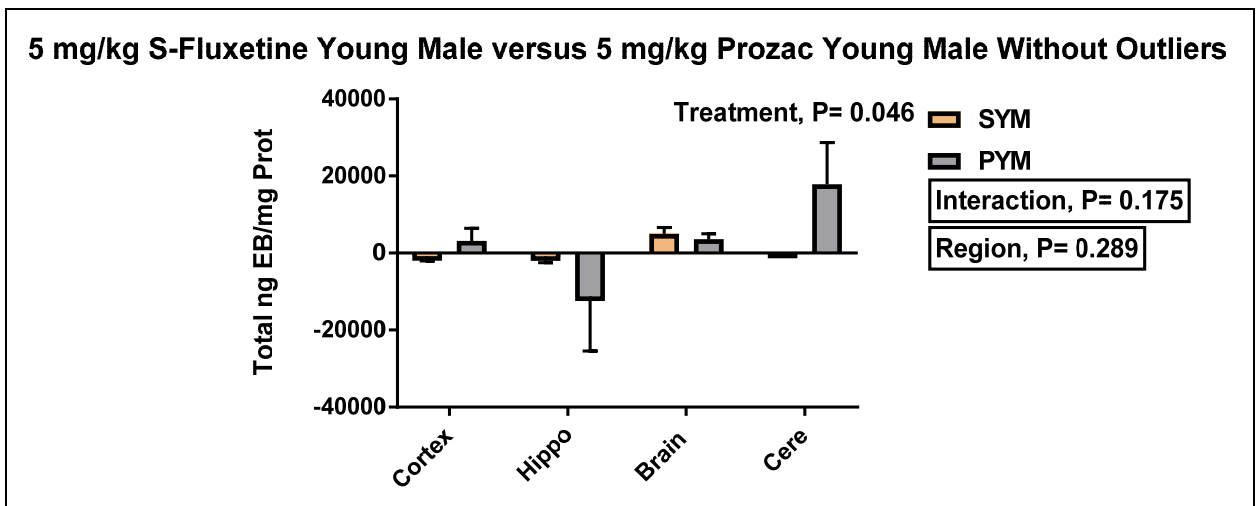


Figure 42: Comparison between young male rats that have given 5 mg/kg S-fluoxetine, and young male rats that have given 5 mg/kg of Prozac (SYM vs. PYM) for three days. The x-axis represents the different brain regions: cortex, peri-ventricular and hippocampus, striatum-caudate putamen-hypothalamus, and cerebellum. The y-axis represents the total ng EB/mg protein. Two-way ANOVA was performed. Columns represent the mean for each

group and error bars show standard error of mean (SEM). Interaction, $P=0.175$. Region, $P=0.289$. Treatment, $P=0.046$. The n for the animal groups of the SYM was as follow: the n for the cortex was 6, the n for the hippocampus was 7, the n for the brain was 7, the n for the cerebellum was 6. The n for the PYM = 7.

Figure 42 shows the data from Figure 41 with the statistical outliers removed. The data shows that there was no significant difference in ng Evans Blue/mg protein for the interaction between the different brain regions and the drug treatment ($P = 0.175$; S-fluoxetine versus Prozac). Also, there was no significant difference between the different brain regions in the young male rats ($P = 0.289$). In addition, there was a significant difference between the drug treatments ($P = 0.046$; S-Fluoxetine versus Prozac). The root mean square error, which is defined as the residual mean square. It is used to estimate the common within-group standard deviation which also known as the standard error of the estimate were as the following. The mean \pm the standard error of the mean for the different brain regions are as follow: cortex: 1207.318 ± 3150.173 , peri-ventricular and hippocampus: 1369.637 ± 3026.589 , striatum-caudate putamen-hypothalamus (brain): 4149.152 ± 3026.589 and the cerebellum: 8820.290 ± 3150.173 . The mean \pm the standard error of the mean for the treatment groups was as follow: SYM: 724.661 ± 2227.509 , PYM: 7048.537 ± 2140.121 .

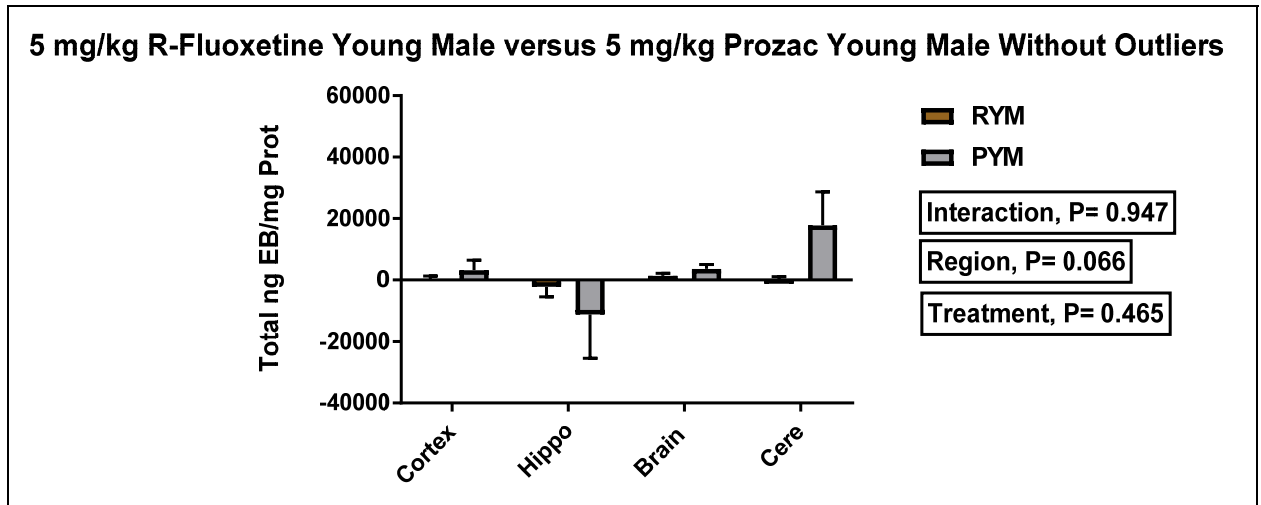


Figure 43: Comparison between young male rats that have given 5 mg/kg R-fluoxetine, and young male rats that have given 5 mg/kg Prozac (RYM vs. PYM) for three days. The x-axis represents the different brain regions: cortex, peri-ventricular and hippocampus, striatum-caudate putamen-hypothalamus (brain), cerebellum. The y-axis represents the total ng Evans Blue/mg protein. Two-way ANOVA was performed. Columns represent the mean for each group and error bars show standard error of mean (SEM). Interaction, $P=0.947$, Region, $P=0.066$, Treatment, $P=0.465$. The n for the different animal groups was as follow, RYM=11, PYM =7 .

Figure 43 shows there was no significant difference in ng Evans Blue/mg protein for the interaction between the different brain regions and drug treatment groups ($P = 0.947$; R-fluoxetine versus Prozac). Also, there was no significant difference between the different brain regions between the groups ($P = 0.066$), although this P value does show a strong trend. In addition, there was no significant difference between the different drug treatment groups ($P = 0.465$; R-fluoxetine versus Prozac). The outliers were determined by using the ROUT analysis at medium setting. The RYM group had four outliers. The first outlier (134723.409) was located at the cortex. In contrast, the rest outliers (24064.006, 41496.548

and 197113.231) were located at the cerebellum. The root mean square error, which is defined as the residual mean square. It is used to estimate the common within-group standard deviation which also known as the standard error of the estimate were as the following. The mean \pm the standard error of the mean: RYM: 8898.305 ± 4905.524 , PYM: 3342.441 ± 5752.236 . The mean \pm the standard error of the mean for the different brain regions was as follow: cortex: 7750.548 ± 7866.338 , hippo: -6717.974 ± 6555.282 , brain: 2495.001 ± 7866.338 , cerebellum: 20953.918 ± 7866.338 . The mean \pm the standard error of the mean: RYM: 8898.305 ± 4905.524 , PYM: 3342.441 ± 5752.236 . The mean \pm the standard error of the mean for the different brain regions are as follow: cortex: 7750.548 ± 7866.338 , hippo: -6717.974 ± 6555.282 , brain: 2495.001 ± 7866.338 , cerebellum: 20953.918 ± 7866.338 .

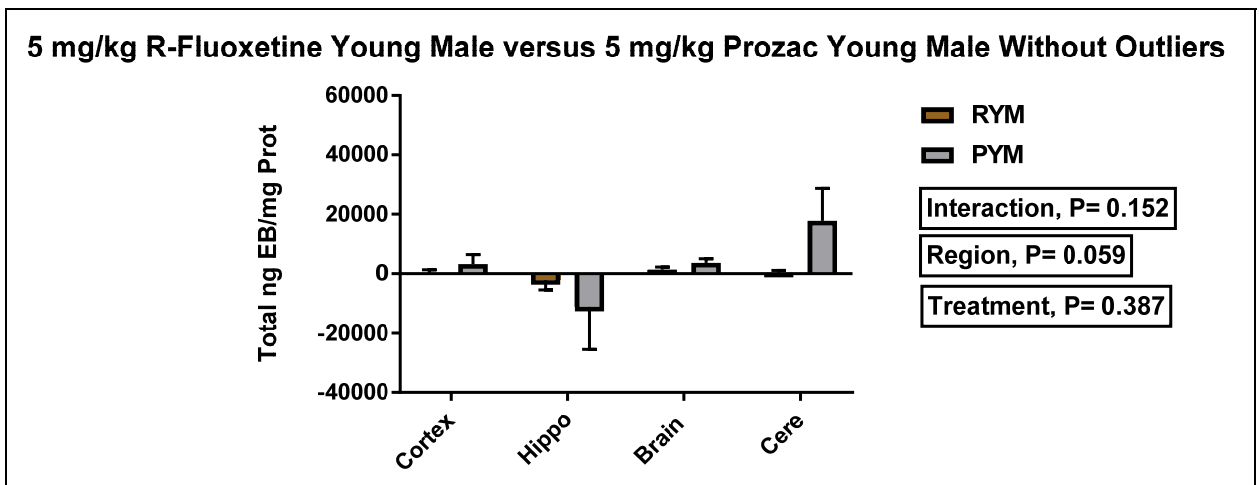


Figure 44: Comparison between young male rats that have given 5 mg/kg R-fluoxetine, and young male rats that have taken 5mg/kg of Prozac (RYM vs. PYM) for three days. The x-axis represents the different brain regions: cortex, peri-ventricular and hippocampus, striatum-caudate putamen-hypothalamus, and cerebellum. The y-axis represents the total ng EB/mg protein. Two-way ANOVA was performed. Columns represent the mean for each

group and error bars show standard error of mean (SEM). Interaction, $P= 0.152$, Region, $P=0.059$, Treatment, $P= 0.387$. The n of the animal groups of the RYM were as follow: the n for the cortex was 9, the n for the hippo was 11, the n for the brain was 11 and the n for the cerebellum was 8. The n for the PYM =7.

Figure 44 shows the data from Figure 43 without the statistical outliers. The data shows that there was no significant difference in ng Evans Blue/mg protein for the interaction between the different brain regions and drug treatments ($P = 0.152$; R-fluoxetine versus Prozac) although the P value is low and does show a trend. Also, there was no significant difference between the different brain regions in the young male rats ($P = 0.059$), with this P value just missing significance, showing a very strong trend. In addition, there was no significant difference between the drug treatments ($P = 0.387$; R-fluoxetine versus Prozac). The root mean square error, which is defined as the residual mean square. It is used to estimate the common within-group standard deviation which also known as the standard error of the estimate were as the following. The mean \pm the standard error of the mean for the different brain regions are as follow: cortex: 1629.792 ± 3950.262 , peri-ventricular and hippocampus: -6717.974 ± 3875.621 , striatum-caudate putamen-hypothalamus (brain): 2495.001 ± 3875.621 and the cerebellum: 9054.164 ± 4148.604 . The mean \pm the standard error of the mean for the treatment groups was as follow: RYM: -111.950 ± 2556.352 , PYM: 3342.441 ± 3029.712 .

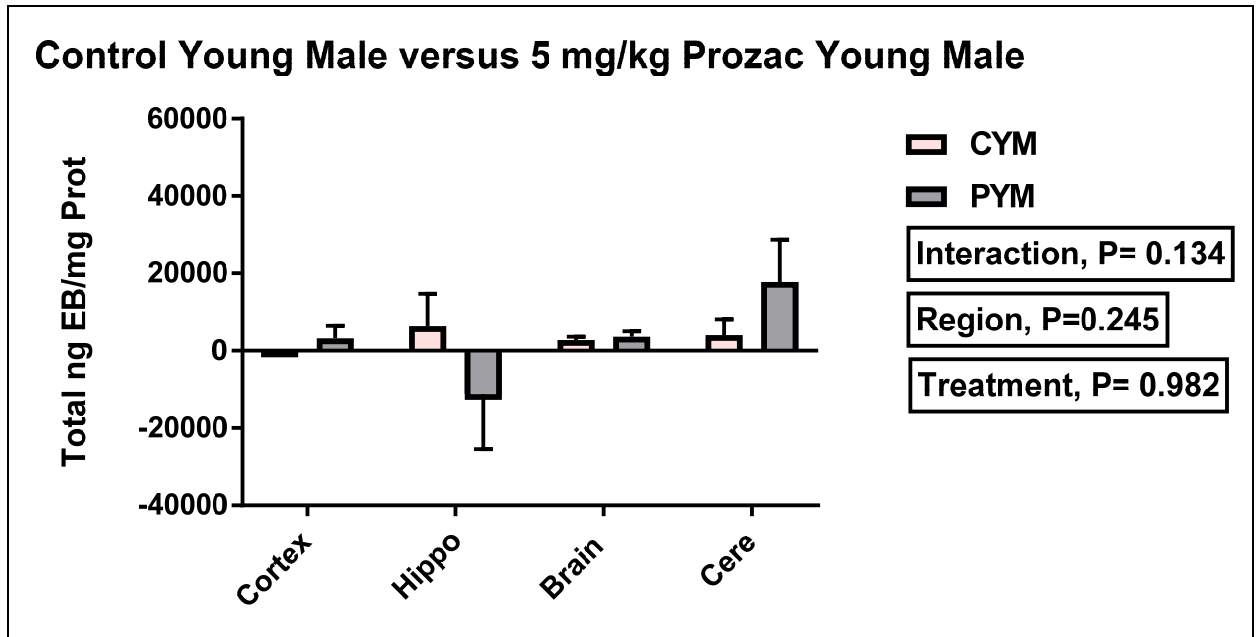


Figure 45: Comparison between young male rats that have not given any drug, and young male rats that have given 5 mg/kg Prozac for three days (CYM vs. PYM). The x-axis represents the different brain regions: cortex, peri-ventricular and hippocampus, striatum-caudate putamen-hypothalamus (brain), cerebellum. The y-axis represents the total ng Evans Blue/mg protein. Two-way ANOVA was performed. Columns represent the mean for each group and error bars show standard error of mean (SEM). Interaction, $P= 0.134$, Region, $P=0.245$, Treatment, $P= 0.982$. The n for the animal groups was as follow: CYM =10, PYM =7.

Figure 45 shows there was no significant difference in ng Evans Blue/mg protein for the interaction between the different brain regions and drug treatment groups ($P = 0.134$). Also, there was no significant difference between the different brain regions for the young male rats ($P = 0.245$). In addition, there was no significant difference between the different drug treatment groups ($P =0.982$). The outliers were determined by using the ROUT analysis at medium settings. The CYM had two outliers. The first outlier

(80868.926) was located at the hippocampus region while the second outlier (40375.985) was located at the cerebellum region. The root mean square error, which is defined as the residual mean square. It is used to estimate the common within-group standard deviation which also known as the standard error of the estimate were as the following. The mean \pm the standard error of the mean: CYM: 3760.815 ± 3939.969 , PYM: 1492.191 ± 4097.067 . The mean \pm the standard error of the mean for the different brain regions was as follow: cortex: 969.421 ± 5320.791 , hippo: -3701.888 ± 4483.520 , brain: 1620.648 ± 7493.500 , cere: 9516.984 ± 5320.791 .

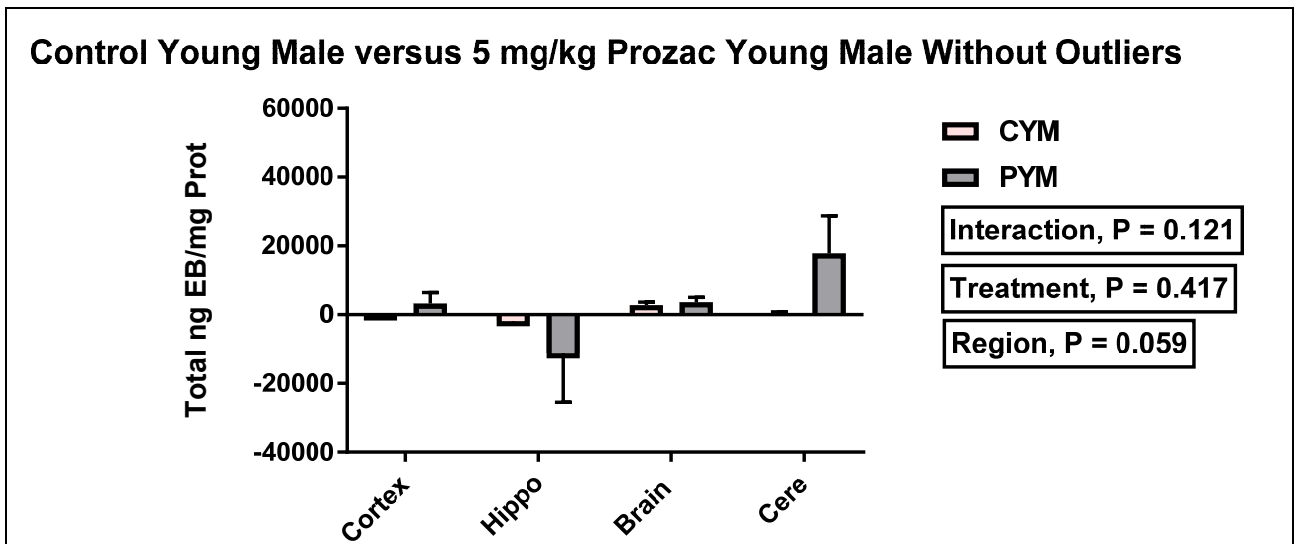


Figure 46: Comparison between young male rats that have given 5 mg/kg of Prozac, and young male rats that have not given any drug (CYM vs. PYM). The x-axis represents the different brain regions: cortex, peri-ventricular and hippocampus, striatum-caudate putamen-hypothalamus, and cerebellum. The y-axis represents the total ng EB/mg protein. Two-way ANOVA was performed. Columns represent the mean for each group and error bars show standard error of mean (SEM). Interaction, $P= 0.121$, Region, $P=0.059$, Treatment, $P= 0.417$. The n of the animal groups of the CYM were as follow: the n for the

cortex was 10, the n for the hippo was 9, the n for the brain was 10, and the n for the cerebellum was 9. The n for the PYM=7.

Figure 46 shows the data from Figure 45 without the statistical outliers. The data shows that there was no significant difference in ng Evans Blue/mg protein for interaction between the different brain regions and the drug treatment ($P = 0.121$; Prozac versus Control). Also, there was no significant difference between the different brain regions in young male rats ($P = 0.059$). In addition, there was no significant difference between the drug treatment ($P = 0.417$). The root mean square error, which is defined as the residual mean square. It is used to estimate the common within-group standard deviation which also known as the standard error of the estimate were as the following. The mean \pm the standard error of the mean for the different brain regions are as follow: cortex: 1473.077 ± 3855.508 , peri-ventricular and hippocampus: -6560.820 ± 3942.719 , striatum-caudate putamen-hypothalamus (brain): 3173.998 ± 3855.508 and the cerebellum: 8913.678 ± 3942.719 . The mean \pm the standard error of the mean for the treatment groups was as follow: CYM: 157.526 ± 2541.831 , PYM: 3342.441 ± 2957.040 .

Summary: When total ng Evans blue in regions is normalized by the amount of protein measured from the tissue in milligrams. We also compared the different treatment groups (R-fluoxetine and S-fluoxetine) with Prozac treatment group. We found there was no significant difference in interaction, region and treatments. The hippocampus showed the lowest blood brain barrier permeability among the different brain regions and the cerebellum showed the highest blood brain barrier permeability among the different brain regions.

3.6 Comparisons among the Old Males Groups

One Way ANOVA of total ng EB/mg protein

The listed figures represent the comparison of the normalized measurements of Evans blue among the different old male rat groups (COM vs. SOM, COM vs. ROM and ROM vs. SOM). The amount of Evans blue was normalized by measuring the total amount of Evans blue in (ng). Then, dividing it by the amount of the protein concentration in mg which was determined by a Bradford protein assay.

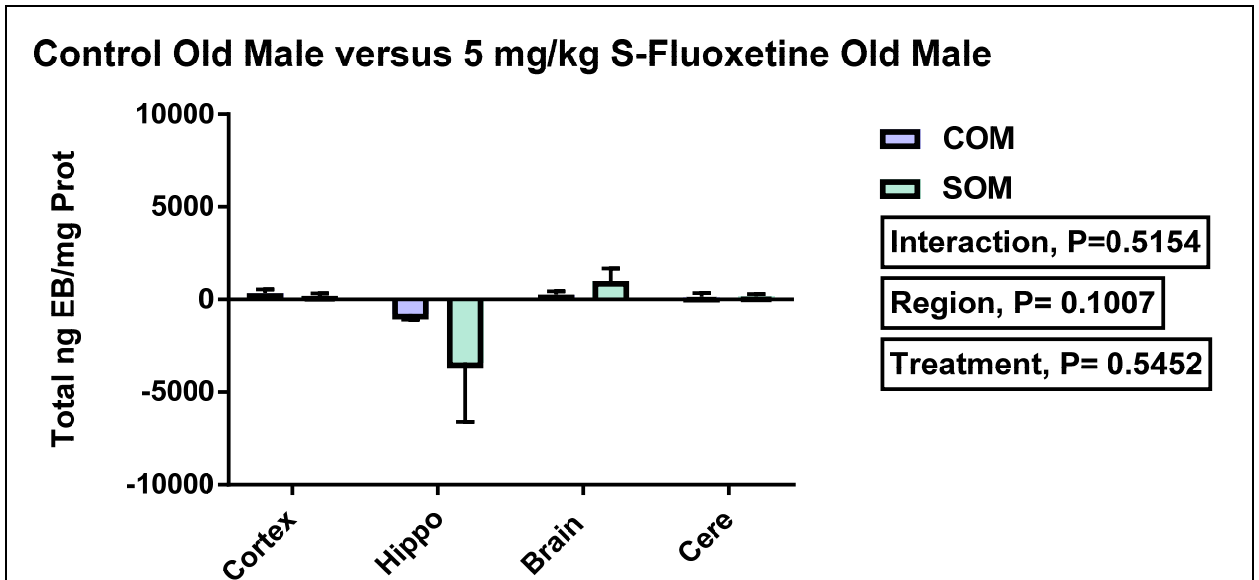


Figure 47: Comparison between old male rats that have not taken any drug, and old male rats that have taken 5 mg/kg S-fluoxetine for three days. The x-axis represents the different brain regions: cortex, peri-ventricular and hippocampus, striatum-caudate putamen-hypothalamus (brain), and cerebellum. The y-axis represents the total ng EB/mg protein. Two-way ANOVA was performed. Columns represent the mean for each group and error

bars show standard error of mean (SEM). Interaction, P= 0.5154. Region, P= 0.1007. Treatment, P= 0.5452. The n of the animals groups were as follow: COM = 7, SOM=7.

Figure 47 shows that there was no significant difference in the amount of Evans Blue/mg protein for interaction between the different brain regions and drug treatment groups (P = 0.5154). Also, there was no significant difference between the different brain regions (P = 0.1007), although this did show a strong trend. In addition, there was no significant difference between the drug treatment groups (P =0.5452) comparing control and S-fluoxetine in old male rats. The outliers were determined by using the ROUT analysis at medium setting. The outliers were found in the SOM group. The outlier 22521.990 was located in the hippocampus while the outlier 4306.475 was located at the brain region. The root mean square error, which is defined as the residual mean square. It is used to estimates the common within-group standard deviation which also known as the standard error of the estimate were as the following. The mean \pm the standard error of the mean for COM: 18.412 ± 508.142 , SOM: -559.024 ± 543.227 . The mean \pm the standard error of the mean for the different brain regions was as follow: cortex: 270.698 ± 665.315 , hippo: -2091.274 ± 768.239 , brain: 541.472 ± 768.239 , cerebellum: 197.881 ± 768.239 .

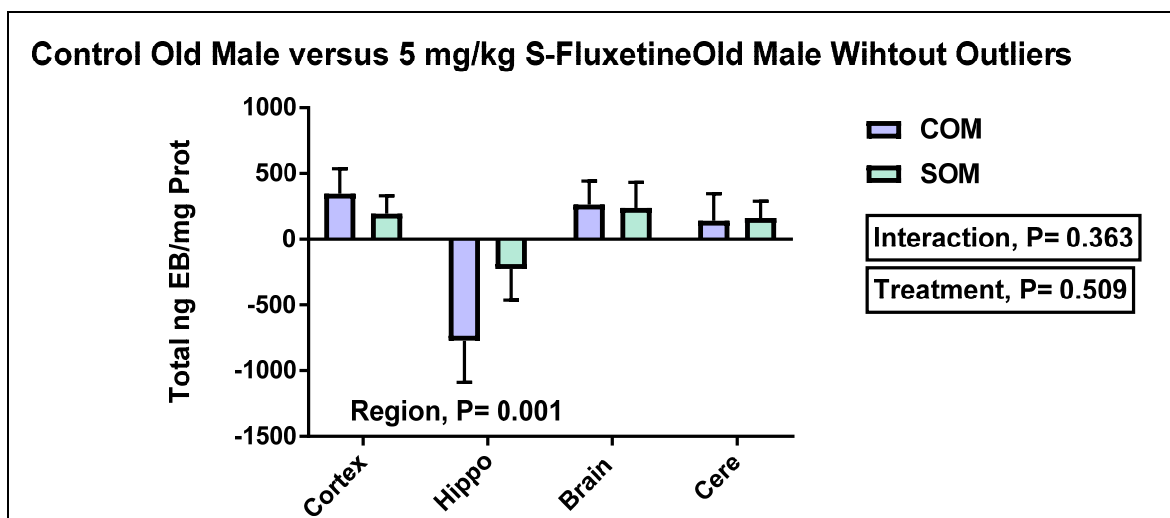


Figure 48: Comparison between old male rats that have not taken any drug, and old male rats that have taken 5 mg/kg S-fluoxetine for three days (COM vs. SOM) without outliers. The x-axis represents the different brain regions: cortex, peri-ventricular and hippocampus, striatum-caudate putamen-hypothalamus (brain), and cerebellum. The y-axis represents the total ng EB/mg protein. Two-way ANOVA was performed. Columns represent the mean for each group and error bars show standard error of mean (SEM). Interaction, $P = 0.363$. Region, $P = 0.001$. Treatment, $P = 0.509$. The n of the SOM for the different animal groups were as follow: the n for the cortex was 7, the n for the hippocampus was 6, the n for the brain was 6, and the n for the cerebellum was 7. The n for the COM = 7.

Figure 48 shows the data from figure 47 without the statistical outliers. The data shows that there was no significant difference in the amount of Evans Blue/mg protein for interaction between the different brain regions and the drug treatment groups ($P = 0.363$). However, there was a significant difference in the amount of Evans Blue/protein between the different brain regions ($P = 0.001$). There was no significant difference between the drug treatment groups ($P = 0.509$). The root mean square error, which is defined as the

residual mean square. It is used to estimate the common within-group standard deviation which is also known as the standard error of the estimate were as the following. The mean \pm the standard error of the mean: COM: -5.023 ± 101.053 , SOM: 92.014 ± 105.180 . The mean \pm the standard error of the mean for the different brain regions: cortex: 270.698 ± 142.911 , the hippo: -498.726 ± 148.747 , brain: 250.928 ± 148.747 , cerebellum: 151.082 ± 142.911 .

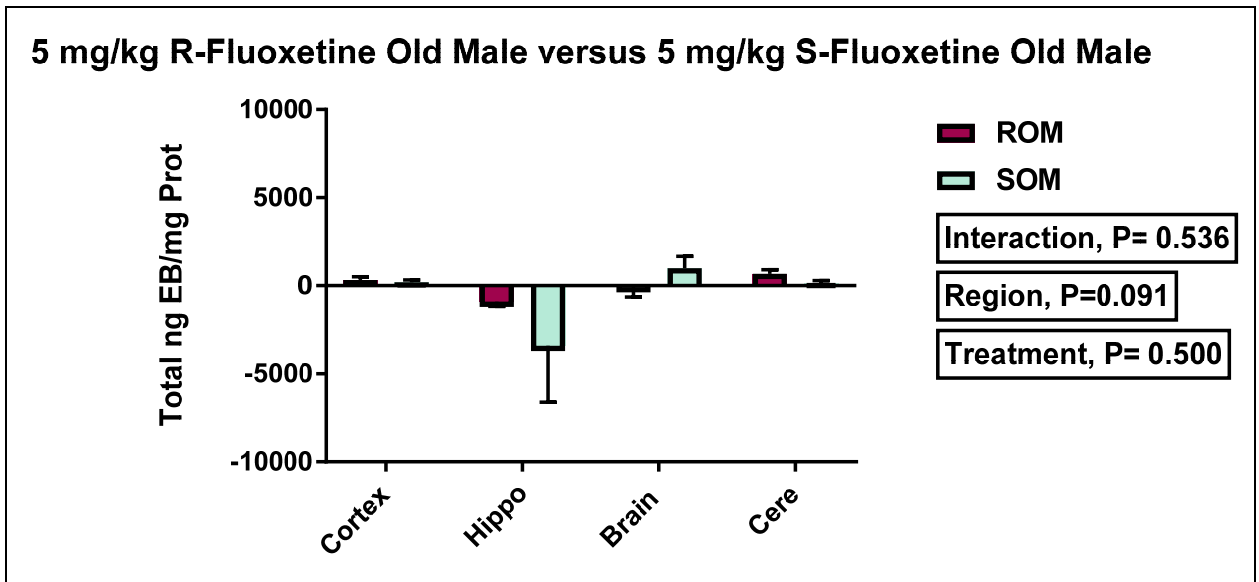


Figure 49: Comparison between old male rats that have given R-fluoxetine, and old male rats that have taken 5 mg/kg S-fluoxetine for three days (ROM vs. SOM). The x-axis represents the different brain regions: cortex, peri-ventricular and hippocampus, striatum-caudate putamen-hypothalamus (brain), and cerebellum. The y-axis represents the total ng EB/mg protein. Two-way ANOVA was performed. Columns represent the mean for each group and error bars show standard error of mean (SEM). Interaction, $P= 0.536$. Region, $P=0.091$. Treatment, $P= 0.500$.

$P = 0.091$. Treatment, $P = 0.500$. The n of the animal groups were as follow: ROM =7, SOM =7.

Figure 49 shows that there was no significant difference in the amount of Evans Blue/mg protein for the interaction between the different brain regions and drug treatment groups ($P = 0.536$). Also, there was no significant difference between the different brain regions ($P = 0.091$), although the P value shows there is a strong trend. In addition, there was no significant difference between the drug treatment ($P = 0.500$). The outliers were determined by using the ROUT analysis at medium setting. The outliers were only found in the SOM group. The outlier 22521.990 was located in the hippocampus while the outlier 4306.475 was located at the lower brain region. The root mean square error, which is defined as the residual mean square. It is used to estimate the common within-group standard deviation which also known as the standard error of the estimate were as the following. The mean \pm the standard error of the mean, ROM: 5.780 ± 137.701 , SOM: 120.155 ± 147.132 . The mean \pm the standard error of the mean for the different brain regions are as follow: cortex: 260.137 ± 194.739 , hippo: -564.159 ± 202.691 , brain: 139.670 ± 213.326 , cerebellum: 416.222 ± 194.739 .

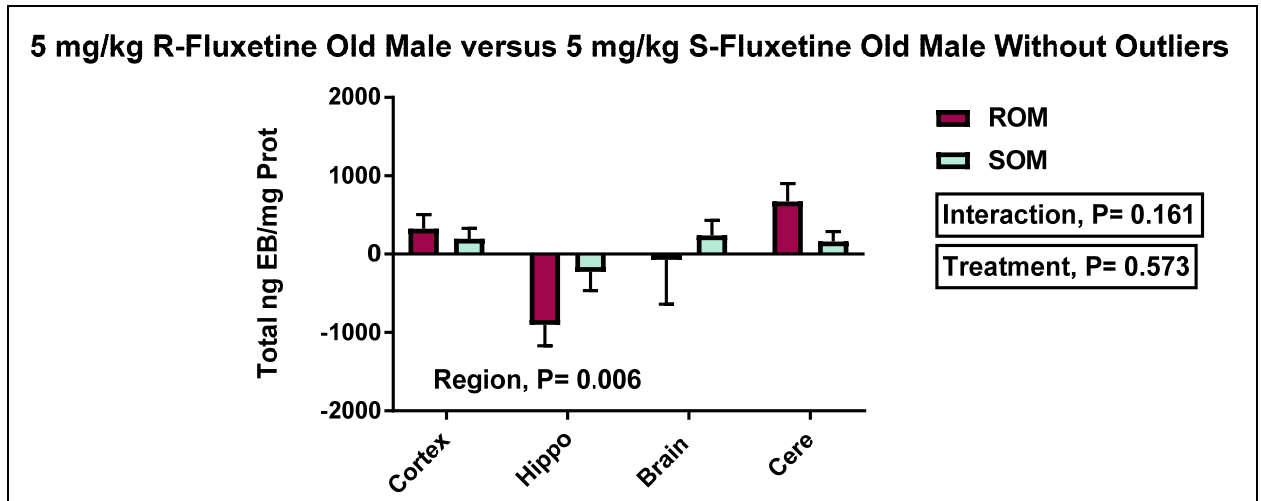


Figure 50: Comparison between old male rats that have given R-fluoxetine, and old male rats that have taken 5 mg/kg S-fluoxetine (ROM vs. SOM). The x-axis represents the different brain regions: cortex, peri-ventricular and hippocampus, striatum-caudate putamen-hypothalamus (brain), and cerebellum. The y-axis represents the total ng EB/mg protein. Two-way ANOVA was performed. Columns represent the mean for each group and error bars show standard error of mean (SEM). Interaction, $P= 0.161$. Region, $P= 0.006$. Treatment, $P= 0.573$. The n for the SOM of the animal groups were as follow: the n for the cortex was 7, the n for the hippo was 6, the n for the brain was 6, and the n for the cerebellum was 7. The n for the ROM =7.

Figure 50 shows that there was no significant difference for interaction between the different brain regions and treatment groups ($P = 0.161$). Also, there was a significant difference between the different brain regions ($P = 0.006$). In addition, there was no significant difference between the treatment ($P=0.573$). The root mean square error, which is defined as the residual mean square. It is used to estimates the common within-group standard deviation which also known as the standard error of the estimate were as the following. The mean \pm the standard error of the mean for the different brain regions are as

follow: cortex: 260.137 ± 194.739 , peri-ventricular and hippocampus: -564.159 ± 202.691 , striatum-caudate putamen-hypothalamus (brain): 139.670 ± 213.326 and the cerebellum: 416.222 ± 194.739 . The mean \pm the standard error of the mean for the treatment groups was as follow: ROM: 5.780 ± 137.701 , SOM: 120.155 ± 147.132 .

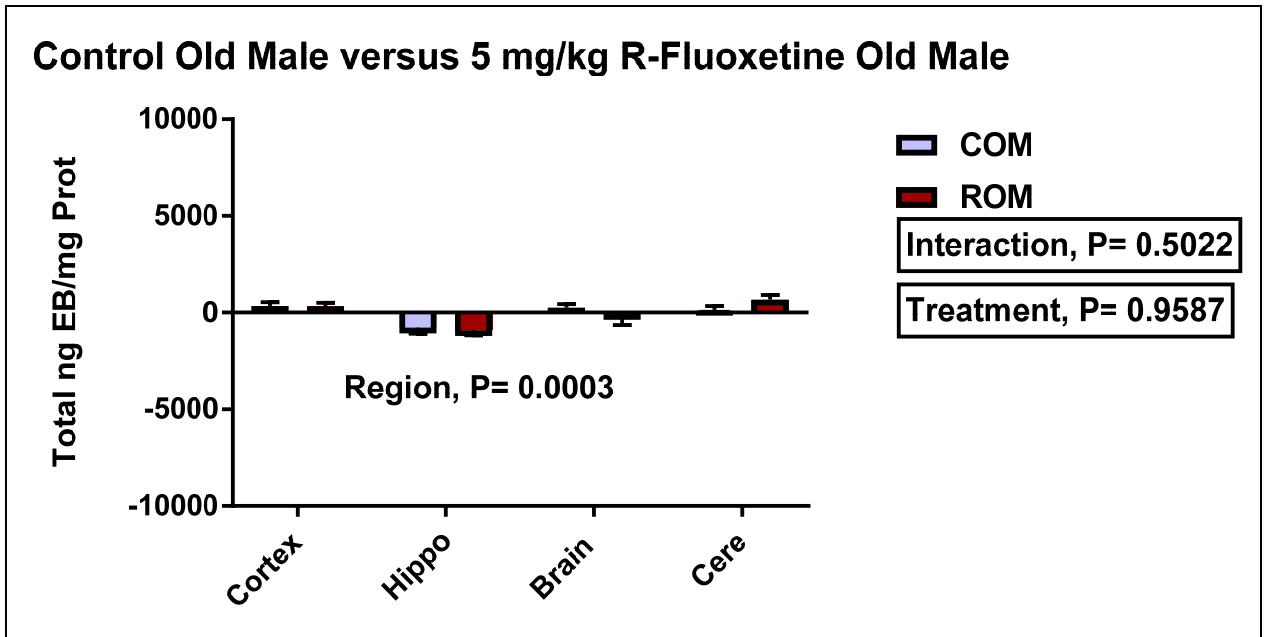


Figure 51: Comparison between old male rats that have given 5 mg/kg R-fluoxetine, and old male rats that have not taken any drug (ROM vs. COM). The x-axis represents the different brain regions: cortex, peri-ventricular and hippocampus, striatum-caudate putamen-hypothalamus (brain), and cerebellum. The y-axis represents the total ng EB/ mg Protein. Two-way ANOVA was performed. Columns represent the mean for each group and error bars show standard error of mean (SEM). Interaction, P= 0.5022. Region, P =

0.0003. Treatment, $P= 0.9587$. The n of the animal groups were as follow: COM =7, ROM =7.

Figure 51 shows that there was no significant difference for ng Evans Blue/mg protein in interaction between the different brain regions and drug treatment groups ($P = 0.5022$). However, there was a significant difference between the different brain regions ($P = 0.0003$), with the hippocampal region showing significantly lower permeability. In addition, there was no significant difference between the drug treatments for the old male rats ($P=0.9587$). The root mean square error, which is defined as the residual mean square. It is used to estimate the common within-group standard deviation which also known as the standard error of the estimate were as the following. The mean \pm the standard error of the mean for the different treatment groups were as follow: COM: -5.023 ± 146.680 , ROM: 71.334 ± 146.680 . The mean \pm the standard error of the mean for the different regions were as follow: cortex: 336.672 ± 207.437 , hippocampus: -705.451 ± 207.437 , brain: 95.381 ± 207.437 , cerebellum: 406.022 ± 207.437 .

Summary: Our statistical analysis for different drug treatments in old male rats showed that there was a significant difference for the blood brain barrier permeability for the different brain regions with the hippocampus showing the lowest blood brain barrier permeability. S-fluoxetine and R-fluoxetine seemed to have no effect on the blood brain barrier permeability because the treatment effect was not significantly different. Also, there was no interaction between the different brain regions and the treatment groups.

3.7 Comparison among Old Female Rats

Two-Way ANOVA of total ng EB/mg Protein

In the next set of figures, we normalized the amount of Evans blue in a region by dividing the total ng Evans blue in that region by the protein concentration in mg, determined by a Bradford protein assay. Then, we compared the total amount of ng Evans blue divided by the amount of protein (mg) in old female rats versus old male rats.

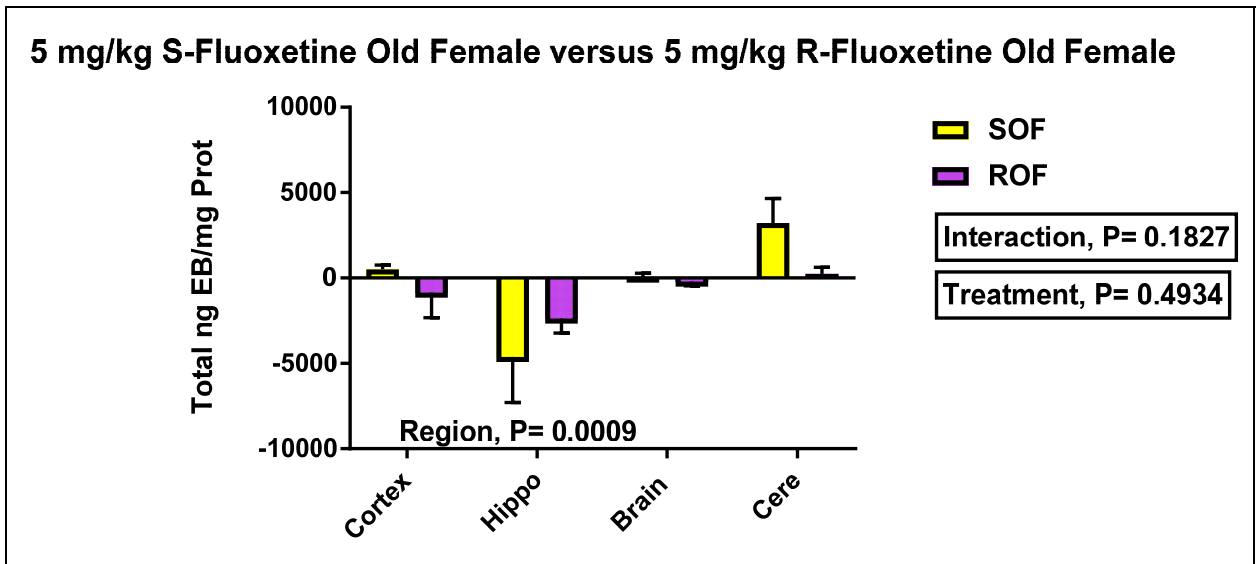


Figure 52: Comparison between old female rats that have given 5 mg/kg R-fluoxetine, and old female rats that have given 5 mg/kg S-fluoxetine (ROF vs. SOF) for three days. The x-axis represents the different brain regions: cortex, peri-ventricular and hippocampus, striatum-caudate putamen-hypothalamus (brain), cerebellum. The y-axis represents the total ng EB/mg protein. Two-way ANOVA was performed. Columns represent the mean for each group and error bars show standard error of mean (SEM). Interaction, $P=0.1827$. Region, $P=0.0009$. Treatment, $P=0.4934$. The n of the animal groups were as follow: SOF =6, ROF=7.

Figure 52 shows that there was no significant difference in the ng Evans Blue/mg protein for the interaction between the different brain regions and drug treatment groups ($P = 0.1827$). However, there was significant difference between the different brain regions

for the old female rats ($P = 0.0009$), with the hippocampal region showing the lowest permeability to Evan Blue. In addition, there was no significant difference between the drug treatment groups ($P = 0.4934$: R-fluoxetine versus S-Fluoxetine). Statistical outliers were determined by using the ROUT analysis at medium setting. The outlier (9420.832) was found in the cortical region of the old female rats receiving R-fluoxetine. The root mean square error, which is defined as the residual mean square. It is used to estimate the common within-group standard deviation which also known as the standard error of the estimate were as the following. The mean \pm the standard error of the mean for SOF: -212.614 ± 582.205 , ROF: -797.972 ± 504.204 . The mean \pm the standard error of the mean for the brain regions are as follow: cortex: -173.417 ± 793.412 , hippo: -3495.600 ± 793.412 , brain: -88.753 ± 793.412 , cerebellum: 1736.597 ± 695.868 .

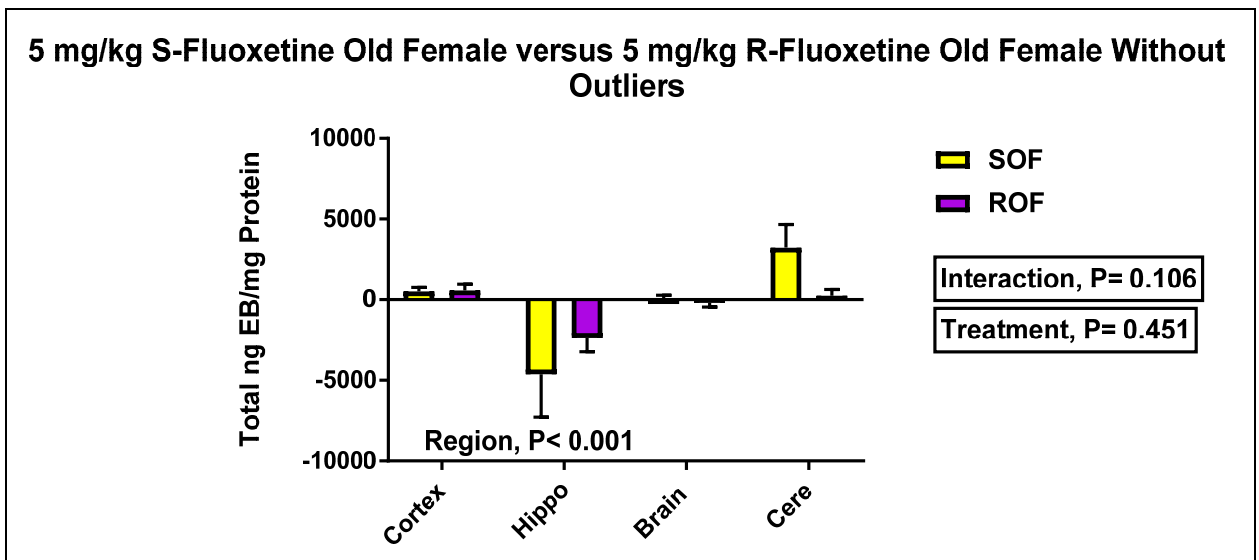


Figure 53: Comparison between old female rats that have taken 5mg/kg R-fluoxetine (ROF), and old female rats that have taken 5 mg/kg S-fluoxetine (SOF) for three days. The x-axis represents the different brain regions: cortex, peri-ventricular and hippocampus, striatum-caudate putamen-hypothalamus, and cerebellum. The y-axis represents the total

ng EB. Two-way ANOVA was performed. Columns represent the mean for each group and error bars show standard error of mean (SEM). Interaction, $P=0.106$. Region, $P<0.001$. Treatment, $P=0.451$. The n for the SOF = 6, the n for the ROF was as follow: the n for the cortex = 6, the n for the hippocampus = 7, the n for the lower brain region = 7, the n for the cerebellum = 7.

Figure 53 shows the same data as Figure 52 but without the statistical outliers. The data shows that there was no significant difference for ng Evans Blue/mg protein for interaction between the different brain regions and drug treatment groups ($P = 0.106$; S-fluoxetine versus R-fluoxetine). However, there was a significant difference between the different brain regions between old female rats given different Fluoxetine enantiomers as drug treatments ($P < 0.001$), with the hippocampal region showing the lowest permeability to Evan Blue. In addition, there was no significant difference between the drug treatment ($P = 0.451$; Fluoxetine enantiomers). The root mean square error, which is defined as the residual mean square. It is used to estimates the common within-group standard deviation which also known as the standard error of the estimate were as the following. The mean \pm the standard error of the mean for the different brain regions are as follow: cortex: -173.417 ± 793.412 , peri-ventricular and hippocampus: -3495.600 ± 793.412 , striatum-caudate putamen-hypothalamus (brain): -88.753 ± 793.412 and the cerebellum: 1736 ± 695.868 . The mean \pm the standard error of the mean for the treatment groups was as follow: SOF: -212.614 ± 582.205 , ROF: -797.972 ± 504.204 .

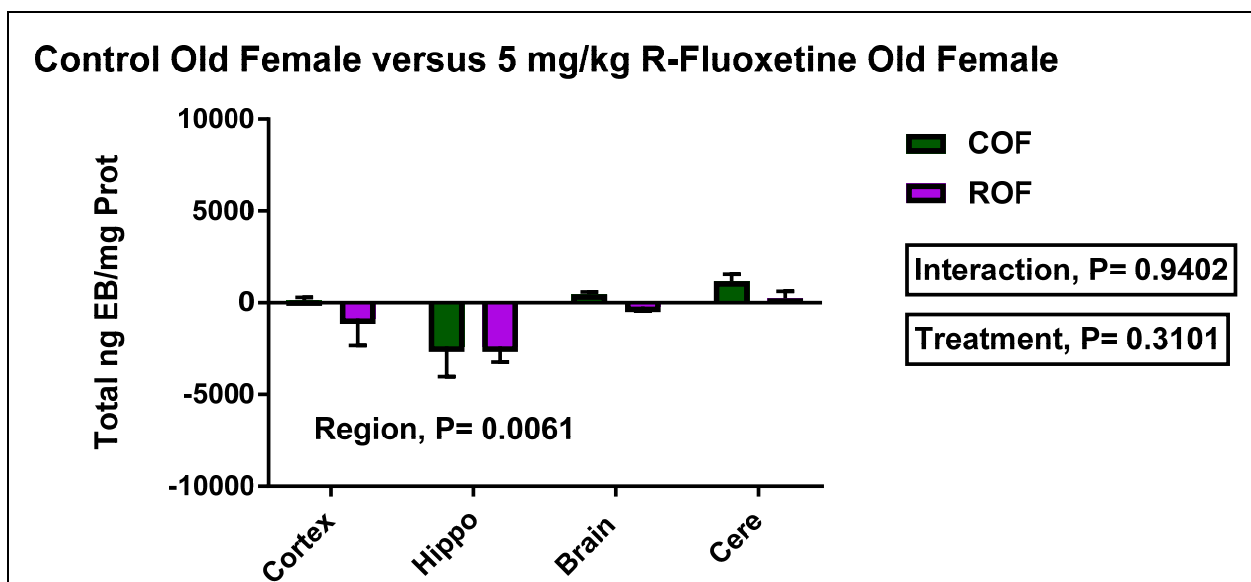


Figure 54: Comparison between old female rats that have given 5 mg/kg R-fluoxetine for three days, and old female rats that have not given any drug (ROF vs. COF). The x-axis represents the different brain regions: cortex, peri-ventricular and hippocampus, striatum-caudate putamen-hypothalamus (brain), cerebellum. The y-axis represents the total ng EB/mg protein. Two-way ANOVA was performed. Columns represent the mean for each group and error bars show standard error of mean (SEM). Interaction, $P=0.9402$. Region, $P=0.0061$. Treatment, $P=0.3101$. The n of the animal groups were as follow: COF = 7, ROF = 7.

Figure 54 shows that there was no significant difference in the total ng Evans Blue/mg protein for interaction between the different brain regions and drug treatment groups ($P = 0.9402$; control versus R-fluoxetine). However, there was a significant difference between the different brain regions for the old female rats ($P = 0.0061$), with the hippocampal region showing the lowest permeability to Evans Blue. There was no significant difference between the drug treatment groups ($P = 0.3101$; control versus R-fluoxetine). The ROUT analysis at medium setting was used to determine the outliers. One outlier was found at the

cortex in the ROF group. The outlier was 9420.832. The COF group had two outliers. One outlier was found in the cortex which was 4503.975. The other outlier was found in the hippocampus, the outlier was -12021.576. Cere: 706.182. The root mean square error, which is defined as the residual mean square. It is used to estimate the common within-group standard deviation which also known as the standard error of the estimate were as the following. The mean \pm the standard error of the mean: COF: 245.048 ± 346.805 , ROF: -797.972 ± 333.199 . The mean \pm the standard error of the mean for the different brain regions was as follow: the cortex: -367.930 ± 490.456 , hippo: -1568.491 ± 490.456 , brain: 124.390 ± 471.215 , cerebellum: 706.182 ± 471.215 .

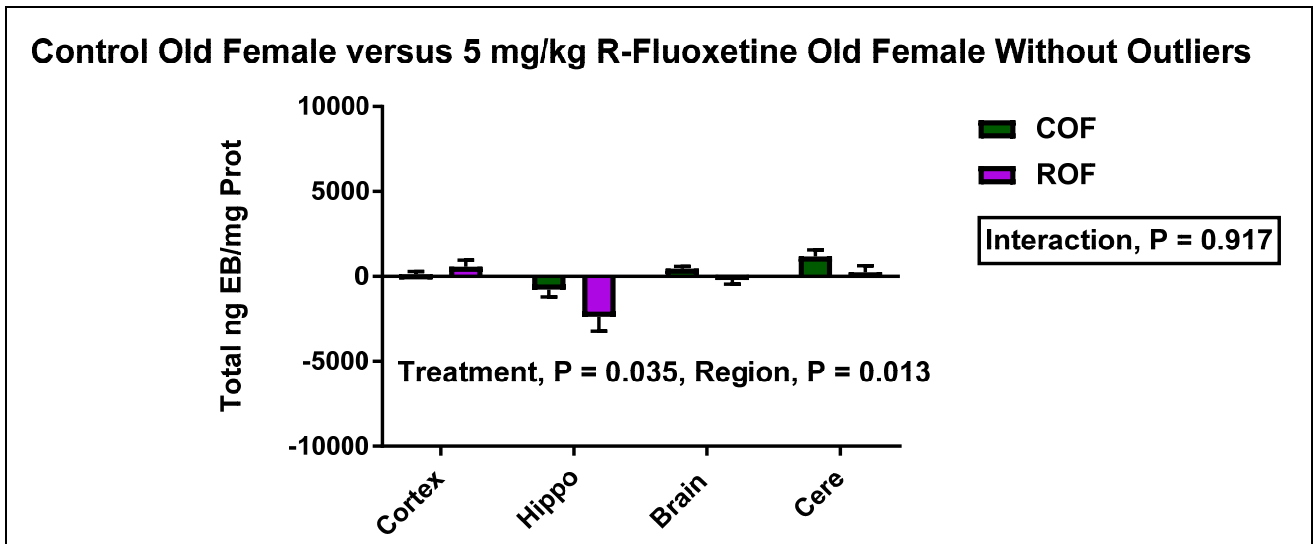


Figure 55: Comparison between old female rats that have given 5 mg/kg R-fluoxetine for three days, and old female rats that have not given any drug (ROF vs. COF). The x-axis represents the different brain regions: cortex, peri-ventricular and hippocampus, striatum-caudate putamen-hypothalamus (brain), and cerebellum. The y-axis represents the total ng EB. Two-way ANOVA was performed. Columns represent the mean for each group and

error bars show standard error of mean (SEM). Interaction, P=0.917. Region, P=0.013. Treatment, P=0.035. The number of animals, n for the COF different brain regions were as follow: the n for the cortex = 6, the n for the hippocampus = 6, the n for the lower brain region = 7, the n for the cerebellum = 7.

Figure 55 the same data as Figure 54, but without the statistical outliers. The data shows that there was no significant difference in ng Evans Blue/mg protein for interaction between the different brain regions and drug treatment groups (P = 0.917). However, there was a significant difference between the different brain regions for the old female groups being compared (P = 0.013), with cerebellum showing increased permeability and the hippocampus showing the lowest permeability. There was also a significant difference between the drug treatment groups (P = 0.035), with the R-fluoxetine tightening the blood brain barrier compared to the control animals. The root mean square error, which is defined as the residual mean square. It is used to estimate the common within-group standard deviation which also known as the standard error of the estimate were as the following. The mean \pm the standard error of the mean for the different brain regions are as follow: cortex: -368.180 ± 490.460 , peri-ventricular and hippocampus: -1568.492 ± 490.460 , striatum-caudate putamen-hypothalamus (brain): 124.390 ± 471.219 and the cerebellum: 706.182 ± 471.219 . The mean \pm the standard error of the mean for the treatment groups was as follow: COF: 244.922 ± 346.808 , ROF: -797.972 ± 333.202 .

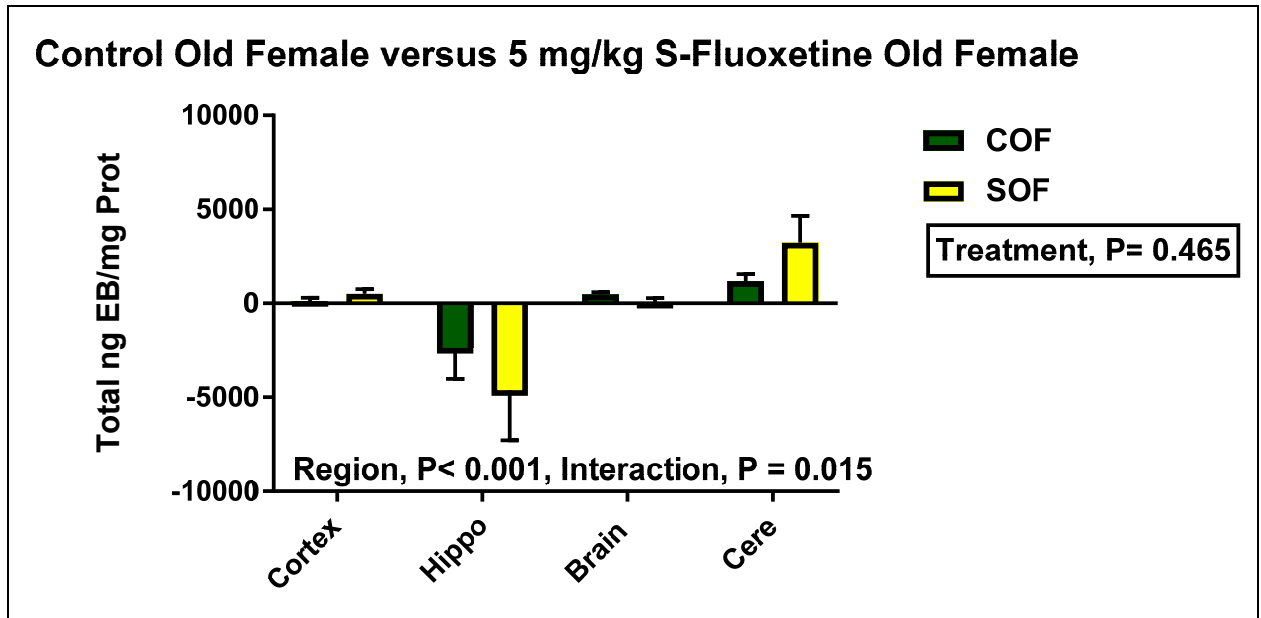


Figure 56: Comparison between old female rats that have given 5 mg/kg S-fluoxetine for three days, and old female rats that have not given any drug (SOF vs. COF). The x-axis represents the different brain regions: cortex, peri-ventricular and hippocampus, striatum-caudate putamen-hypothalamus (brain), cerebellum. The y-axis represents the total ng EB/mg protein. Two-way ANOVA was performed. Columns represent the mean for each group and error bars show standard error of mean (SEM). Interaction, $P=0.015$. Region, $P<0.001$. Treatment, $P=0.465$. The n of the animal groups were as follow: COF = 7, SOF = 6.

Figure 56 that there was a significant difference in ng Evans Blue/mg protein for the interaction between the different brain regions and the drug treatment groups ($P = 0.015$; control versus S-fluoxetine). Also, there was significant difference between the different brain regions in these old female drug groups ($P < 0.001$), with the hippocampus showing the lowest permeability of the BBB and the cerebellum showing the highest permeability. There was no significant difference between the different drug treatment groups (P

=0.465). The ROUT analysis was used to determine the outliers. The outlier 4503.975 was located in the cortex while the outlier -12021.576 was found in the hippocampus. The root mean square error, which is defined as the residual mean square. It is used to estimate the common within-group standard deviation which also known as the standard error of the estimate were as the following. The mean \pm the standard error of the mean: COF: 245.048 \pm 433.250, SOF: -212.614 \pm 447.155. The mean \pm the standard error of the mean for the different brain regions are as follow: Cortex: 315.195 \pm 585.463, the hippo: -2695.107 \pm 676.034, the brain: 242.768 \pm 651.443, the cerebellum: 2202.011 \pm 571.353.

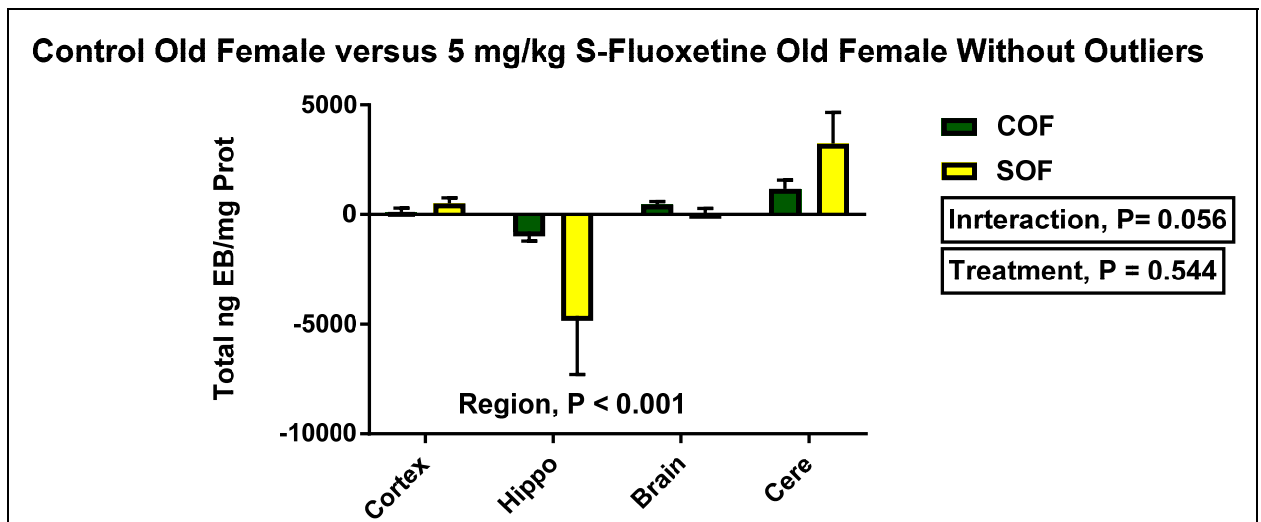


Figure 57: Comparison between old female rats that have given no drugs, and old female rats that have taken 5 mg/kg S-fluoxetine for three days (COF vs. SOF). The x-axis represents the different brain regions: cortex, peri-ventricular and hippocampus, striatum-caudate putamen-hypothalamus, and cerebellum. The y-axis represents the total ng EB. Two-way ANOVA was performed. Columns represent the mean for each group and error bars show standard error of mean (SEM). Interaction, $P=0.056$. Region, $P<0.001$.

Treatment, P=0.544. The animal numbers, n for the SOF = 6, the n for the ROF different brain regions were as follow: the n for the cortex = 6, the n for the hippocampus = 7, the n for the lower brain region = 7, and the n for the cerebellum = 7.

Figure 57 shows the same data as Figure 56, but with the statistical outliers removed. The data shows that we just missed having a significant difference in ng Evans Blue/mg protein for interaction between the different brain regions and drug treatment groups ($P = 0.056$; control versus S-fluoxetine), showing a very strong trend. Interestingly, the S-fluoxetine increased permeability in the cerebellum, but appears to lower permeability in the hippocampus. Also, there was a significant difference between the different brain regions between the groups ($P < 0.001$), with the hippocampal region showing low BBB permeability and the cerebellum showing high BBB permeability. In addition, there was no significant difference between the drug treatment groups ($P = 0.544$; control versus S-Fluoxetine). The root mean square error, which is defined as the residual mean square. It is used to estimate the common within-group standard deviation which also known as the standard error of the estimate were as the following. The mean \pm the standard error of the mean for the different brain regions are as follow: cortex: 315.195 ± 762.731 , periventricular and hippocampus: -2695.107 ± 762.731 , striatum-caudate putamen-hypothalamus (brain): 242.768 ± 734.986 and the cerebellum: 2202.011 ± 734.986 . The mean \pm the standard error of the mean for the treatment groups was as follow: COF: 245.048 ± 519.714 , SOF: -212.614 ± 539.332 .

Summary: When total ng Evans blue in regions is normalized by the amount of protein measured from the tissue in milligrams for old female rats, we compared the blood

brain barrier permeability under different drug treatments. The analysis showed that there was a significant difference in the total ng Evans Blue/mg protein among the different brain regions in old female rats with the hippocampus showing the lowest blood brain barrier permeability and the cerebellum showing the highest permeability. When we compared R-fluoxetine to control in old female rats, we did see a significant drug treatment effect on the permeability, with the R-fluoxetine consistently reducing the permeability

3.8 Comparison of All treatment groups across a Brain Regions

3.8.1 Cortex

Two-Way ANOVA of total ng EB/mg Protein

In the coming figures, we compared the total amount of Evans blue in the cortex region for the young male rats, old male rats and old female rats. We normalized the amount of Evans blue in a region by dividing the total ng Evans blue in that region by the protein concentration in mg, determined by a Bradford protein assay.

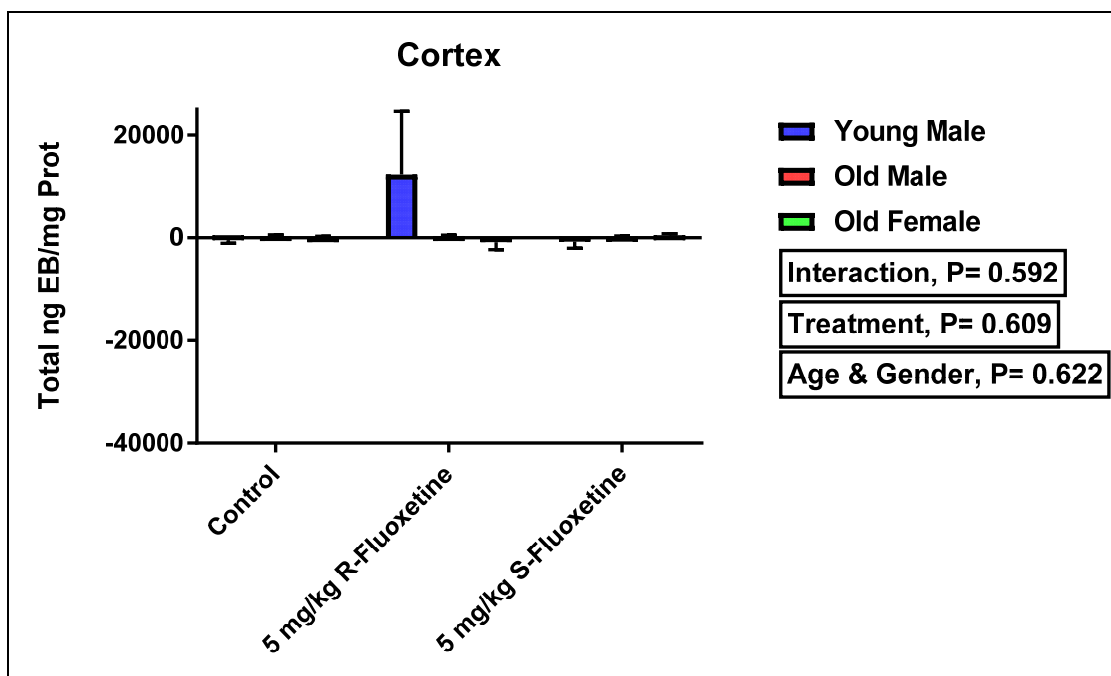


Figure 58: Comparison between cortex region for the young male, old male and old female rats. The x-axis represents the different treatment groups. The y-axis represents the total ng Evans Blue/mg protein. Columns represent the mean for each group and error bars show standard error of mean (SEM). Two-way ANOVA was performed. Interaction, $P=0.592$. Treatment, $P=0.609$. Age and gender $P=0.622$. The n of the animal groups were as follow: CYM =10, ROM =7, SOF=6.

Figure 58 shows that there no significant difference in the amount of Evans Blue/mg protein in the cortex for the interaction between the different drug treatments and the different animal groups (age and gender differences) ($P = 0.592$). Also, there is no significant difference between the different drug treatments for this region of the brain ($P = 0.609$). In addition, there is no significant difference between the animal groups (young male rats, old male rats, old female rats) ($P= 0.622$). The outliers were determined by using the ROUT analysis at medium setting. The outliers were found at the RYM, COF, and ROF groups. The outlier at the cortex region of the RYM was 134723.4088. The outlier at the

cortex region of the COF was -4503.975. The outlier at the cortex region of the ROF was -9420.832. The root mean square error, which is defined as the residual mean square. It is used to estimate the common within-group standard deviation which also known as the standard error of the estimate were as the following. The mean \pm the standard error of the mean for the cortex of the young males: 3673.030 ± 2812.087 , cortex of the old males: 289.169 ± 3515.386 , the cortex of the old female: -295.748 ± 3611.716 . The mean \pm the standard error of the mean for the treatment groups was as follow: the control: -234.732 ± 3334.988 . R-fluoxetine treatment group: 3925.951 ± 3295.452 . S-fluoxetine treatment group: -24.768 ± 3365.726 .

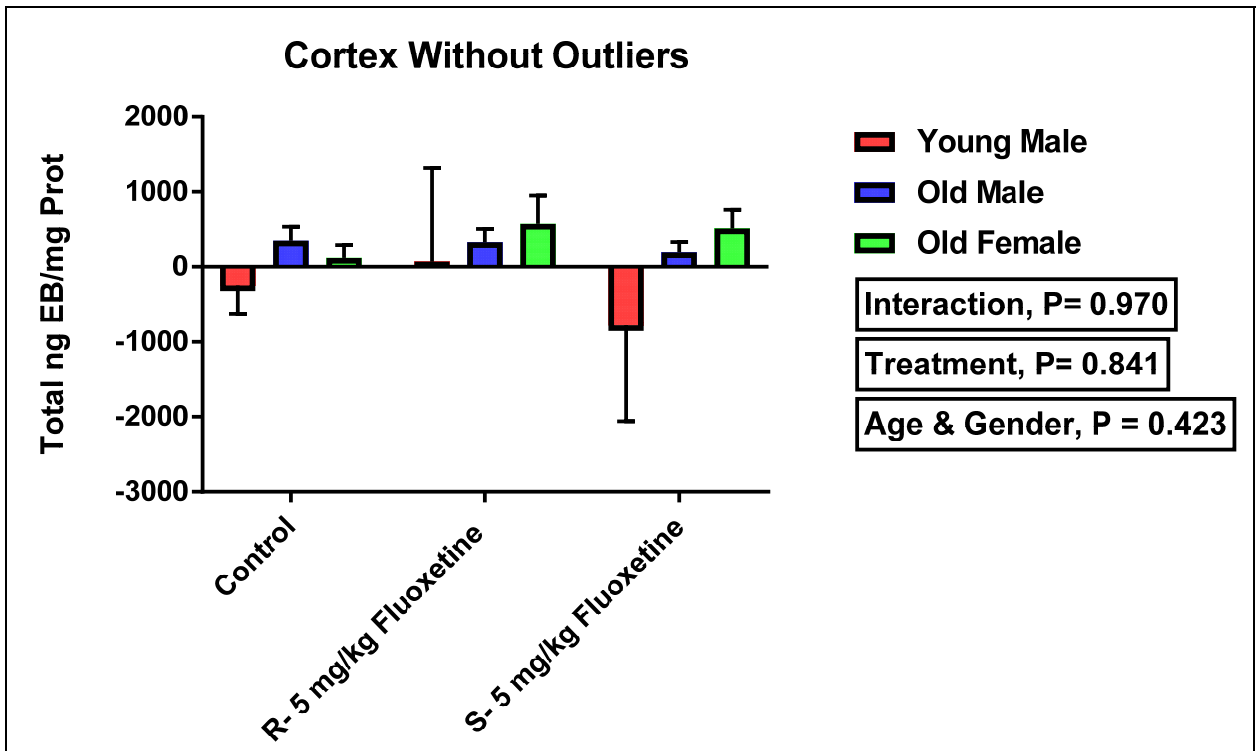


Figure 59: Comparison between Cortex regions for the young males, old males and old female rats that have not taken any drug, have taken 5 mg/kg R-fluoxetine and the ones

that have taken the 5 mg/kg S-fluoxetine. The x-axis represents the different drug treatment groups. The y-axis represents the total ng Evans Blue/mg protein. Columns represent the mean for each group and error bars show standard error of mean (SEM). Two-way ANOVA was performed. Interaction, $P=0.970$. Treatment, $P=0.841$. Age and gender $P=0.423$. The n of the animal groups were as follow: the n for the cortex of the CYM = 10, the n for the hippocampus =9, the n for the lower brain region = 10, the n for the cerebellum =9, ROM =7, SOF =6.

Figure 59 shows the data from Figure 58 without the statistical outliers. The data shows that there was no significant difference in the ng Evans Blue/mg protein for the interaction between the different drug treatments and the age/gender of the animals ($P = 0.970$). Also, there was no significant difference between the different drug treatments for the cortex ($P = 0.841$). In addition, there was no significant differences in the BBB permeability between young males, old males and old females ($P = 0.423$) in the cortex. The root mean square error, which is defined as the residual mean square. It is used to estimates the common within-group standard deviation which also known as the standard error of the estimate were as the following. The mean \pm the standard error of the mean for the cortex of the young male: -379.011 ± 399.901 , hippocampus of the old males: 333.287 ± 484.877 , the hippocampus of the old females: 444.361 ± 517.246 . The mean \pm the standard error of the mean: R-group: 357.508 ± 426.051 , S-group: -81.992 ± 413.714 , control group: -9.232 ± 594.026 .

3.8.2 Hippocampus

Two-Way ANOVA of total ng EB/mg Protein: All treatment groups compared across the hippocampal brain region

In the following set of figures, we measured the amount of the protein concentration in mg by using the Bradford protein assay. Then, we normalized the data by dividing the total ng Evans blue in that region by the amount of the protein (mg). Then, we compared the total amount of Evans blue (ng) divided by the amount of protein (mg) in the hippocampus region for the young male, old male and old female rats with the following drug treatment: 1) control, 2) 5 mg/kg R-fluoxetine and 3) 5 mg/kg S-Fluoxetine.

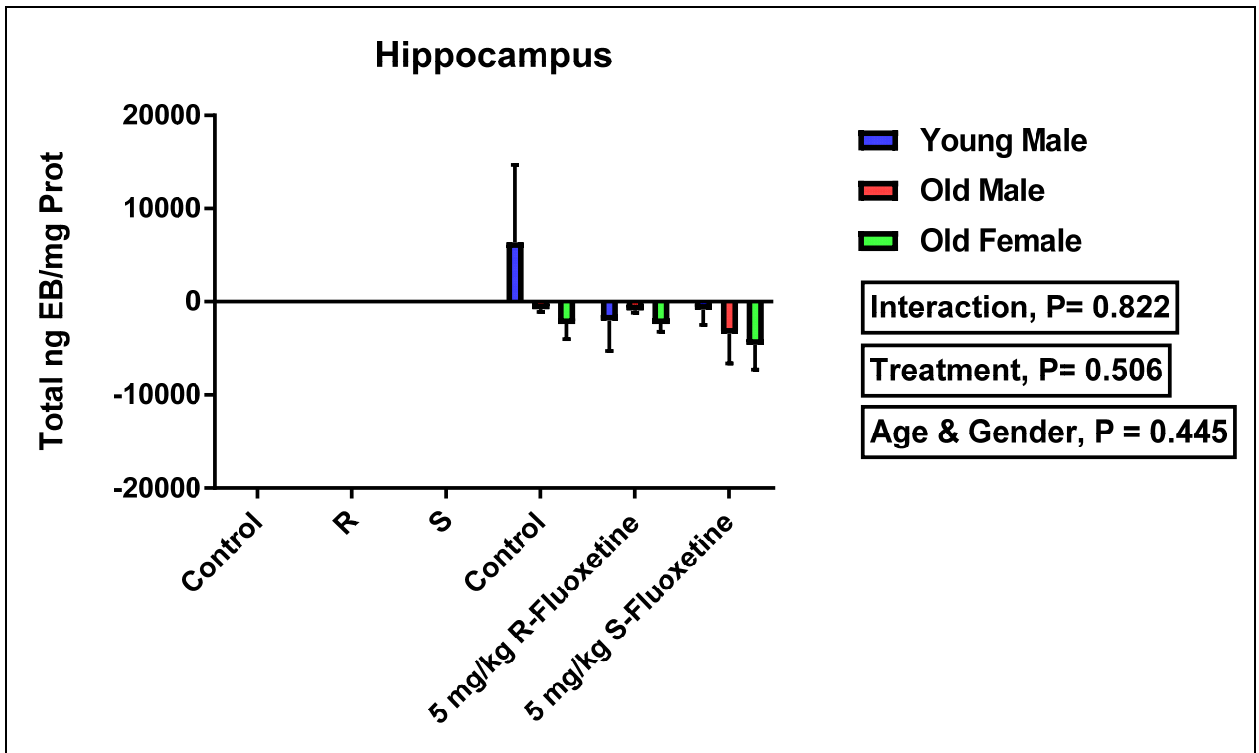


Figure 60: Comparison between hippocampal region for the young males, old males and old female rats that have not taken any drug, have taken 5 mg/kg R-fluoxetine and the ones that have taken the 5 mg/kg S-fluoxetine. The x-axis represents the different drug treatment groups. The y-axis represents the total ng Evans Blue/mg protein. Columns represent the mean for each group and error bars show standard error of mean (SEM). Two-way

ANOVA was performed. Interaction, P=0.822. Drug Treatment, P=0.506. Age and gender P=0.445. The n of the animal groups were as follow: CYM =10, ROM =7, SOF=6.

Figure 60 shows a comparison of the different drug treatments for all of the different age and gender groups on blood brain barrier permeability in the hippocampal region. There was no significant difference in the ng Evans Blue/mg protein for interaction between the different drug treatments (listed on the X axis) and the age or gender of the animals ($P = 0.822$). Also, there was no significant difference between the different drug treatments ($P = 0.506$) for this region. In addition, there was no significant difference in the blood brain barrier permeability in this region based on either age or gender ($P = 0.445$). The outliers were determined by the ROUT analysis at medium setting. The outliers were found in the CYM, SOM and COF groups. The outlier at the hippocampus region in the CYM was 80868.926. The outlier at the hippocampus of the SOM was -22521.990. The outlier at the COF was -12021.576. The root mean square error, which is defined as the residual mean square. It is used to estimates the common within-group standard deviation which also known as the standard error of the estimate were as the following. The mean \pm the standard error of the mean for the hippo region of the young male: 1166.939 ± 2262.869 , the hippo region of the old male: -1694.846 ± 2564.188 , for the hippo region of the old females: -3122.296 ± 2634.453 . The mean \pm the standard error of the mean for the treatment groups was as follow: control: 1079.616 ± 2432.602 , R-fluoxetine treatment group: -1767.342 ± 2403.764 , S-fluoxetine: -2962.479 ± 2634.453 .

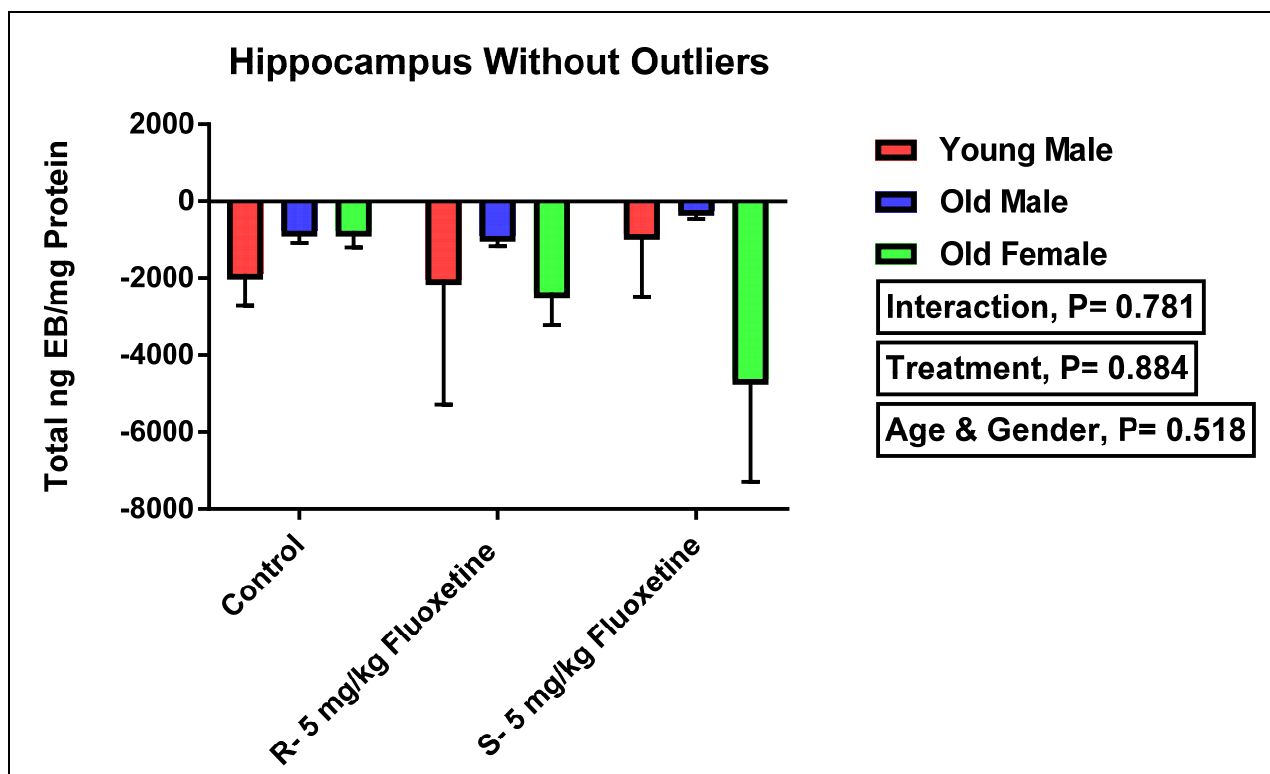


Figure 61: Comparison in BBB permeability (ng Evans Blue/mg protein) in the hippocampal region for the different groups (young males, old males and old female rats) and the different drug treatments (control: that have not taken any drug, have taken 5 mg/kg R-fluoxetine and the ones that have taken the 5 mg/kg S-fluoxetine). The x-axis represents the different drug treatment groups. The y-axis represents the total ng Evans Blue/mg protein. Columns represent the mean for each group and error bars show standard error of mean (SEM). Two-way ANOVA was performed. Interaction, P=0.781. Drug Treatment, P=0.884. Age and gender P=0.518. The n of the animal groups were as follow: the n for the cortex = 10, the n for the hippocampus = 9, the n for the lower brain region =10, the n for the cerebellum =9, ROM =7, SOF= 6.

Figure 61 shows the data from Figure 60 but with the statistical outliers removed. The data indicates that there was no significant difference for ng Evans Blue/mg protein in

the interaction between the different drug treatments and the age & gender of the animals ($P = 0.781$). Also, there was no significant difference between the different drug treatments in this brain region ($P = 0.884$). In addition, there was no significant difference between the young males, old males and the old females ($P = 0.518$). The root mean square error, which is defined as the residual mean square. It is used to estimate the common within-group standard deviation which also known as the standard error of the estimate were as the following. The mean \pm the standard error of the mean for the hippocampus of the young male: -1381.897 ± 1315.295 , the hippocampus of the old male: -468.675 ± 1454.796 , the hippocampus of the old females: -1803.768 ± 1921.934 .

3.8.3 Brain

Two-Way ANOVA of total ng EB/mg Protein

In the following figures, we divided the total amount of Evans blue in a region (ng) by the protein concentration (mg) which was determined by using Bradford protein assay in order to normalize the data. Then, we compared the total amount of Evans blue (ng) divided the amount of the protein (mg) in the lower brain region (striatum, caudate putamen, hypothalamus) for the young male, old male and old female receiving the following drug treatments: 1) control, 2) 5 mg/kg R-fluoxetine, and 3) 5 mg/kg S-fluoxetine.

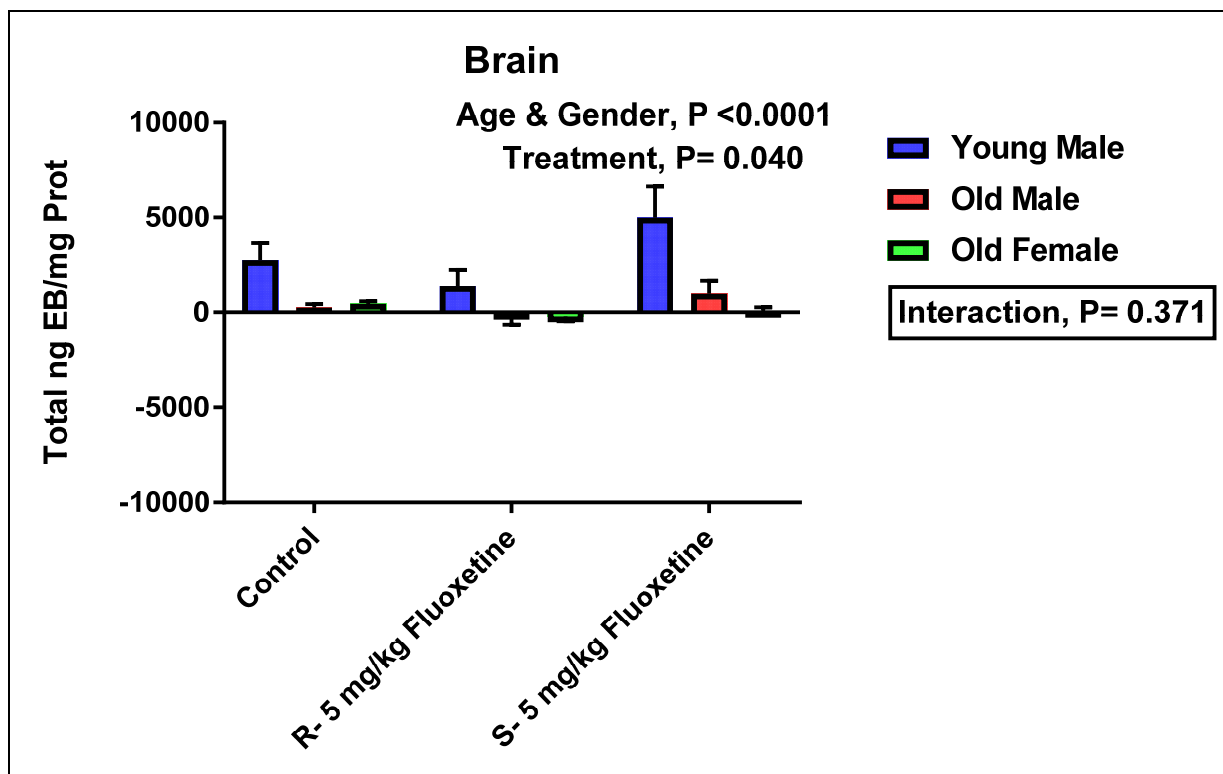


Figure 62: Comparison of Blood Brain for the young males, old males and old female rats.

The x-axis represents the different drug treatment groups. The y-axis represents the total ng Evans Blue/mg protein. Columns represent the mean for each group and error bars show standard error of mean (SEM). Two-way ANOVA was performed. Interaction, $P=0.371$. Drug Treatment, $P=0.040$. Age and gender $P<0.0001$. The n of the animal groups were as follow: CYM = 10, ROM = 7, SOF = 6.

Figure 62 shows that there no significant difference in the ng Evans Blue/mg protein for interaction between the different drug treatments and the different animal groups (age and gender differences) ($P = 0.371$). Also, there is no significant difference between the different drug treatments in the lower brain ($P = 0.040$), although the low P value does indicate a strong trend here. There is significant difference between in the blood brain barrier permeability of the young male rats and the older male and female rats, $P < 0.0001$.

The younger rats show enhanced permeability in this region, which includes the choroid plexus, while the older animals show reduced permeability. The statistical outliers were determined by ROUT analysis at medium setting. The outlier (4306.475) at brain region was found at the SOM group. The root mean square error, which is defined as the residual mean square. It is used to estimate the common within-group standard deviation which also known as the standard error of the estimate were as the following. The mean \pm the standard error of the mean for the brain region of the young male: 3047.635 ± 457.498 , brain of the old males: 757.866 ± 518.418 , brain of the old females: 92.802 ± 532.624 . The mean \pm the standard error of the mean for the treatment groups was as follow: control: 1157.955 ± 491.814 , R-fluoxetine treatment group: 434.820 ± 485.984 , S-fluoxetine treatment group: 2305.529 ± 532.624 .

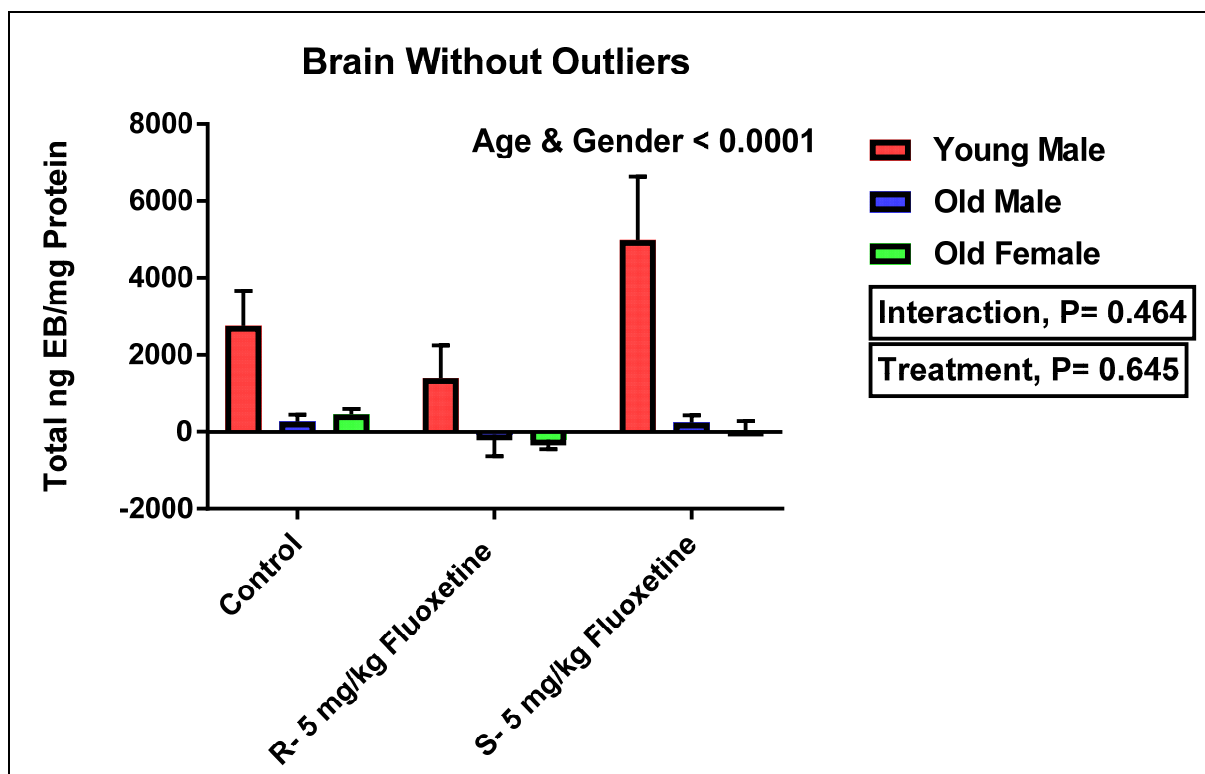


Figure 63: Comparison between brain regions for the young males, old males and old female rats that have not taken any drug, have taken 5 mg/kg R-fluoxetine and the ones that have taken the 5 mg/kg S-fluoxetine. The x-axis represents the different treatment groups. The y-axis represents the total ng Evans Blue/mg protein. Columns represent the mean for each group and error bars show standard error of mean (SEM). Two-way ANOVA was performed. Interaction, $P=0.464$. Treatment, $P=0.645$. Age and gender $P<0.0001$. The animal number, n for the different groups of the CYM were as follow: the n for the cortex = 10, the n for the hippocampus =9, the n for the lower brain region =10, and the n for the cerebellum =9, ROM=7, SOF=6.

Figure 63 shows the same data for Figure 62, but with the one statistical outlier removed. This data indicates that there was no significant difference in the ng Evans Blue/mg protein for the interaction between the drug treatment and the age/gender of the

animal groups ($P = 0.464$). Also, there was no significant difference between the different drug treatments ($P = 0.645$). However, there was a significant difference young males, old males and old females ($P < 0.0001$), with the young males showing enhanced permeability in the lower brain region. The root mean square error, which is defined as the residual mean square. It is used to estimate the common within-group standard deviation which also known as the standard error of the estimate were as the following. The mean \pm the standard error of the mean: the brain of the young male: 2983.164 ± 532.173 , the brain of the old male: 611.074 ± 589.604 , the brain of the old female: 35.867 ± 638.137 . The mean for the different treatment groups was as follow: control: 1135.939 ± 513.319 , R-group: 252.743 ± 504.818 , S-group: 2613.634 ± 629.453 .

3.8.4 Cerebellum

Two-Way ANOVA of total ng EB/mg Protein

The figures below represent the normalized amount of Evans blue in the cerebellum region of the brain in young male, old male and old female with different drug treatment: 1) control; 2) 5 mg/kg R-fluoxetine, 3) 5 mg/kg S-fluoxetine. The data were normalized by dividing the amount of Evans blue (ng) by the amount of protein (mg) that was measured by using the Bradford protein assay.

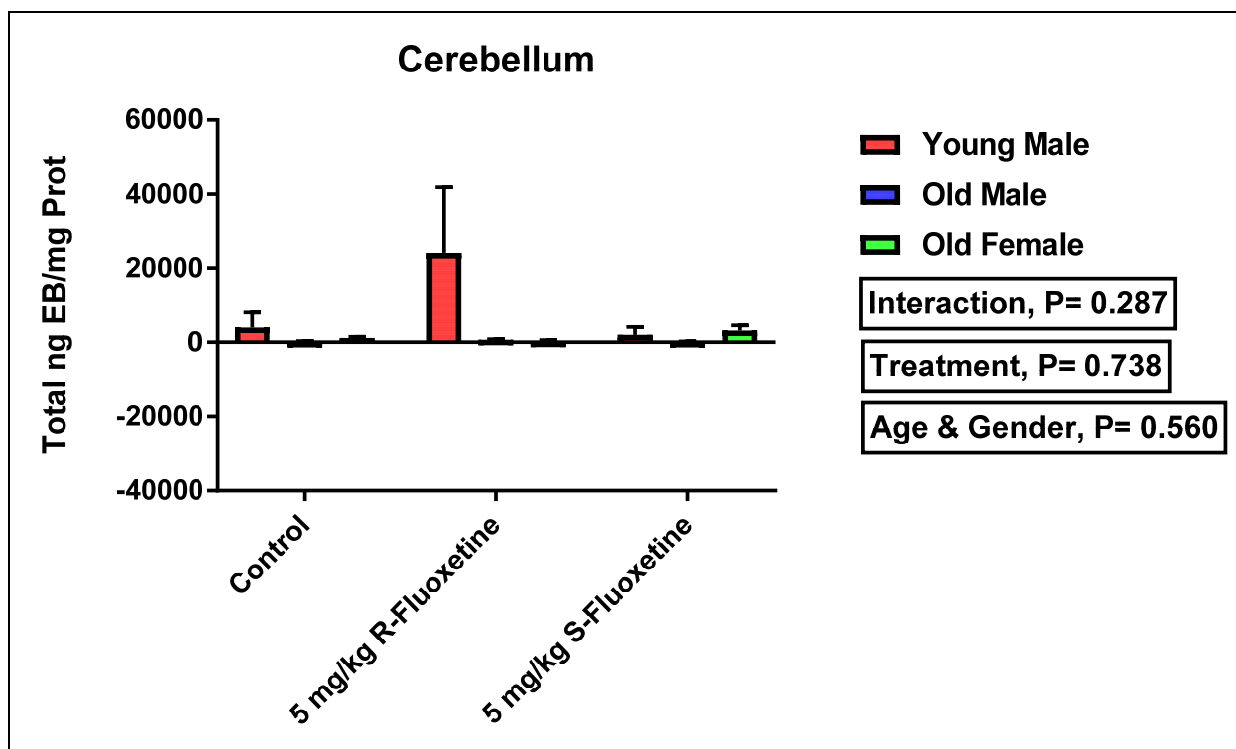


Figure 64: Comparison between cerebellum region for the young males, old males and old female rats that have not taken any drug (control), have taken 5 mg/kg R-fluoxetine and the ones that have taken 5 mg/kg S-fluoxetine. The x-axis represents the different drug treatment groups. The y-axis represents the total ng Evans Blue/mg protein. Columns represent the mean for each group and error bars show standard error of mean (SEM). Two-way ANOVA was performed. Interaction, $P=0.287$. Treatment, $P=0.738$. Age and gender $P=0.560$. The n of the animal groups were as follow: CYM =10, ROM = 7, SOF =6.

Figure 64 shows that there was no significant difference in the ng Evans Blue/mg protein for interaction between the different animal groups (age and gender differences) and the drug treatments ($P = 0.287$) in the cerebellum. Also, there is no significant difference between the different the different drug treatments for this region of the brain (P

= 0.738). In addition, there is no significant difference between the animal groups (age and gender differences) in the cerebellum ($P = 0.560$). The statistical outliers were determined by using the ROUT analysis at medium setting. The outliers were found in the CYM, RYM, and SYM groups. The CYM's outlier was 40375.9851. The SYM's outlier was 15175.1144. The RYM's outliers were 24064.006, 41496.548, and 197113.231. The root mean square error, which is defined as the residual mean square. It is used to estimate the common within-group standard deviation which also known as the standard error of the estimate were as the following. The mean \pm the standard error of the mean for the cerebellum of the young male: 11987.928 ± 6323.456 , the cerebellum of the old male: 9720.010 ± 6541.153 , the cerebellum of the old female: 1613.656 ± 7553.072 .

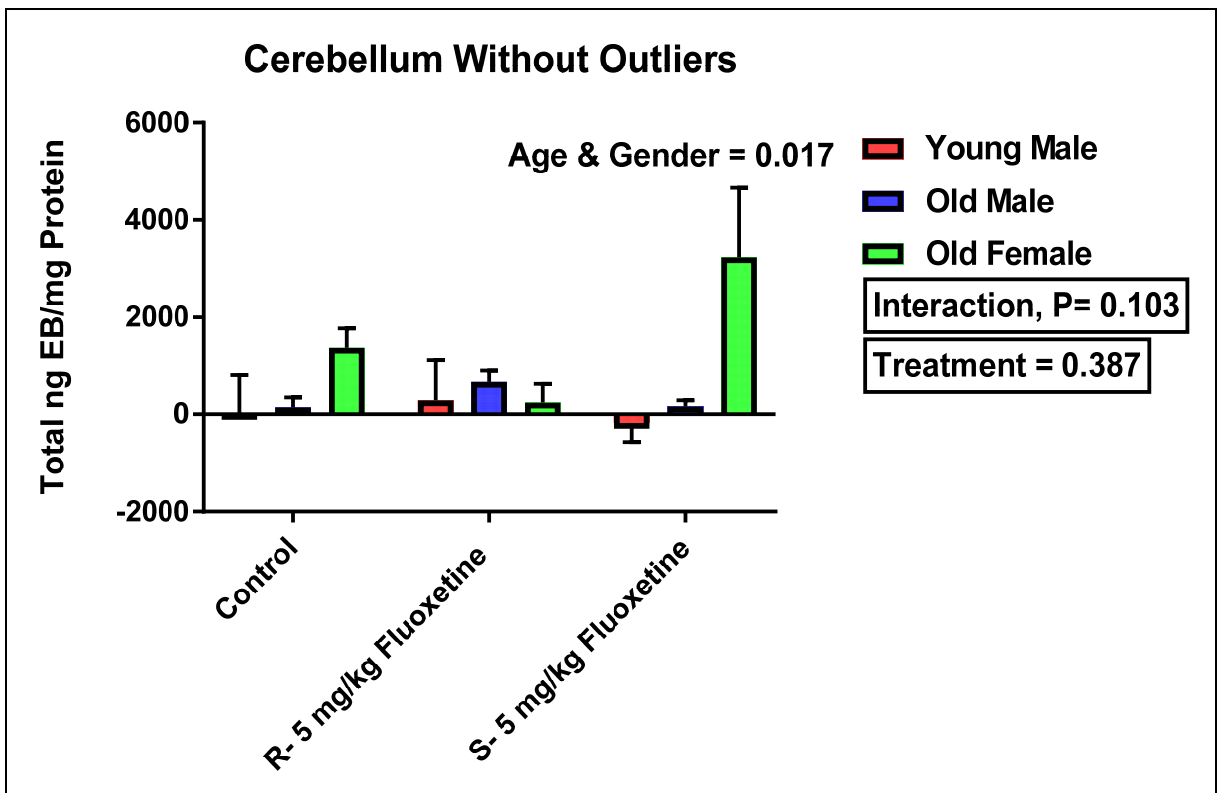


Figure 65: Comparison between cerebellum region for the young males, old males and old female rats that have not taken any drug (control), have taken 5 mg/kg R-fluoxetine and

the ones that have taken the 5 mg/kg S-fluoxetine. The x-axis represents the different treatment groups. The y-axis represents the total ng Evans Blue/mg protein. Columns represent the mean for each group and error bars show standard error of mean (SEM). Two-way ANOVA was performed. Interaction, P=0.103. Drug Treatment, P=0.387. Age and gender P=0.017. The animal numbers, n for the CYM different brain regions were as follow: the n for the cortex =10, the n for the hippocampus =9, the n for the lower brain region=10, the n for the cerebellum =9, ROM = 7, SOF=6.

Figure 65 shows the data from Figure 64, but with the statistical outliers removed. The data indicates that there was no significant difference in ng Evans Blue/mg protein for the interaction between the drug treatment and the different ages/gender of the animals groups (P = 0.103), but the low P value indicates a strong trend. Also, there was no significant difference between the different drug treatments (P = 0.387) in this region of the brain. There was a significant difference young males, old males and old females (P = 0.017), showing an influence of age and gender on the permeability. In particular, the female rat had greater permeability in the cerebellum in the control condition and in the presence of S-fluoxetine. The root mean square error, which is defined as the residual mean square. It is used to estimates the common within-group standard deviation which also known as the standard error of the estimate were as the following. The mean \pm the standard error of the mean for the cerebellum of the young males: -84.739 ± 391.646 , cerebellum of the old males: 327.434 ± 417.002 , the cerebellum of the old females: 1490.404 ± 457.757 . The mean \pm the standard error of the mean for the different treatment groups: control: 586.748 ± 496.978 , R-treatment group: 426.862 ± 378.740 , S-treatment group: 906.113 ± 361.394 .

Summary:

Two-Way ANOVA of Total ng EB/mg Protein

Total ng Evans blue in regions was normalized by the amount of protein measured from the tissue in milligrams. In this analysis we compared the different brain region (cortex, hippocampus, brain region and the cerebellum) among the young male rats, the old male rats and old female rats for each of the different drug treatments. In the cortex, our analysis showed that there were no significant difference in the interaction between the drug treatment and the age and gender factor of the animal groups. Also, there no significant difference in the either the drug treatments nor the age and gender factor.

In hippocampus, our analysis showed that there was no significant difference in the interaction between the drug treatment and the age and gender factor. Also, there were no significant difference in the drug treatment, or the age and gender factor in this region of the brain.

In the lower brain, our analysis showed that there was a significant difference in age and gender. The young males showed the highest blood brain barrier permeability, while older animals had much lower permeability. In the young male rats, we saw a strong trend ($P=0.1319$) for differences in drug treatment, with the S-fluoxetine increasing the blood brain barrier permeability while the R-fluoxetine decreased the blood brain barrier permeability. There was no significant difference in the interactions between drug treatment and age/gender in this region.

In cerebellum, there were no significant difference in the interaction between drug treatment and age /gender of the animal groups, but the P-value indicated a very strong

trend. S-fluoxetine increased the blood brain barrier permeability while the R-fluoxetine decreased the blood brain barrier permeability in old female rats. There was a significant difference in the BBB permeability when age and gender was considered, with an increase in the blood brain barrier in the old female rats compared to the two male groups.

IV. Discussion

The following table represents significant differences in BBB permeability (measured with Evans Blue permeability based on either Age or the interaction between Age and the region of the brain. In Figure 63, we see a highly significant P value (<0.0001) based on age, when we examined permeability in the lower brain region across the three basic groups (young males (YM), old males (OM) and old females (OF)). The YM had enhanced permeability in the lower brain region compared to either the OM or OF (Holm-Sidak post-hoc analysis). The lower two rows in this table refer to the analysis on Figure 34, which compares COM and CYM. We see an significant interaction ($P = 0.0302$) between age and region. In the middle row, we see an increased permeability of the lower Brain region compared to the Cortex, Hippocampus and Cerebellum within the CYM. In the last row, we see another interaction between age in region, with CYM showing enhanced permeability compared to COM, but only in the Brain region (Holm-Sidak post-hoc analysis).

P-Value	The Animal Groups	Variable	Significant difference		
<0.0001	Brain	Age	Increased permeability in YM compared to either OM or OF		Figure 63
0.0302	COM vs. CYM	Region and Age Interaction	Brain	Increased permeability in Brain versus Cortex, Hippo and Cere within CYM	Figure 34
0.0302	COM vs. CYM	Age and Region Interaction	CYM versus COM	Brain	Figure 34

Table 4: Significant P-values for the Age. YM: young males; OM old males; OF old females; COM: control old males; CYM control young males; Brain: lower brain region; Hippo: hippocampus; Cere: Cerebellum.

The lower brain region showed more blood brain barrier permeability in the young males compared to the old males. It contains a region called the choroid plexuses. The choroid plexuses have important functions which involve the production of cerebrospinal fluid and regulating the movement of molecules across the brain (116). That regulation plays an important role in ensuring having a homeostatic state in the brain. However, as we get older the brain function changes due to changes in its structure. These changes cause changes in cerebrospinal fluid homeostasis. For example, the hippocampus, the prefrontal cortex and the choroid plexus decreases in size with aging. The size of the choroid plexuses is changed by changing the height of its epithelial cells and the total volume and length of its apical microvilli (117). The change in the choroid plexuses size cause a decrease in the cerebrospinal fluid production due to a decrease in the expression of certain proteins in the choroid plexuses (118). The following proteins are the main proteins that are associated with choroidal CSF production: carbonic anhydrase II, aquaporin 1 (AQP1) and sodium-potassium exchanging ATPase (Na, K-ATPase) (118). In addition, the blood vessel's wall gets thicker with aging (117), so that electrolytes that could cross in young rats can no longer cross well in older rats.

4.2 The results of the total ng EB/mg protein in male versus female (Gender difference)

The next table represents significant differences in BBB permeability based on gender differences. We compared the blood brain barrier's permeability under different drug treatments by measuring the total amount of Evans blue in different brain regions. In figure 65, we saw a significant increase in the BBB permeability in the cerebellum (P value of 0.0149) based on gender. The results showed that old females showed the highest

permeability for the blood brain barrier in the cerebellum when compared to old males and young males (Holm-Sidak post-hoc analysis). The cerebellum is the region of the brain that is the focus for classical conditioning with the eyeblink response and coordination of motor control. Other studies have shown that the cerebellum has increased blood brain barrier permeability when the body is trying to clear viruses, but ours is the first report of a gender difference of BBB permeability. One other study has shown that removing the ovaries from female rats, which would cause premature estrogen loss, caused a significant increase in BBB permeability, but they did not evaluate regional changes in permeability. Our female rats at 10 months of age are generally thought to have lost their estrogen due to menopause. We would really like to test the BBB permeability of the cerebellum in young female rats, to determine if the increase in permeability in the cerebellum in old female rats is related to estrogen loss. Research studies found that there is a sex differences in response to selective serotonin reuptake inhibitor. Studies have found that females respond better than males in response to selective serotonin reuptake inhibitor (119).

P-Value	The Animal Groups	Variable	Significant difference	
0.0149	Cerebellum	Gender	Increased permeability in cerebellum old females versus either old males or young males	Figure 65

Table 5: Significant P-values for the gender.

4.3 Comparison of All treatment groups across a Brain region

Lower Brain Region

We measured the permeability for the blood brain barrier for the lower brain region by using Evans blue method. Then, we normalized the data by measuring the amount of Evans blue divided the concentrations of the protein. Table 9 represents the significant p-values in the lower brain region of the brain.

P-Value	The Animal Groups	Variable		Significant difference	Related Figure
0.0012	CYM	Region	Brain	Increased permeability	Figure 14
0.0164	SYM				Figure 18
< 0.001	COM vs. CYM			Increased permeability in brain vs. hippo, cortex and cerebellum within CYM	Figure 34
< 0.0001	CYM vs. SYM			Increased permeability in Brain vs. hippo, brain vs. cortex, and brain vs. cerebellum. The increased permeability of brain vs. hippo is within CYM. The increased permeability of brain vs. hippo, brain vs. cortex and brain vs. cerebellum is within SYM	Figure 36
< 0.001	COM vs. CYM			Region and Age In	Increased permeability in brain vs. hippo, brain vs. cortex, and brain vs. cerebellum within CYM

Table 6: Significant P-values in the lower brain region of the brain. COM: control old males; CYM control young males; SYM: S-fluoxetine young males; Brain: lower brain region; Hippo: hippocampus

In figure 14, we found a significant P value in the brain region of CYM (0.0012), the lower brain region showed the highest blood brain barrier permeability. In figure 18, we saw a significant P value in the brain region of SYM (0.0164), and the lower brain region showed the highest blood brain barrier permeability among the different brain regions. In the comparison between COM vs. CYM, we saw a significant P value (<0.001)

associated with the lower brain region. There was an increased permeability in brain vs. hippo, cortex and cerebellum within CYM (Holm-Sidak post-hoc analysis). In figure 36, we found out that the significant P value is < 0.0001 : We saw an increased permeability in brain vs. hippo, brain vs. cortex, and brain vs. cerebellum. The increased permeability of brain vs. hippo is within CYM. The increased permeability of brain vs. hippo, brain vs. cortex and brain vs. cerebellum is within SYM. The last row of the table, in figure 34, we saw a significant p value (<0.001) with an increased permeability in brain vs. hippo, brain vs. cortex and brain vs. cerebellum within CYM.

Hippocampus

Evans blue method was used to measure the permeability of the blood brain barrier. Then, the results were normalized by dividing the amount of Evans blue by the amount of the protein concentrations that was measured by using Bradford protein assay. We found that the hippocampus showed the lowest permeability of all of the tested brain regions for the following groups: control old males, old males that have given 5 mg/kg of R-fluoxetine, old females that given 5 mg/kg of S-fluoxetine and old females group that have given 5 mg/kg of R-fluoxetine (see Table 7) .

P-value	Animal Group(s)	Variable		Significant Difference	Related Figure
0.0074	COM	Region	Hippocampus	Decreased permeability	Figure 20
0.0221	ROM				Figure 23
0.0136	SOF				Figure 26
0.0028	ROF				Figure 28
0.001	COM vs. SOM			Decreased permeability in hippocampus compared to cortex, or lower brain, or cerebellum within COM	Figure 48
0.006	ROM vs. SOM			Decreased permeability in hippocampus versus cerebellum or lower brain region	Figure 50
0.001	COM vs. ROM			Decreased permeability in hippocampus versus cerebellum within ROM	Figure 51
0.013	COF vs. ROF			Decreased permeability in hippocampus versus cerebellum within ROF	Figure 55
<0.001	COF vs. SOF			Decreased permeability in hippocampus versus cerebellum, cortex or lower brain regions	Figure 57

Table 7: Significant P-values for the hippocampus region of the brain. COM: control old males, ROM: R-fluoxetine treated old males, SOF: S-fluoxetine old females, ROF: R-fluoxetine old females, SOM: S-fluoxetine old males, COF: control old females.

Cerebellum

The permeability of the blood brain barrier was evaluated by using Evans blue method. The Evans blue was normalized by measuring the total ng of Evans blue and dividing it by the protein concentration that was determined by using Bradford protein assay. We saw a significant p value (<0.001) with an increased permeability in cerebellum vs. hippo, cortex vs. hippo, and brain vs. hippo within SOF in figure 51. In figure 23, we found a significant p value (0.0023). There was an increased permeability in the cerebellum region of COF.

P-Value	The Animal Groups		Significant difference		
<0.001	SOF vs. ROF	Region	Cerebellum	Increased permeability in cerebellum versus cortex, hippocampus or lower brain within SOF	Figure 51
0.0023	COF			Increased permeability of cerebellum compared to other brain regions	Figure 23

Table 8: Significant P-values for the cerebellum region of the brain. SOF: S-fluoxetine treated old females; ROF: R-fluoxetine treated old females; COF: control old females (old females without treatment).

4.4 The Treatment Effect among the Different Animal Groups

We used the total amount of normalized Evans blue to measure the blood brain barrier permeability. In figure 55, the significant p value is 0.0353. We saw a decreased permeability of COF vs. ROF whereas R-fluoxetine decreased the permeability in the hippocampus region of the brain (Holm-Sidak post-hoc analysis). In figure 56, the significant P value is 0.015. We saw a decreased permeability in COF vs. SOF whereas S-fluoxetine decreased permeability in the hippocampus region of the brain. In figure 42,

which represents SYM vs. PYM, we saw an increased permeability in the cerebellum region of the brain. In the brain region, we saw an increased permeability in young males who have taken 5mg/kg of S-fluoxetine (Holm-Sidak post-hoc analysis).

P-Value	The Animal Groups		Significant difference	
0.0353	COF vs. ROF	Treatment	Decreased permeability of in old female rats that took R-fluoxetine	Figure 55
0.015	COF vs. SOF	Treatment and region interaction	Increased permeability in old female rats that took S-fluoxetine in the cerebellum only	Figure 56
0.046	SYM vs. PYM	Treatment	Increased permeability in the cerebellum	Figure 42
0.040	Brain		Increased permeability in young males who have taken 5 mg/kg of S-fluoxetine	Figure 62

Table 9: Significant P-values for Treatment Effect. COF: Control Old Females; ROF: R-fluoxetine Old Females, SOF: S-fluoxetine Old Females; SYM: S-fluoxetine Young Males; PYM: Prozac Young Males

4.5 The Activity of the Fluoxetine Metabolites

The S-fluoxetine enantiomer is metabolized principally to the S-norfluoxetine, whereas the R-fluoxetine is metabolized to the R-norfluoxetine. The S-enantiomers show stronger action when compared against the R-enantiomer forms: about 1.5 times higher for the fluoxetine forms, and 20 times as much for norfluoxetine (120, 121). In other words, the S-norfluoxetine is active, while the R-norfluoxetine is relatively inactive.

Previous studies have demonstrated that fluoxetine and norfluoxetine get passed from the mother to the fetus through the placenta. Also, the serum of the newborn will contain the medications and its metabolites even after its birth. In regard to the potential pharmacological actions of the drug, the selective disposition of fluoxetine show more

impact on the foetus than on the mother specifically the S-norfluoxetine (122). Studies have showed the presence of fluoxetine and its active metabolites in the brain and the serum of the Sprague Dawley rats (106, 107) with the presence of norfluoxetine found in brain samples over 2 weeks after the drug fluoxetine was given in a single dose.

Effect of Fluoxetine on Connexin 43

Astrocytes from the striatum have less number of functional channels formed by Connexin 43 than the astrocytes of the hypothalamus. Immunoblotting was used to determine the amount of Cx43. It was found that the Cx43 protein in the hypothalamus is approximately four times than that found in cultures from striatum. Northern blot analysis showed that connexin 43 mRNA levels were also approximately 4-fold greater in the hypothalamic cultures consistent with the difference seen by immunoblotting (123). In the prefrontal cortex, other labs have found that fluoxetine increases Cx43 protein expression. Antidepressant like behavioral activities results when Cx43 gets knocked down. Research studies found that Fluoxetine and Corticosterone have opposite effects. Corticosterone increases the hippocampal amounts of phosphorylated form of Cx43. Also, it caused anxiety and depression-like abnormalities. Fluoxetine exhibit an opposite effect of corticosterone. Antidepressant drugs provide therapeutic activity by decreasing the expression of Cx43. Anawa trading was used to purchase Fluoxetine hydrochloride. The medicine was used for one month. The concentration of fluoxetine was 18 mg/kg per day. Old male transgenic were during this research study (124).

Our results showed that R-fluoxetine caused a decrease in permeability compared to control in old female rats. That provided us an evidence that fluoxetine is more effective

in females. Dr. Debra found out that there is an increase in connexin 43 in the hippocampus. However, during this research study the medications were administrated for three days that might was not enough period to cause a change in connexin 43 density. Also, fluoxetine stimulates VEGF (vascular endothelial growth factor) which enhances the blood brain barrier permeability because it increases angiogenesis (125).

4.6 Previous Research Studies

In a thesis named, "Examination Of a Post-stroke Drug Treatment For Its Effect on Blood Brain Barrier Permeability, and Gene Expression Changes in the Prei-infarct Region" The blood brain barrier permeability was quantified by using Evans blue method after stroke induction. The animals of this research study had stroke (brain injury) while the animals of our research study were healthy and did not suffer from brain injury. Also, in our research study we did not use unpaired-t-test with Welch's corrections while this research study used unpaired-t-test with Welch's corrections. The animals that was used in this study were aged animals (10-12 months old) while in our study both old (10-12 months) and young animals (1.5 months) were used.

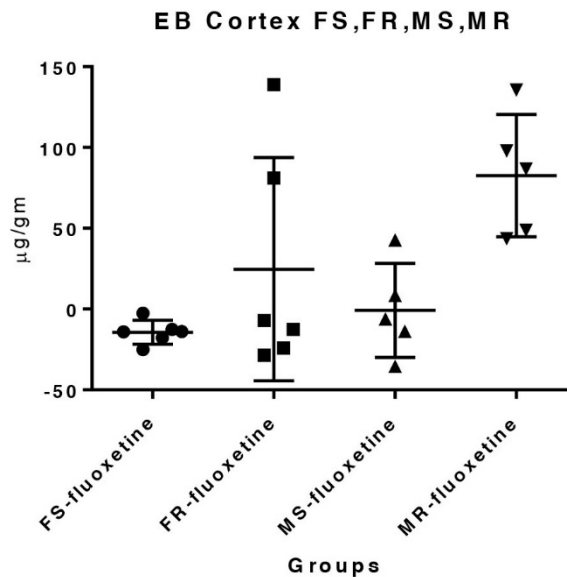


Figure 66: Blood brain barrier permeability measurement in the cerebral cortex of the males and the females' animal groups.

The above figure shows the measurement of the blood brain barrier permeability in the cortex of both the male and female rats. No outlier was found by using the ROUT analysis. The data shows that there was significant difference in the results. The p-value was 0.0091. The male S-fluoxetine showed the least amount of the blood brain barrier permeability in comparison to the other groups. The graph shows that the male and the female rats that have taken S-fluoxetine showed less blood brain barrier permeability than the R-fluoxetine. Unpaired t-test with Welch's corrections showed the p-value for the female S-fluoxetine and the female R-fluoxetine are significantly different. The p-value for that test was 0.0041. Also, the unpaired t-test with Welch's corrections showed that the male S-fluoxetine is significantly different from the male R-fluoxetine with a P-value of 0.0045. That confirms that the S-fluoxetine decreased the blood brain barrier permeability while the R-fluoxetine increased the blood brain barrier permeability. When we saw significant effects

of the drug treatments in normal brains, we saw basically the opposite of these results: the R-fluoxetine tightened the BBB compared to controls, and the S-Fluoxetine increased the permeability of the BBB compared to controls in the cerebellar region of old female rats. We believe that the fluoxetine is working on activated microglia in the injured brain, turning them into beneficial M2 microglia, which support neuronal survival. In a normal brain, one might expect more inflammatory microglia as an animal ages (126), but the overall effect would be very different from an injured animals in terms of the sheer number of activated microglia.

In this research study, we saw a tight BBB in both cortex and hippocampus of all animals tested. Our 10 months rats corresponded to about 45 years old person. Neurodegenerative changes occur generally after 65 years of age (human). So, we would like to evaluate older animals to see if we see an increased in BBB permeability.

V. Future Directions

For future experiments, the remaining pellets of the experiment are still available and we kept them at -80 freezer. For future experiments, we could look for the density of the proteins that are found in the tight junctions such as ZO-1, and Cx43. Also, we could possibly continue the work of Dr. Debra Mayes while she is looking for the density of Cx43 and the level of estrogen. In addition, we interested to see if we could find a shift in tight junction proteins that corresponds to the changes in BBB permeability that we see. Also, we would like to use older animals (24 months old) to see if we could see an increased BBB permeability.

VI. Conclusion

In this study, we found out that there were regional differences in blood brain barrier permeability in rats at all ages examined, with the hippocampal region generally showing the tightest BBB. As we expected in the hypotheses with aging the blood brain barrier permeability changes. Younger animals showed enhanced BBB permeability in the lower brain region compared to older animals, which may reflect age related changes to the choroid plexus region. We also saw that old female rats had enhanced BBB permeability in the cerebellum, which may possibly be due to estrogen loss, but we would need to test the BBB permeability in young female rats to make that conclusion. When we saw the fluoxetine enantiomer treatment effects, they were generally opposite what we had seen in injured rats (stroked rats): The R-fluoxetine seemed to tighten the BBB barrier and the S-fluoxetine loosened the BBB in the cerebellum in old female rats. In a model BBB that was used in Dr. Maye's lab, endothelial cells and astrocytes were the only cells that were present at the model. The results of Dr. Maye's showed that R-fluoxetine tightened the BBB while S-fluoxetine increased permeability of the BBB. Microglia play a role in live animal. So our results did not matches our expectations from the hypothesis about stroke studies. In stroke models, microglial are activated and we see that S-fluoxetine tightening the BBB while R-fluoxetine increased permeability. The long-lasting S-fluoxetine and S-norfluoxetine act to suppress inflammatory response from the microglia in this case. Since

R-fluoxetine is only active a short time, the microglial can become inflammatory again within a short time (hours). In the animals in this study, the microglia probably are not activated or inflammatory. So fluoxetine might be working directly on the endothelial cells or astrocytes. Interestingly, the R-fluoxetine and S-fluoxetine worked in the same way as Dr. Mayes saw in her model BBB. We have negative Evans blue because we used the linear regression line. It is the best fitting line for the data. The y-intercept for the line was 15 which was equivalent to zero. Any value less than 15 represents a negative number which means that it is negative relative to the other Evans blue values.

VII. References

1. Arlt S. Non-Alzheimer's disease-related memory impairment and dementia. *Dialogues Clin Neurosci*. 2013 Dec;15(4):465-73. PubMed PMID: 24459413. Pubmed Central PMCID: 3898684.
2. Erdo F, Denes L, de Lange E. Age-associated physiological and pathological changes at the blood-brain barrier: A review. *J Cereb Blood Flow Metab*. 2017 Jan;37(1):4-24. PubMed PMID: 27837191. Pubmed Central PMCID: 5363756.
3. Gianaros PJ, Jennings JR, Sheu LK, Greer PJ, Kuller LH, Matthews KA. Prospective reports of chronic life stress predict decreased grey matter volume in the hippocampus. *Neuroimage*. 2007 Apr 01;35(2):795-803. PubMed PMID: 17275340. Pubmed Central PMCID: 1868546.
4. Corti O, Fournier M, Brice A. Neurodegeneration in Parkinson's disease: genetics enlightens physiopathology. *J Neural Transm Suppl*. 2009 (73):215-21. PubMed PMID: 20411780.
5. Obermeier B, Daneman R, Ransohoff RM. Development, maintenance and disruption of the blood-brain barrier. *Nat Med*. 2013 Dec;19(12):1584-96. PubMed PMID: 24309662. Pubmed Central PMCID: 4080800.
6. Bradbury MW, Stubbs J, Hughes IE, Parker P. The Distribution of Potassium, Sodium, Chloride and Urea between Lumbar Cerebrospinal Fluid and Blood Serum in Human Subjects. *Clin Sci*. 1963 Aug;25:97-105. PubMed PMID: 14058246.
7. Hansen AJ. Effect of anoxia on ion distribution in the brain. *Physiol Rev*. 1985 Jan;65(1):101-48. PubMed PMID: 3880896.
8. Abbott NJ, Ronnback L, Hansson E. Astrocyte-endothelial interactions at the blood-brain barrier. *Nat Rev Neurosci*. 2006 Jan;7(1):41-53. PubMed PMID: 16371949.
9. Bernacki J, Dobrowolska A, Nierwinska K, Malecki A. Physiology and pharmacological role of the blood-brain barrier. *Pharmacol Rep*. 2008 Sep-Oct;60(5):600-22. PubMed PMID: 19066407.
10. Gingrich MB, Junge CE, Lyuboslavsky P, Traynelis SF. Potentiation of NMDA receptor function by the serine protease thrombin. *J Neurosci*. 2000 Jun 15;20(12):4582-95. PubMed PMID: 10844028.
11. Gingrich MB, Traynelis SF. Serine proteases and brain damage - is there a link? *Trends Neurosci*. 2000 Sep;23(9):399-407. PubMed PMID: 10941185.
12. Melissa B. Gingrich CEJ, Polina Lyuboslavsky, and Stephen F. Traynelis. Potentiation of NMDA Receptor Function by the Serine Protease Thrombin. *The Journal of Neuroscience*. 2000.
13. Wolburg H, Noell S, Mack A, Wolburg-Buchholz K, Fallier-Becker P. Brain endothelial cells and the glio-vascular complex. *Cell Tissue Res*. 2009 Jan;335(1):75-96. PubMed PMID: 18633647.
14. Dejana E, Simionescu M, Wolburg H. Endothelial cell biology and pathology. *Cell Tissue Res*. 2009 Jan;335(1):1-3. PubMed PMID: 19015887.

15. Carvey PM, Hendey B, Monahan AJ. The blood-brain barrier in neurodegenerative disease: a rhetorical perspective. *J Neurochem.* 2009 Oct;111(2):291-314. PubMed PMID: 19659460. Pubmed Central PMCID: 2761151.
16. Abbott NJ, Friedman A. Overview and introduction: the blood-brain barrier in health and disease. *Epilepsia.* 2012 Nov;53 Suppl 6:1-6. PubMed PMID: 23134489. Pubmed Central PMCID: 3625728.
17. Kandel. *Principles of Neural Science* New York: McGraw-Hill; 2000.
18. Wolburg H, Paulus W. Choroid plexus: biology and pathology. *Acta Neuropathol.* 2010 Jan;119(1):75-88. PubMed PMID: 20033190.
19. Marques F, Sousa JC, Brito MA, Pahnke J, Santos C, Correia-Neves M, et al. The choroid plexus in health and in disease: dialogues into and out of the brain. *Neurobiol Dis.* 2016 Aug 18. PubMed PMID: 27546055.
20. Maktabi MA, Heistad DD, Faraci FM. Effects of angiotensin II on blood flow to choroid plexus. *Am J Physiol.* 1990 Feb;258(2 Pt 2):H414-8. PubMed PMID: 2309908.
21. Spector R, Keep RF, Robert Snodgrass S, Smith QR, Johanson CE. A balanced view of choroid plexus structure and function: Focus on adult humans. *Experimental neurology.* 2015 May;267:78-86. PubMed PMID: 25747036.
22. Brightman MW, Reese TS. Junctions between intimately apposed cell membranes in the vertebrate brain. *J Cell Biol.* 1969 Mar;40(3):648-77. PubMed PMID: 5765759. Pubmed Central PMCID: 2107650.
23. Nabeshima S, Reese TS, Landis DM, Brightman MW. Junctions in the meninges and marginal glia. *J Comp Neurol.* 1975 Nov 15;164(2):127-69. PubMed PMID: 810497.
24. Brochner CB, Holst CB, Møllgaard K. Outer brain barriers in rat and human development. *Front Neurosci.* 2015;9:75. PubMed PMID: 25852456. Pubmed Central PMCID: 4360706.
25. Ronaldson PT, Davis TP. Blood-brain barrier integrity and glial support: mechanisms that can be targeted for novel therapeutic approaches in stroke. *Curr Pharm Des.* 2012;18(25):3624-44. PubMed PMID: 22574987. Pubmed Central PMCID: 3918413.
26. Raivich G, Bohatschek M, Kloss CU, Werner A, Jones LL, Kreutzberg GW. Neuroglial activation repertoire in the injured brain: graded response, molecular mechanisms and cues to physiological function. *Brain Res Brain Res Rev.* 1999 Jul;30(1):77-105. PubMed PMID: 10407127.
27. Ronaldson PT, Persidsky Y, Bendayan R. Regulation of ABC membrane transporters in glial cells: relevance to the pharmacotherapy of brain HIV-1 infection. *Glia.* 2008 Dec;56(16):1711-35. PubMed PMID: 18649402.
28. Speth C, Dierich MP, Sopper S. HIV-infection of the central nervous system: the tightrope walk of innate immunity. *Mol Immunol.* 2005 Feb;42(2):213-28. PubMed PMID: 15488609.
29. Aloisi F. Immune function of microglia. *Glia.* 2001 Nov;36(2):165-79. PubMed PMID: 11596125.
30. Zlokovic BV. The blood-brain barrier in health and chronic neurodegenerative disorders. *Neuron.* 2008 Jan 24;57(2):178-201. PubMed PMID: 18215617.
31. Faff L, Ohlemeyer C, Kettenmann H. Intracellular pH regulation in cultured microglial cells from mouse brain. *J Neurosci Res.* 1996 Nov 01;46(3):294-304. PubMed PMID: 8933368.
32. Klee R, Heinemann U, Eder C. Voltage-gated proton currents in microglia of distinct morphology and functional state. *Neuroscience.* 1999;91(4):1415-24. PubMed PMID: 10391447.
33. Newell EW, Schlichter LC. Integration of K⁺ and Cl⁻ currents regulate steady-state and dynamic membrane potentials in cultured rat microglia. *J Physiol.* 2005 Sep 15;567(Pt 3):869-90. PubMed PMID: 16020460. Pubmed Central PMCID: 1474215.

34. Eder C. Regulation of microglial behavior by ion channel activity. *J Neurosci Res.* 2005 Aug 01;81(3):314-21. PubMed PMID: 15929071.
35. Eder C. Ion channels in microglia (brain macrophages). *Am J Physiol.* 1998 Aug;275(2 Pt 1):C327-42. PubMed PMID: 9688586.
36. Noda M, Nakanishi H, Nabekura J, Akaike N. AMPA-kainate subtypes of glutamate receptor in rat cerebral microglia. *J Neurosci.* 2000 Jan 01;20(1):251-8. PubMed PMID: 10627602.
37. Maher F. Immunolocalization of GLUT1 and GLUT3 glucose transporters in primary cultured neurons and glia. *J Neurosci Res.* 1995 Nov 01;42(4):459-69. PubMed PMID: 8568932.
38. Bar T, Wolff JR. The formation of capillary basement membranes during internal vascularization of the rat's cerebral cortex. *Z Zellforsch Mikrosk Anat.* 1972;133(2):231-48. PubMed PMID: 5082884.
39. Canfield AE, Schor AM, Loskutoff DJ, Schor SL, Grant ME. Plasminogen activator inhibitor-type I is a major biosynthetic product of retinal microvascular endothelial cells and pericytes in culture. *Biochem J.* 1989 Apr 15;259(2):529-35. PubMed PMID: 2497739. Pubmed Central PMCID: 1138540.
40. Barber AJ, Lieth E. Agrin accumulates in the brain microvascular basal lamina during development of the blood-brain barrier. *Dev Dyn.* 1997 Jan;208(1):62-74. PubMed PMID: 8989521.
41. Sorokin L. The impact of the extracellular matrix on inflammation. *Nat Rev Immunol.* 2010 Oct;10(10):712-23. PubMed PMID: 20865019.
42. Wu C, Ivars F, Anderson P, Hallmann R, Vestweber D, Nilsson P, et al. Endothelial basement membrane laminin alpha5 selectively inhibits T lymphocyte extravasation into the brain. *Nat Med.* 2009 May;15(5):519-27. PubMed PMID: 19396173.
43. Daneman R, Prat A. The blood-brain barrier. *Cold Spring Harb Perspect Biol.* 2015 Jan 05;7(1):a020412. PubMed PMID: 25561720. Pubmed Central PMCID: 4292164.
44. Aird WC. Phenotypic heterogeneity of the endothelium: I. Structure, function, and mechanisms. *Circ Res.* 2007 Feb 02;100(2):158-73. PubMed PMID: 17272818.
45. Aird WC. Phenotypic heterogeneity of the endothelium: II. Representative vascular beds. *Circ Res.* 2007 Feb 02;100(2):174-90. PubMed PMID: 17272819.
46. Coomber BL, Stewart PA. Morphometric analysis of CNS microvascular endothelium. *Microvasc Res.* 1985 Jul;30(1):99-115. PubMed PMID: 4021842.
47. Reese TS, Karnovsky MJ. Fine structural localization of a blood-brain barrier to exogenous peroxidase. *J Cell Biol.* 1967 Jul;34(1):207-17. PubMed PMID: 6033532. Pubmed Central PMCID: 2107213.
48. Westergaard E, Brightman MW. Transport of proteins across normal cerebral arterioles. *J Comp Neurol.* 1973 Nov 01;152(1):17-44. PubMed PMID: 4765853.
49. Henninger DD, Panes J, Eppihimer M, Russell J, Gerritsen M, Anderson DC, et al. Cytokine-induced VCAM-1 and ICAM-1 expression in different organs of the mouse. *J Immunol.* 1997 Feb 15;158(4):1825-32. PubMed PMID: 9029122.
50. Daneman R, Zhou L, Kebede AA, Barres BA. Pericytes are required for blood-brain barrier integrity during embryogenesis. *Nature.* 2010 Nov 25;468(7323):562-6. PubMed PMID: 20944625. Pubmed Central PMCID: 3241506.
51. Thiebaut F, Tsuruo T, Hamada H, Gottesman MM, Pastan I, Willingham MC. Immunohistochemical localization in normal tissues of different epitopes in the multidrug transport protein P170: evidence for localization in brain capillaries and crossreactivity of one antibody with a muscle protein. *J Histochem Cytochem.* 1989 Feb;37(2):159-64. PubMed PMID: 2463300.

52. Loscher W, Potschka H. Blood-brain barrier active efflux transporters: ATP-binding cassette gene family. *NeuroRx*. 2005 Jan;2(1):86-98. PubMed PMID: 15717060. Pubmed Central PMCID: 539326.
53. Cordon-Cardo C, O'Brien JP, Casals D, Rittman-Grauer L, Biedler JL, Melamed MR, et al. Multidrug-resistance gene (P-glycoprotein) is expressed by endothelial cells at blood-brain barrier sites. *Proc Natl Acad Sci U S A*. 1989 Jan;86(2):695-8. PubMed PMID: 2563168. Pubmed Central PMCID: 286540.
54. Mittapalli RK, Manda VK, Adkins CE, Geldenhuys WJ, Lockman PR. Exploiting nutrient transporters at the blood-brain barrier to improve brain distribution of small molecules. *Ther Deliv*. 2010 Dec;1(6):775-84. PubMed PMID: 22834013.
55. Thiebaut. immunohistochemical localization in normal tissues of different epitopes in the multidrug transport protein P170: evidence for localization in brain capillaries and crossreactivity of one antibody with a muscle protein. *Histochem Cytochem*. 1989.
56. Lee SW, Kim WJ, Choi YK, Song HS, Son MJ, Gelman IH, et al. SSeCKS regulates angiogenesis and tight junction formation in blood-brain barrier. *Nat Med*. 2003 Jul;9(7):900-6. PubMed PMID: 12808449.
57. Pelligrino DA, Vetri F, Xu HL. Purinergic mechanisms in gliovascular coupling. *Semin Cell Dev Biol*. 2011 Apr;22(2):229-36. PubMed PMID: 21329762. Pubmed Central PMCID: 3070818.
58. Goldberg M, De Pitta M, Volman V, Berry H, Ben-Jacob E. Nonlinear gap junctions enable long-distance propagation of pulsating calcium waves in astrocyte networks. *PLoS Comput Biol*. 2010 Aug 26;6(8). PubMed PMID: 20865153. Pubmed Central PMCID: 2928752.
59. Deli MA. Potential use of tight junction modulators to reversibly open membranous barriers and improve drug delivery. *Biochim Biophys Acta*. 2009 Apr;1788(4):892-910. PubMed PMID: 18983815.
60. Fournier G, Cabaud O, Josselin E, Chaix A, Adelaide J, Isnardon D, et al. Loss of AF6/afadin, a marker of poor outcome in breast cancer, induces cell migration, invasiveness and tumor growth. *Oncogene*. 2011 Sep 08;30(36):3862-74. PubMed PMID: 21478912.
61. Abbott NJ. Dynamics of CNS barriers: evolution, differentiation, and modulation. *Cell Mol Neurobiol*. 2005 Feb;25(1):5-23. PubMed PMID: 15962506.
62. Hawkins BT, Davis TP. The blood-brain barrier/neurovascular unit in health and disease. *Pharmacol Rev*. 2005 Jun;57(2):173-85. PubMed PMID: 15914466.
63. Schneeberger EE, Lynch RD. The tight junction: a multifunctional complex. *Am J Physiol Cell Physiol*. 2004 Jun;286(6):C1213-28. PubMed PMID: 15151915.
64. Liu WY, Wang ZB, Zhang LC, Wei X, Li L. Tight junction in blood-brain barrier: an overview of structure, regulation, and regulator substances. *CNS Neurosci Ther*. 2012 Aug;18(8):609-15. PubMed PMID: 22686334.
65. Furuse M, Hirase T, Itoh M, Nagafuchi A, Yonemura S, Tsukita S, et al. Occludin: a novel integral membrane protein localizing at tight junctions. *J Cell Biol*. 1993 Dec;123(6 Pt 2):1777-88. PubMed PMID: 8276896. Pubmed Central PMCID: 2290891.
66. Del Maschio A, De Luigi A, Martin-Padura I, Brockhaus M, Bartfai T, Fruscella P, et al. Leukocyte recruitment in the cerebrospinal fluid of mice with experimental meningitis is inhibited by an antibody to junctional adhesion molecule (JAM). *J Exp Med*. 1999 Nov 01;190(9):1351-6. PubMed PMID: 10544206. Pubmed Central PMCID: 2195675.
67. Dejana E, Lampugnani MG, Martinez-Estrada O, Bazzoni G. The molecular organization of endothelial junctions and their functional role in vascular morphogenesis and permeability. *Int J Dev Biol*. 2000;44(6):743-8. PubMed PMID: 11061439.

68. Yeung D, Manias JL, Stewart DJ, Nag S. Decreased junctional adhesion molecule-A expression during blood-brain barrier breakdown. *Acta Neuropathol.* 2008 Jun;115(6):635-42. PubMed PMID: 18357461.
69. Hoffman WH, Stamatovic SM, Andjelkovic AV. Inflammatory mediators and blood brain barrier disruption in fatal brain edema of diabetic ketoacidosis. *Brain Res.* 2009 Feb 13;1254:138-48. PubMed PMID: 19103180.
70. Haarmann A, Deiss A, Prochaska J, Foerch C, Weksler B, Romero I, et al. Evaluation of soluble junctional adhesion molecule-A as a biomarker of human brain endothelial barrier breakdown. *PLoS One.* 2010 Oct 21;5(10):e13568. PubMed PMID: 21060661. Pubmed Central PMCID: 2958838.
71. Bangsow T, Baumann E, Bangsow C, Jaeger MH, Pelzer B, Gruhn P, et al. The epithelial membrane protein 1 is a novel tight junction protein of the blood-brain barrier. *J Cereb Blood Flow Metab.* 2008 Jun;28(6):1249-60. PubMed PMID: 18382472.
72. Gonzalez-Mariscal L, Betanzos A, Avila-Flores A. MAGUK proteins: structure and role in the tight junction. *Semin Cell Dev Biol.* 2000 Aug;11(4):315-24. PubMed PMID: 10966866.
73. Stevenson BR, Siliciano JD, Mooseker MS, Goodenough DA. Identification of ZO-1: a high molecular weight polypeptide associated with the tight junction (zonula occludens) in a variety of epithelia. *J Cell Biol.* 1986 Sep;103(3):755-66. PubMed PMID: 3528172. Pubmed Central PMCID: 2114282.
74. Fanning AS, Jameson BJ, Jesaitis LA, Anderson JM. The tight junction protein ZO-1 establishes a link between the transmembrane protein occludin and the actin cytoskeleton. *J Biol Chem.* 1998 Nov 06;273(45):29745-53. PubMed PMID: 9792688.
75. Gottardi CJ, Arpin M, Fanning AS, Louvard D. The junction-associated protein, zonula occludens-1, localizes to the nucleus before the maturation and during the remodeling of cell-cell contacts. *Proc Natl Acad Sci U S A.* 1996 Oct 01;93(20):10779-84. PubMed PMID: 8855257. Pubmed Central PMCID: 38232.
76. Betanzos A, Huerta M, Lopez-Bayghen E, Azuara E, Amerena J, Gonzalez-Mariscal L. The tight junction protein ZO-2 associates with Jun, Fos and C/EBP transcription factors in epithelial cells. *Exp Cell Res.* 2004 Jan 01;292(1):51-66. PubMed PMID: 14720506.
77. Jalife Z. 2004.
78. Ambrosi C, Ren C, Spagnol G, Cavin G, Cone A, Grintsevich EE, et al. Connexin43 Forms Supramolecular Complexes through Non-Overlapping Binding Sites for Drebrin, Tubulin, and ZO-1. *PLoS One.* 2016;11(6):e0157073. PubMed PMID: 27280719. Pubmed Central PMCID: 4900556.
79. Axelsen LN, Calloe K, Holstein-Rathlou NH, Nielsen MS. Managing the complexity of communication: regulation of gap junctions by post-translational modification. *Front Pharmacol.* 2013 Oct 22;4:130. PubMed PMID: 24155720. Pubmed Central PMCID: 3804956.
80. Edward. The connexin 43 C-terminus: A tail of many tales. *Biochimica et Biophysica Acta.* 2017:17.
81. Goodenough DA, Paul DL. Gap junctions. *Cold Spring Harb Perspect Biol.* 2009 Jul;1(1):a002576. PubMed PMID: 20066080. Pubmed Central PMCID: 2742079.
82. Hare JF. Mechanisms of membrane protein turnover. *Biochim Biophys Acta.* 1990 Feb 28;1031(1):71-90. PubMed PMID: 2407292.
83. Hare JF, Taylor K. Mechanisms of plasma membrane protein degradation: recycling proteins are degraded more rapidly than those confined to the cell surface. *Proc Natl Acad Sci U S A.* 1991 Jul 01;88(13):5902-6. PubMed PMID: 2062868. Pubmed Central PMCID: 51986.
84. Herve JC, Derangeon M, Bahbouhi B, Mesnil M, Sarrouilhe D. The connexin turnover, an important modulating factor of the level of cell-to-cell junctional communication: comparison

with other integral membrane proteins. *J Membr Biol.* 2007 Jun;217(1-3):21-33. PubMed PMID: 17673963.

85. Fallon RF, Goodenough DA. Five-hour half-life of mouse liver gap-junction protein. *J Cell Biol.* 1981 Aug;90(2):521-6. PubMed PMID: 7287816. Pubmed Central PMCID: 2111874.

86. Laird DW, Puranam KL, Revel JP. Turnover and phosphorylation dynamics of connexin43 gap junction protein in cultured cardiac myocytes. *Biochem J.* 1991 Jan 01;273(Pt 1):67-72. PubMed PMID: 1846532. Pubmed Central PMCID: 1149880.

87. Laird DW. Life cycle of connexins in health and disease. *Biochem J.* 2006 Mar 15;394(Pt 3):527-43. PubMed PMID: 16492141. Pubmed Central PMCID: 1383703.

88. Axelsen LN CK, Holstein-Rathlou NH, Nielsen MS. Managing the complexity of communication: regulation of gap junctions by post-translational modification. *Frontiers in Pharmacology.* 2013.

89. Wong AD, Ye M, Levy AF, Rothstein JD, Bergles DE, Searson PC. The blood-brain barrier: an engineering perspective. *Frontiers in neuroengineering.* 2013 Aug 30;6:7. PubMed PMID: 24009582. Pubmed Central PMCID: 3757302.

90. Avdeef A. Physicochemical profiling (solubility, permeability and charge state). *Curr Top Med Chem.* 2001 Sep;1(4):277-351. PubMed PMID: 11899112.

91. Lipinski CA, Lombardo F, Dominy BW, Feeney PJ. Experimental and computational approaches to estimate solubility and permeability in drug discovery and development settings. *Adv Drug Deliv Rev.* 2001 Mar 01;46(1-3):3-26. PubMed PMID: 11259830.

92. Pardridge WM. CNS drug design based on principles of blood-brain barrier transport. *J Neurochem.* 1998 May;70(5):1781-92. PubMed PMID: 9572261.

93. Pardridge WM. Biopharmaceutical drug targeting to the brain. *J Drug Target.* 2010 Apr;18(3):157-67. PubMed PMID: 20064077.

94. Enerson BE, Drewes LR. The rat blood-brain barrier transcriptome. *J Cereb Blood Flow Metab.* 2006 Jul;26(7):959-73. PubMed PMID: 16306934.

95. Kostrzewa RM. The blood-brain barrier for catecholamines - revisited. *Neurotox Res.* 2007 Apr;11(3-4):261-71. PubMed PMID: 17449463.

96. Robberecht W. Oxidative stress in amyotrophic lateral sclerosis. *J Neurol.* 2000 Mar;247 Suppl 1:11-6. PubMed PMID: 10795881.

97. van Horsen J, Witte ME, Schreibelt G, de Vries HE. Radical changes in multiple sclerosis pathogenesis. *Biochim Biophys Acta.* 2011 Feb;1812(2):141-50. PubMed PMID: 20600869.

98. Olmez I, Ozyurt H. Reactive oxygen species and ischemic cerebrovascular disease. *Neurochem Int.* 2012 Jan;60(2):208-12. PubMed PMID: 22122807.

99. Pun PB, Lu J, Moochhala S. Involvement of ROS in BBB dysfunction. *Free radical research.* 2009 Apr;43(4):348-64. PubMed PMID: 19241241.

100. French JA, Pedley TA. Clinical practice. Initial management of epilepsy. *N Engl J Med.* 2008 Jul 10;359(2):166-76. PubMed PMID: 18614784.

101. Marchi N, Angelov L, Masaryk T, Fazio V, Granata T, Hernandez N, et al. Seizure-promoting effect of blood-brain barrier disruption. *Epilepsia.* 2007 Apr;48(4):732-42. PubMed PMID: 17319915. Pubmed Central PMCID: 4135474.

102. Wingerchuk DM, Lennon VA, Lucchinetti CF, Pittock SJ, Weinshenker BG. The spectrum of neuromyelitis optica. *Lancet Neurol.* 2007 Sep;6(9):805-15. PubMed PMID: 17706564.

103. Molloy B, and Schmiegel, K. K. , inventor Aryloxphenylpropylamines 1982.

104. Gossen D, de Suray JM, Vandenhende F, Onkelinx C, Gangji D. Influence of fluoxetine on olanzapine pharmacokinetics. *AAPS PharmSci.* 2002;4(2):E11. PubMed PMID: 12102620. Pubmed Central PMCID: 2751291.

105. Maertens C, Wei L, Voets T, Droogmans G, Nilius B. Block by fluoxetine of volume-regulated anion channels. *Br J Pharmacol*. 1999 Jan;126(2):508-14. PubMed PMID: 10077245. Pubmed Central PMCID: 1565822.
106. Hiemke C, Hartter S. Pharmacokinetics of selective serotonin reuptake inhibitors. *Pharmacol Ther*. 2000 Jan;85(1):11-28. PubMed PMID: 10674711.
107. Unceta N, Ugarte A, Sanchez A, Gomez-Caballero A, Goicolea MA, Barrio RJ. Development of a stir bar sorptive extraction based HPLC-FLD method for the quantification of serotonin reuptake inhibitors in plasma, urine and brain tissue samples. *J Pharm Biomed Anal*. 2010 Jan 05;51(1):178-85. PubMed PMID: 19660886.
108. Megan. Classics in chemical neuroscience: fluoxetine (prozac). *ACS Chemical NEUROSCIENCE*. 2013.
109. Gao HM, Hong JS. Why neurodegenerative diseases are progressive: uncontrolled inflammation drives disease progression. *Trends Immunol*. 2008 Aug;29(8):357-65. PubMed PMID: 18599350. Pubmed Central PMCID: 4794280.
110. Zhang F, Zhou H, Wilson BC, Shi JS, Hong JS, Gao HM. Fluoxetine protects neurons against microglial activation-mediated neurotoxicity. *Parkinsonism Relat Disord*. 2012 Jan;18 Suppl 1:S213-7. PubMed PMID: 22166439. Pubmed Central PMCID: 3608679.
111. Su F, Yi H, Xu L, Zhang Z. Fluoxetine and S-citalopram inhibit M1 activation and promote M2 activation of microglia in vitro. *Neuroscience*. 2015 May 21;294:60-8. PubMed PMID: 25711936.
112. Oztas B. Sex and Blood-Brain Barrier 1997;37.
113. Corbett A, McGowin A, Sieber S, Flannery T, Sibbitt B. A method for reliable voluntary oral administration of a fixed dosage (mg/kg) of chronic daily medication to rats. *Laboratory animals*. 2012 Oct;46(4):318-24. PubMed PMID: 22969146.
114. Macleod MR, Fisher M, O'Collins V, Sena ES, Dirnagl U, Bath PM, et al. Reprint: Good laboratory practice: preventing introduction of bias at the bench. *Int J Stroke*. 2009 Feb;4(1):3-5. PubMed PMID: 19236488.
115. Gage GJ, Kipke DR, Shain W. Whole animal perfusion fixation for rodents. *J Vis Exp*. 2012 Jul 30(65). PubMed PMID: 22871843. Pubmed Central PMCID: 3476408.
116. Cserr HF. Physiology of the choroid plexus. *Physiol Rev*. 1971 Apr;51(2):273-311. PubMed PMID: 4930496.
117. Marques F, Sousa JC, Sousa N, Palha JA. Blood-brain-barriers in aging and in Alzheimer's disease. *Mol Neurodegener*. 2013 Oct 22;8:38. PubMed PMID: 24148264. Pubmed Central PMCID: 4015275.
118. Maseguin C, LePanse S, Corman B, Verbavatz JM, Gabrion J. Aging affects choroidal proteins involved in CSF production in Sprague-Dawley rats. *Neurobiol Aging*. 2005 Jun;26(6):917-27. PubMed PMID: 15718051.
119. Jasmina Kercmar GM. Sex-specific behavioral effects of fluoxetine treatment in animal models of depression and anxiety 2014.
120. Stokes PE, Holtz A. Fluoxetine tenth anniversary update: the progress continues. *Clin Ther*. 1997 Sep-Oct;19(5):1135-250. PubMed PMID: 9385500.
121. Zienowicz. Enancjomery i ich rola w psychopharmakologii na przykladzie escitalopramu. 2003. p. 71-83.
122. Kim J. Stereoselective disposition of fluoxetine and norfluoxetine during pregnancy and breast-feeding. *British Journal of Clinical pharmacology*. 2005.
123. David K. Batter RAC, Christineroy, David C. Spray, Elliot L. Hertzberg, John A. Kessler. Heterogeneity in Gap Junction Expression in Astrocytes Cultured From Different Brain Regions. 1992.

124. Quesseveur G, Portal B, Basile JA, Ezan P, Mathou A, Halley H, et al. Attenuated Levels of Hippocampal Connexin 43 and its Phosphorylation Correlate with Antidepressant- and Anxiolytic-Like Activities in Mice. *Frontiers in cellular neuroscience*. 2015;9:490. PubMed PMID: 26733815. Pubmed Central PMCID: 4686612.
125. Jiayi Wang XZ, Hiayan Lu, Mingrui Song, Jinglong Zhao, and Qiaoshu Wang. Fluoxetine induces vascular endothelial growth factor/Netrin over-expression via the mediation of hypoxia-inducible factor 1-alpha in SH-SY5Y cells *Journal of Neurochemistry* 2016;136(6).
126. Godbout DMNaJP. Review: Microglia of the aged brain: primed to be activated and resistant to regulation. *Neuropathology and Applied Neurobiology* 2013.